Regulation of chromatin structure in genome stability

Laura Lee

A dissertation

submitted in partial fulfillment of the

requirements for the degree of

Doctor of Philosophy

University of Washington

2016

Reading Committee:

Toshio Tsukiyama, Chair

Mosur Raghuraman

Toshi Taniguchi

Program Authorized to Offer Degree:

Molecular and Cellular Biology

University of Washington

Abstract

Regulation of chromatin structure in genome stability

Laura Lee

Chair of the Supervisory Committee:
Toshio Tsukiyama
Member
Division of Basic Sciences
Fred Hutchinson Cancer Research Center
Affiliate Associate Professor, Department of Biochemistry

In eukaryotic cells, DNA is tightly packaged into chromatin. Because chromatin is inhibitory to DNA-binding proteins, it must be modified so that necessary DNA-protein interactions can occur. Chromatin structure can be modified or altered by chromatin regulators. One class of chromatin regulators is the ATP-dependent chromatin remodeling factor family. Chromatin remodeling enzymes utilize ATP hydrolysis to alter chromatin structure and thus affect many DNA-dependent processes. Mutations in these complexes can cause disease and cell death, signifying their importance. Here I use *Saccharomyces cerevisiae* as a model organism to characterize the roles of chromatin structure and remodeling factors in essential biological processes. In this study, I show that budding yeast remodeling factors Isw2 and Ino80 act in opposition to checkpoint activators and promote accessibility of chromatin during replication

stress. I also suggest novel roles for these enzymes in telomere homeostasis and rRNA transcriptional regulation. Finally, I show that nucleosome occupancy is a novel parameter for origin activities and that a chromatin regulator is likely responsible for establishing occupancy at origins. Taken together my work demonstrates the importance of chromatin regulation in cellular mechanisms that are crucial for genome integrity.

TABLE OF CONTENTS

LIST OF FIGURES

LIST OF TABLES

ACKNOWLEDGEMENTS

This work and my graduate school career would not have been possible without the contributions and support of so many people. First and foremost, I would like to thank my advisor, Toshio Tsukiyama. He continuously challenged me and taught me to be a better scientist, and his constant enthusiasm for science has been contagious. I am very grateful to have been a part of Toshi's lab. I also want to thank all members of the Tsukiyama lab for their advice, assistance and most importantly their friendships. I am thankful for Tracey for initially training me in lab. I also want to thank Jairo for his collaboration on multiple projects and Sam for carrying on my project after I leave. Joe, Keean, and Sarah have become great friends and I am thankful for their support and discussions. I am particularly thankful for Jeff and Eric. Jeff has been like a second mentor to me. He has been critical in my graduate school training and I am definitely a better scientist because of it. I am grateful to have had Eric join the lab the same time as me. He is a great friend, scientist and sports fanatic. I would have not have been able to survive the hostile Seahawks territory without a fellow Bay Area fan. I am also thankful to Janine Alcid and Laura McKnight for always supporting and understanding me.

There are many people at both the Fred Hutch and UW that I would like to acknowledge. I want to thank my committee members: Steve Henikoff, Steve Hahn, M.K. Raghuraman, and Toshi Taniguchi, specifically Raghu and Toshi for serving on my reading committee. The Henikoff, Gottschling, Smith and Biggins labs were very sincere and always helpful. I particularly want to thank the Biggins lab for the joint lab meetings and Sue for her advice and mentorship. I acknowledge Jeremy Msetif for being our wonderful lab manager and making everything functional in lab. Luna Yu and Pat Heath were always very friendly and I am thankful they were here to fix all the computer problems. I also would like to acknowledge the Core facilities at the Hutch that were always great. I particularly thank Andy Marty, Phil Gafken and Jeff Delrow. I want to thank the MCB program, specifically the administration at the Hutch, Michele Karantsavelos and Maia Lowe. I am very thankful to my fellow classmate Tony Abeyta for all his continued support and understanding throughout graduate school.

Lastly, I would like to thank my friends and family for their enormous support and encouragement throughout my graduate school career. I would have not made it through graduate school without all of them. I want to thank my Seattle community, specifically Sarah Lee, Mike Kim, Jooyeon and Jinman Choe, Lisa Rho, David and Alison Staples, Jessica Shin, Jinny and Jason Koh, John Lee, Alyssa Chung, Alisa So, Lance Park and Elise Cho. I also want to thank my best friends from college, Janice Cho, Eugenie Hong, Hana Lee, Tam Duong, Rebecca Zabinsky and Kelsey Tanaka. I particularly want to thank Kelsey Tanaka, along with her parents, Steve and Carol, for being like a second family to me in Seattle. Kelsey has always been there for me through my grad school career, so for that I will be forever grateful. I am extremely thankful for my sister and brother-in-law, Lydia and Daniel You. They have been some of my biggest supporters. I am so grateful for my parents for always believing in me and supporting me in every way possible. Most importantly, I am grateful for my husband Alex for making me the best person I can be. I love him so much and none of this would have been possible without him.

DEDICATION

To my wonderful parents,
for their tremendous love and support.
Also to my sister and brother-in-law,
For their constant encouragement.
And of course to my amazing husband Alex,
for being my biggest supporter and loving me,
I would not be where I am today without all of you.

CHAPTER 1

Introduction

Chromatin Structure

All of our genetic information is contained in a set of DNA molecules that together stretch out to nearly two meters. In order for DNA to fit into a 10-20μm nucleus, the DNA must be tightly packaged. DNA attains this structure by first wrapping around an octamer of histone proteins, which consist of two copies of H2A, H2B, H3 and H4. About 147 base pairs of DNA wrap 1.65 turns around the histone octamer to form nucleosomes, and variable lengths of linker DNA separate adjacent nucleosomes (Luger et al., 1997). Through intermolecular and intramolecular interactions, nucleosomes and linker DNA further fold into 30nm fibers (Felsenfeld and Groudine, 2003). These fibers further condense into a higher order structure through currently unknown mechanisms. Many studies have attempted to decipher the folding patterns of higher order chromatin, but because of the highly compact structure, resolving the compaction mechanisms has proved to be difficult. Understanding regulation of chromatin structure is integral to elucidating the regulation of biological processes. While all cells have the same genetic information, cells are differentiated to perform different functions. Thus DNA sequence alone cannot define cellular function. Rather chromatin structure is differentially regulated in different types of cells for proper execution of these functions. Certainly, studies have shown that defects in chromatin structure results in misregulation of many cellular processes (Hendrich and Bickmore, 2001).

There are many layers of chromatin regulation. Regulating the accessibility of chromatin is necessary for DNA-dependent processes to occur at a given locus. DNA-dependent processes such as transcription and replication require initiation factors to bind to the target loci. However, nucleosomes can act as barriers to protein binding. Therefore, chromatin must be made accessible in these regions for these processes to occur. Indeed, replication origins (hereafter origins) and transcription start sites (TSSs) of genes have are depleted of nucleosomes to facilitate recruitment of necessary factors (Bernstein et al., 2004; Eaton et al., 2010; Lee et al., 2004). On the other hand, there are regions of the genome that need to remain inaccessible, and are therefore associated with more compacted chromatin structure. These DNA sequences tend to have higher nucleosome occupancy and recruit other factors that reinforce condensation (Woodcock and Ghosh, 2010). The compact, inactive chromatin state is known as heterochromatin, whereas the decondensed, active state is known as euchromatin. Different types of heterochromatin exist: facultative heterochromatin can reversibly transition from inactive to active states, and constitutive heterochromatin is always condensed, enriched in repetitive sequences, and associated with gene poor regions (Woodcock and Ghosh, 2010). Chromatin is also spatially organized within the nucleus. Compared to euchromatin, heterochromatin tends to localize more at the nuclear periphery and has been shown to interact with the nuclear envelope (Marshall, 2002). Moreover, studies suggest that there may be chromatin "territories," in which chromatin with similar properties associate together (Woodcock and Ghosh, 2010). Within this spatial organization, chromatin has been shown to "loop out" specific regions of the genome in order to regulate their accessibility (Kadauke and Blobel, 2009). Enhancer promoter interactions are required for transcriptional activation but enhancers and promoters can be separated by thousands of base pairs. Recent studies suggest that spatial regulation and chromatin looping

serve as mechanisms to regulate interaction between enhancers and promoters (Nolis et al., 2009). Current studies also suggest that chromatin is constantly dynamic and chromatin mobility can range among different regions of the genome, which has functional consequences for DNA-dependent processes (Soutoglou and Misteli, 2007).

In order to regulate these different chromatin states, cells have many proteins whose primary function is to regulate chromatin structure. Histone modifying enzymes can add or remove modifications to histone proteins. Different modifications like acetylation or methylation are associated with various chromatin activities. These modifications can either recruit specific chromatin regulators or regulate activities of chromatin regulators. ATP-dependent chromatin remodeling enzymes are another class of proteins that use the energy of ATP hydrolysis to alter chromatin structure. These chromatin regulators are involved in many DNA-dependent pathways including transcription, DNA replication, DNA repair, and chromosome segregation (Clapier and Cairns, 2009). Mutations in chromatin regulators result in many kinds of disorders or diseases, which highlights their importance in regulating multiple DNA-dependent pathways (Hendrich and Bickmore, 2001).

ATP-dependent chromatin remodeling enzymes

ATP-dependent chromatin remodeling enzymes are multi-subunit complexes that alter chromatin structure in various ways. They have been shown to slide, evict, assemble or restructure nucleosomes (Clapier and Cairns, 2009). Remodeling factors are part of the SNF2 super family that have homology domains to DExx box helicases (Vignali et al., 2000). However they are not known to have helicase activities. Rather, they are stimulated by nucleosomes and use their translocase activity to affect DNA-histone interactions (Clapier and Cairns, 2009). All

chromatin remodeling factors have a catalytic ATPase subunit but each class of ATPases has unique domains that define the different subfamilies of remodeling enzymes. Furthermore, each ATPase associates with different accessory subunits that specializes the factor to execute its specific functions. There are four families of remodeling factors: SWI/SNF (switching defective/sucrose nonfermenting), ISWI (imitation switch), CHD (chromodomain, helicase, DNA binding) and INO80 (inositol requiring 80) (Figure 1.1) (Clapier and Cairns, 2009). Each family of remodeling factors participates in numerous biological processes, and because of their importance each family is highly conserved from yeast to humans.

The SWI/SNF family of enzymes is characterized by an ATPase domain that has two helicase-SANT (HSA) domains and a C-terminal bromodomain (Figure 1.1). The helicase-SANT domain functions to interact with histones and DNA. Bromodomains bind to acetylated lysine residues, and binding can promote recruitment of factors to specific locations or alter ATPase activity. The SWI/SNF family of enzymes has been shown to slide or eject nucleosomes (Clapier and Cairns, 2009). In yeast, there are two complexes in the SWI/SNF family, SWI/SNF and RSC. The catalytic subunit of SWI/SNF is the Snf2 subunit. SWI/SNF has been shown to facilitate transcription (Winston and Carlson, 1992). While mostly known to be involved in activating transcription, there is some evidence of SWI/SNF having roles in transcriptional repression at telomeres and the ribosomal DNA (rDNA) (Dror and Winston, 2004). Furthermore it was shown the SWI/SNF also has roles in replication and the checkpoint response (Flanagan and Peterson, 1999; Kapoor et al., 2015). The catalytic subunit of RSC is Sth1 and RSC has been shown to be involved in chromosome segregation, gene expression, and DNA repair (Clapier and Cairns, 2009).

The ISWI family of proteins has an ATPase that consists of a C-terminal HAND-SANT-SLIDE domain (Figure 1.1), which functions to bind to unmodified histone tails and DNA (Clapier and Cairns, 2009). In yeast, ISWI complexes include Isw1a, Isw1b and Isw2. The ISWI family is mostly known to be involved in transcriptional repression (Fazzio et al., 2001; Goldmark et al., 2000; Ruiz et al., 2003; Sherriff et al., 2007). However, some ISWI complexes like *Drosophila* NURF can promote transcription (Mizuguchi et al., 1997). ISWI complexes have the ability alter nucleosome positioning and assemble nucleosome arrays (Clapier and Cairns, 2009).

The CHD family proteins are distinguishable by an ATPase with tandem chromodomains. Chromodomains function to bind methylated histones (Figure 1.1). CHD remodeling factors have nucleosome sliding and ejecting activities (Clapier and Cairns, 2009). Mammalian Mi-2, which forms the nucleosome remodeling and deacetylase (NuRD) complex, is part of the CHD class of remodeling factors. Yeast only has one known CHD family protein, Chd1. Chd1 has been implicated in transcriptional elongation, as studies show co-localization with elongating Pol II (McDaniel et al., 2008; Murawska et al., 2008). Chd1 functions alongside Isw1 and Isw2 to generate nucleosomal arrays (Gkikopoulos et al., 2011). Indeed in the absence of all three complexes, nucleosome positioning is disrupted genome-wide (Gkikopoulos et al., 2011).

The INO80 family of proteins has a unique ATPase in that the ATPase domain is "split" by a long insertion (Figure 1.1). Ino80 has been implicated in many functions including DNA replication, repair and transcription (Clapier and Cairns, 2009). However, mechanisms of Ino80 activities are far less understood. Budding yeast Ino80 and Swr1 are part of the INO80 family of proteins. Ino80 and Swr1 were shown to have opposing biochemical activities, in which Swr1

exchanges H2A-H2B dimers with H2A.Z-H2B dimers, and Ino80 performs the opposite reaction (Mizuguchi et al., 2004; Papamichos-Chronakis et al., 2011). Ino80 has also been shown to have nucleosome sliding activity (Udugama et al.). Both Ino80 and Swr1 have role in multiple pathways and thought to be important for maintaining genome integrity (Clapier and Cairns, 2009).

Thus far chromatin remodeling factors activities have only been characterized with histone or DNA substrates. However a recent study suggested that chromatin remodeling factor SWI/SNF can regulate activation of a non-chromatin substrate Mec1(Kapoor et al., 2015), which is a central checkpoint kinase. Additionally, Mot1, a protein related to chromatin remodeling factors has the ability to displace TATA-binding protein (TBP) from promoters (Auble et al., 1994). These studies indicate that chromatin remodeling factors may have functions beyond altering histone-DNA interactions to regulate cellular processes.

Budding yeast Isw2

In budding yeast, the ISWI family of remodeling factors consists of Isw1a, Isw1b, and Isw2. Isw2 has been purified as either a two- or a four-subunit complex. The two-subunit complex consists of catalytic subunit Isw2 and Itc1. The four subunit complex is made up of the Isw2, Itc1, Dpb4, and Dls1 (Figure 1.2). Isw2 has mainly been shown slide nucleosomes into the nucleosome depleted region (NDR) of genes to repress transcription at specific sites (Fazzio et al., 2001; Goldmark et al., 2000; Ruiz et al., 2003; Sherriff et al., 2007). Isw2 recruitment and activity is dependent on the basic patch in the N-terminal tail of histone H4 (Dang et al., 2006). Isw2 is specifically recruited to target genes through transcription factor Ume6 by direct interaction or through chromosome looping (Goldmark et al., 2000; Yadon et al., 2013). Isw2 is

also targeted to upstream regions of tRNA genes through Bdp1, a Pol III transcription factor TFIIIB subunit, to affect Ty1 retrotransposon integration sites (Bachman et al., 2005). Recently, Isw2 was also shown to repress long noncoding RNAs (lncRNAs), which can inhibit transcription of the overlapping mRNA (Alcid and Tsukiyama, 2014). Outside of transcription, Isw2 has been implicated in replication and the S phase checkpoint, and shown to be enriched at stalled replication forks (Au et al., 2011; Vincent et al., 2008). Moreover, Isw2 was recently shown to be involved in increasing life span (Dang et al., 2014). Furthermore, Isw2 has the ability to translocate on ssDNA, albeit with lower affinity for ssDNA than nucleosomes (Fischer et al., 2009).

Budding yeast Ino80

The INO80 subfamily consists of Ino80 and Swr1 in budding yeast. Ino80 is a 15 subunit complex that has been implicated in many different cellular processes (Figure 1.2). Ino80 subunits include helicase-related proteins Rvb1 and Rvb2, actin proteins Arp5, Apr8, Apr4 and Actin1, TATA binding protein-associated factor Taf14, and Ino80-specific subunits Ies2, Ies6, Ies1, Ies3, Ies4, Ies5 and Nhp10. The Nhp10 subunit, which is related to mammalian high mobility group proteins, has been shown to bind to DNA. It is currently unknown whether Ino80 exists in multiple subcomplexes. Mechanisms of Ino80 activities are currently not well understood. Thus far, studies have shown that Ino80 has the ability to exchange H2A.Z-H2B dimers with H2A-H2B dimers and slide nucleosomes *in vitro* (Papamichos-Chronakis et al., 2011; Udugama et al.). Ino80 also has roles in DNA repair pathways, as Ino80 is enriched at double-stranded breaks (DSBs) and facilitates H2AX phosphorylation at DSBs (van Attikum et al., 2004). Mutations in Ino80 subunits lead to sensitivity on replication inhibitors because Ino80

promotes replication fork stability and recovery (Shimada et al., 2008). Regulation of Ino80 activity is not well defined, but studies have shown that phosphorylation of Ies4 subunit by Mec1/Tel1 modulates the checkpoint response (Morrison et al., 2007). Ino80 was shown to be enriched at the +1 nucleosome of TSSs, where H2A.Z exchange occurs (Yen et al., 2013). Additionally, Ino80 and its subunits have been implicated in telomere function (Xue et al., 2015; Yu et al., 2007).

Chromatin Structure in DNA replication

DNA replication occurs from multiple sites in the genome called replication origins (origins). In budding yeast, origins are defined by an AT rich autonomous replication sequence (ARS) (Marahrens and Stillman, 1992). Prior to S phase, the ARS consensus sequence (ACS) is bound by the origin recognition complex (ORC) (Bell and Stillman, 1992; Diffley and Cocker, 1992). ORC recruits the mini chromosome maintenance (MCM) helicase complex, via Ctd1 and Cdc6, to form the pre-replicative complex (pre-RC) (Remus et al., 2009). The Cdc45 complex then recruits polymerases for DNA replication, and cyclin dependent kinases (CDKs) and Dbf4-dependent kinase (DDK) to activate the MCM complex (Fragkos et al., 2015). MCM forms a complex with Cdc45 and the GINS to form the CMG helicase, which when activated, unwinds DNA ahead of the fork and results in bi-directional DNA replication. However, replication factors are limiting (Mantiero et al., 2011), hence origins do not all fire simultaneously (Brewer and Fangman, 1991; Dubey et al., 1991). Instead, origins show temporally staggered patterns of initiation, and in addition vary in their efficiency of initiation (Figure 1.3). Origin timing is defined as when in S phase an origin is seen to fire on average in a population of cells. Origin

efficiency is defined as the fraction of cells in which a given origin fires. Origin activation is strictly regulated to ensure that re-replication does not occur.

Chromatin structure is a significant factor in establishing origin activation and modulating DNA replication. Chromatin context has been shown to affect origin activation as origins close to centromeres fire early (McCarroll and Fangman, 1988; Raghuraman et al., 2001), and those close to telomeres fire late (Ferguson and Fangman, 1992; McCarroll and Fangman, 1988). Moreover, a late origin can fire early when placed on a plasmid (Ferguson and Fangman, 1992). Histone acetylation has also been implicated in controlling DNA replication and origin activation (Iizuka et al., 2006; Knott et al., 2009; Unnikrishnan et al., 2010; Vogelauer et al., 2002). Furthermore, origins have ORC-dependent asymmetric nucleosome positions, which affect origin initiation (Eaton et al., 2010). Chromatin remodeling factors have also been implicated in DNA replication. We and others have shown that chromatin remodeling factors are required for proper replication initiation and replication fork progression (Biswas et al., 2008; Flanagan and Peterson, 1999; Vincent et al., 2008).

Chromatin Structure in S phase checkpoint

During DNA replication, cells are prone to endogenous or exogenous stresses that can cause replication stress or DNA damage. Improper resolution of these events can lead to genome instability and cell death. Thus cells have a mechanism in place called the S phase checkpoint to allow cells to properly undergo DNA repair and replication before cell division (Figure 1.4).

Replication protein A (RPA) has a high affinity to ssDNA and accumulation of RPA on DNA serves as one of the first signals for checkpoint activation. RPA binds to Ddc2 (mammalian ATRIP), which recruits binding partner Mec1 (human ATR) to stalled replication forks (Zou and

Elledge, 2003). In budding yeast, Mec1 is the main S phase checkpoint kinase, and is necessary for robust activation of the S phase checkpoint (Zou, 2013). Tel1 also acts in parallel to Mec1, but is a minor contributor to the S phase checkpoint as it is dispensable for checkpoint activation (Zou, 2013). Sensor proteins Rad24 clamp loader and the 9-1-1 clamp (Rad17, Ddc1, and Mec3), Dna2 and Dpb11 are recruited separately to stalled forks and all have the ability to activate Mec1 (Gilbert et al., 2001; Katou et al., 2003; Kondo et al., 2001; Kumar and Burgers, 2013; Majka et al., 2006; Navadgi-Patil and Burgers, 2008). Once activated, Mec1 signals mediator proteins Rad9 and Mrc1, which both function to activate the downstream effector kinases Rad53 and Chk1 (Alcasabas et al., 2001). Rad53 has a greater role in S phase checkpoint activation than Chk1 in budding yeast. Once Rad53 is activated, cells slow down replication, resolve the stress, stabilize replication forks and prevent origin firing. While checkpoint activation is important for genome stability, checkpoint deactivation has also been found to be critical. Cells deficient in checkpoint deactivation cannot recover from replication fork arrest, and eventually replication forks collapse leading to cell death (Szyjka et al., 2008). One mode of checkpoint deactivation occurs through Rad53 phosphatases that function to dephosphorylate Rad53, thereby deactivating the checkpoint (Szyjka et al., 2008). While other modes of checkpoint deactivation exist, these mechanisms are currently unknown.

Chromatin structure has been shown to be important in the S phase checkpoint. We have previously shown that chromatin remodeling factors Isw2 and Ino80 can deactivate the S phase checkpoint (Au et al., 2011). A study has also shown that Mec1 can phosphorylate Ies4 subunit of Ino80 and this regulation can affect Ino80 binding to Rad53 to modulate checkpoint activity (Morrison et al., 2007). Mec1 was also shown to phosphorylate Isw2 (Chen et al., 2010), but

whether these phosphorylations affect the function of Isw2 are unknown. Recently SWI/SNF was shown to directly regulate Mec1 activity to modulate the checkpoint (Kapoor et al., 2015).

Chromatin structure in rDNA stability

Ribosomal RNAs (rRNAs) are transcribed from the rDNA locus, which resides in the nucleolus. rRNAs are the RNA components of the ribosome and are required for proper protein synthesis. Growing cells require robust production of proteins so rRNAs are abundantly transcribed. In fact, rRNAs make up ~80% of total RNA in the cell (Kobayashi, 2014). In order for cells to produce many rRNAs, the rDNA locus contains multiple repeating units of rRNA genes. In budding yeast, the rDNA locus is on chromosome XII, and wild type cells carry around 150 copies of the rDNA unit (Figure 1.5). Each unit is made up of the 35S transcription unit, which gives rise to the 25S, 18S, and 5.8S RNAs, the 5S gene, a replication fork barrier (RFB) and a ribosomal origin of replication (rARS). While the majority of the yeast RNAs are transcribed by Pol II, the rRNAs are transcribed by Pol I and Pol III (Kobayashi, 2014). Pol I transcribes the 35S, while Pol III transcribes the 5S. However, while there are many copies of the rDNA unit, not all of these units are transcribed. Studies have reported that the rDNA exists in two different forms. Early psoralen crosslinking experiments deduced that about half the rDNA copies are nucleosome poor, and the other half have higher levels of nucleosomes (Dammann et al., 1993). The nucleosome poor copies are associated with active rDNA units, whereas the nucleosome rich copies are associated with inactive units (Dammann et al., 1993). In mammals, a chromatin remodeling factor NoRC has been shown to be involved in silencing the inactive copies (Strohner et al., 2004).

rDNA is important for genome stability and has been implicated in aging and cellular senescence (Kobayashi, 2011). The rDNA locus is a hot spot for homologous recombination (HR) because of its highly repetitive nature. When HR occurs at the rDNA locus, cells can both lose or gain rDNA copies. The binding of Fob1 to the RFB and a double strand break (DSB) is required for HR to initiate at the rDNA locus (Burkhalter and Sogo, 2004; Kobayashi et al., 1998; Kobayashi et al., 2004). Through an unknown mechanism cells sense when rDNA copy number is low and a rDNA amplification response is initiated. During HR, cohesion pairs sister chromatids together at the rDNA and the cells undergo equal chromatid recombination, which results in no changes in copy number (Figure 1.6) (Kobayashi and Ganley, 2005). In this instance, NAD^+-dependent histone deacetylase Sir2 functions to silence HR by binding to an E-pro promoter (Kobayashi et al., 2004). However during rDNA amplification, Sir2 is redistributed from the rDNA and in the absence of Sir2, a non-coding RNA (ncRNA) is expressed, which displaces cohesin from the region (Kobayashi and Ganley, 2005). When HR is stimulated in the absence of cohesion, unequal sister chromatid exchange takes place, which results in rDNA amplification (Figure 1.6). Chromatin structure has been shown to be important in regulating genome stability at the rDNA. *SIR2* deletions result in unstable rDNA copy number and reduced replicative life span (Kobayashi et al., 2004).

Chromatin structure at telomere stability

Telomeres are the ends of chromosomes and function to protect the chromosomal ends from degradation or end-to-end chromosomal fusions (Wellinger and Zakian, 2012). Haploid *S. cerevisiae* has 32 telomeres and each telomere consists of both repetitive and heterogeneous DNA sequences. Telomeres have many structural similarities, but they are also unique in their

composition of different types of subtelomeric elements, which have the ability to recruit different types of factors (Wellinger and Zakian, 2012). As cells undergo successive rounds of DNA replication, telomeres begin to shorten. Telomere length is associated with cellular senescence and aging (Wellinger and Zakian, 2012). Once telomeres become too short, cells are programmed to undergo senescence to prevent genome instability. Budding yeast has a telomerase enzyme that functions to lengthen telomeres and prevent genome instability.

Because of their repetitive nature, telomeres are hot spots for recombination. To prevent genome instability, telomeres tend to be in a heterochromatic structure (Wellinger and Zakian, 2012). Transcription and DNA repair is repressed at these regions, as activation of these activities has shown to result in genomic instability (Gravel and Wellinger, 2002; Maicher et al., 2012). Heterochromatin at telomeres is formed through recruitment of Sir (silent information regulator) proteins (Imai et al., 2000; Takahashi et al., 2011). Yeast DNA repair Ku complex (Yku) along with transcription factor Rap1 bind to DNA sequences within the telomeres and recruit Sir proteins to telomeres (Boulton and Jackson, 1996; Gilson et al., 1993). Sirs deacetylate H4K16 acetylation, which compacts chromatin and also recruits more Sirs to spread heterochromatin formation (Imai et al., 2000). Mechanisms of limiting Sir spreading are currently unknown, but recently a study implicated Ino80 to be important for establishing Sir boundaries (Xue et al., 2015).

Description of Dissertation

The goal of my dissertation is to characterize chromatin structure and its effects in biological processes. As discussed above, there are many levels of chromatin regulation, and for my dissertation I specifically focus on how chromatin remodeling factors affect chromatin

structure to regulate essential DNA-dependent processes. *Saccharomyces cerevisiae* is an ideal organism to study many of these processes, and both remodeling factors are highly conserved from yeast to humans.

Chapter 2 focuses on chromatin remodeling factors Isw2 and Ino80. Our lab previously showed that these two remodeling factors function in parallel to facilitate DNA replication and checkpoint deactivation. The goal of my project was to determine the mechanisms by which Isw2 and Ino80 attenuate the S phase checkpoint. I first sought to determine the kinetics checkpoint activation in *isw2 nhp10*. I then systematically screened for interacting checkpoint partners of Isw2 and Ino80 to determine which part of the checkpoint pathway Isw2 and Ino80 functioned in. Furthermore, I investigated whether Isw2 and Ino80 affect chromatin accessibility during replication stress to influence the checkpoint response.

Apart from DNA replication and the S phase checkpoint, in Chapter 3 I investigated the other potential functions of Isw2 and Ino80. I screened for genetic interactions of *ISW2* and *NHP10* to determine whether Isw2 and Ino80 had roles in other cellular processes. Genetic interactions suggested that Isw2 and Ino80 have previously unknown roles at the rDNA and telomeres. Thus I explored functions of Isw2 and Ino80 at the rDNA and telomeres. Moreover, I observed whether Isw2 and Ino80 were targeted to these loci and how they affected chromatin structure. I also discuss the implications of remodeling factors in these processes that regulate genome stability and cellular senescence.

In Chapter 4, I discuss my findings on chromatin structure and its role in origin activation. In collaboration with another post-doc in the lab, I specifically investigated how nucleosome occupancy affects origin activities, and subsequently DNA replication. While we

have yet to identify the factor responsible for establishing nucleosome occupancy around origins, we speculate that this factor is likely a chromatin remodeling factor.

In Chapter 5, I discuss the conclusions of the dissertation and the implications of my findings. I propose possible models for Isw2 and Ino80 in checkpoint deactivation, as well as in rDNA and telomere activities. I also discuss possible mechanisms for chromatin remodeling factors in origin activation. Finally, I suggest future plans that will be needed to answer some of the unanswered questions from my studies.

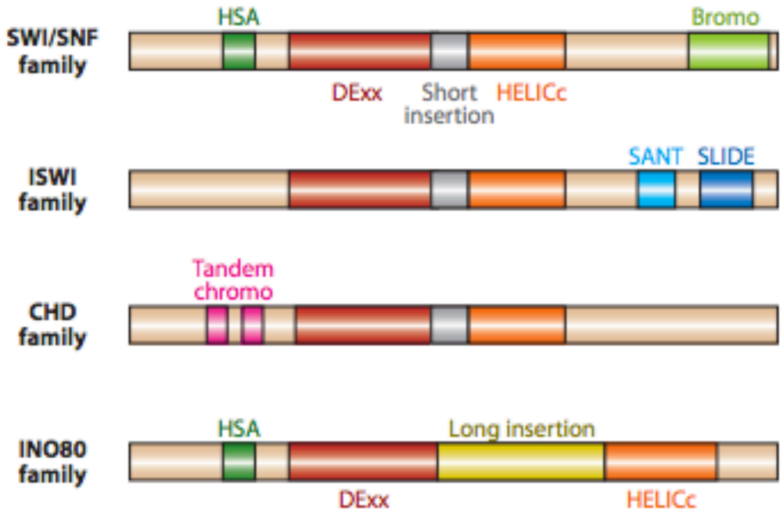

Figure 1.1 ATP-dependent chromatin remodeling families.
The ATPases of the SWI/SNF, ISWI and CHD and INO80 families. The families are separated by the different ATPase domains. Figure from Clapier, C. and Cairns, B. *Annu Rev Biochem* (2009).

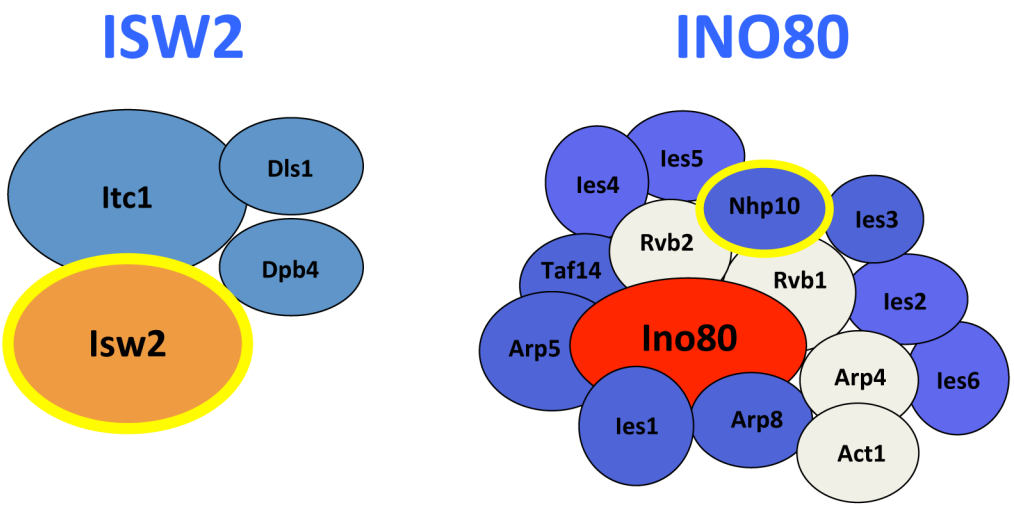

Figure 1.2 *Saccharomyces cerevisiae* Isw2 and Ino80 complexes.
Budding yeast Isw2 complex includes Itc1, Dls1, Dpb4 and Isw2, depicted in orange as the ATPase. Ino80 complex is composed of Rvb1, Rvb2, Apr4, Arp5, Apr8, Act1, Nhp10, Ies1-6, Taf14 and Ino80, which is shown in red as the ATPase. The grey subunits indicate the subunits that exist in other complexes. The blue subunits are known to exist only in Ino80. Isw2 and Nhp10 are highlighted in yellow, which are the subunits of focus in this dissertation.

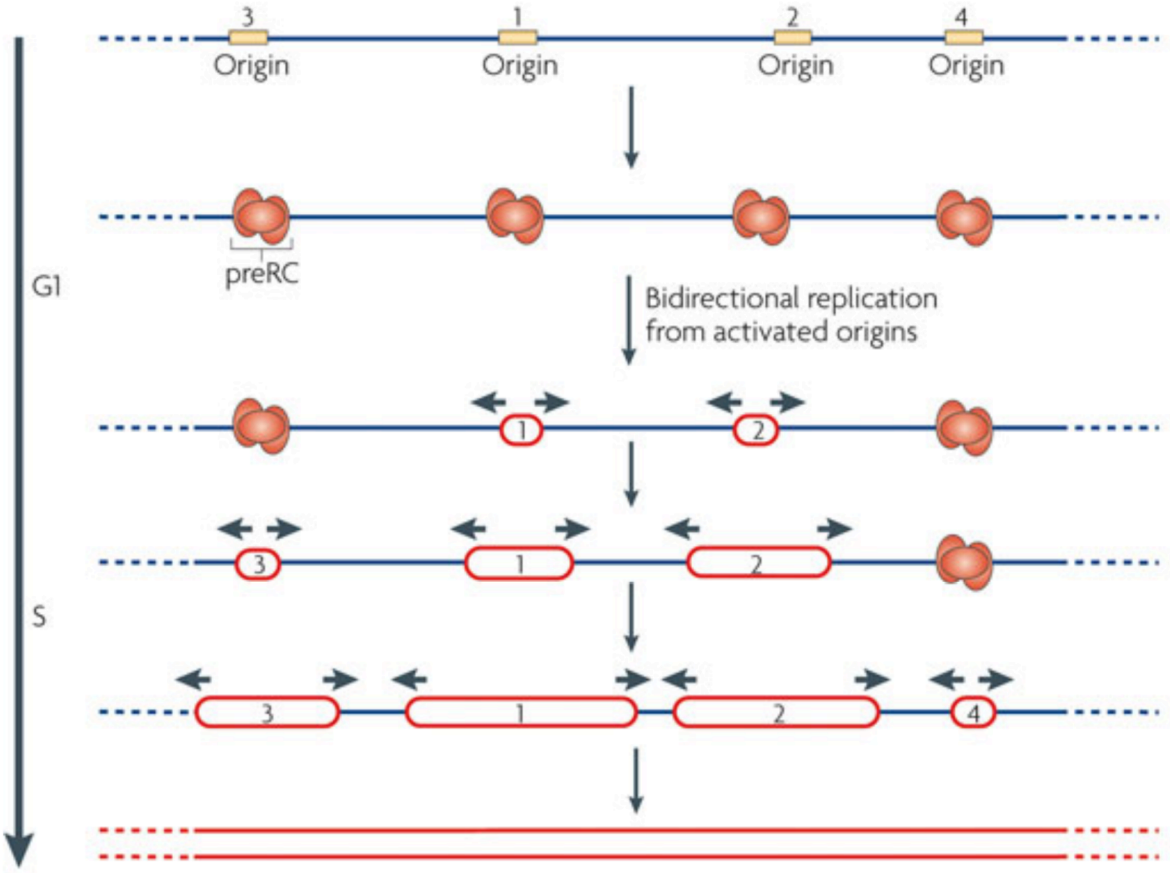

Figure 1.3 Replication origin initiation in a given cell.
The process of origin initiation is depicted from G1 to S phase. Origins have different timing and efficiency patterns. Figure from Mechali, M. *Nat Rev Mol Cell Biol* (2010).

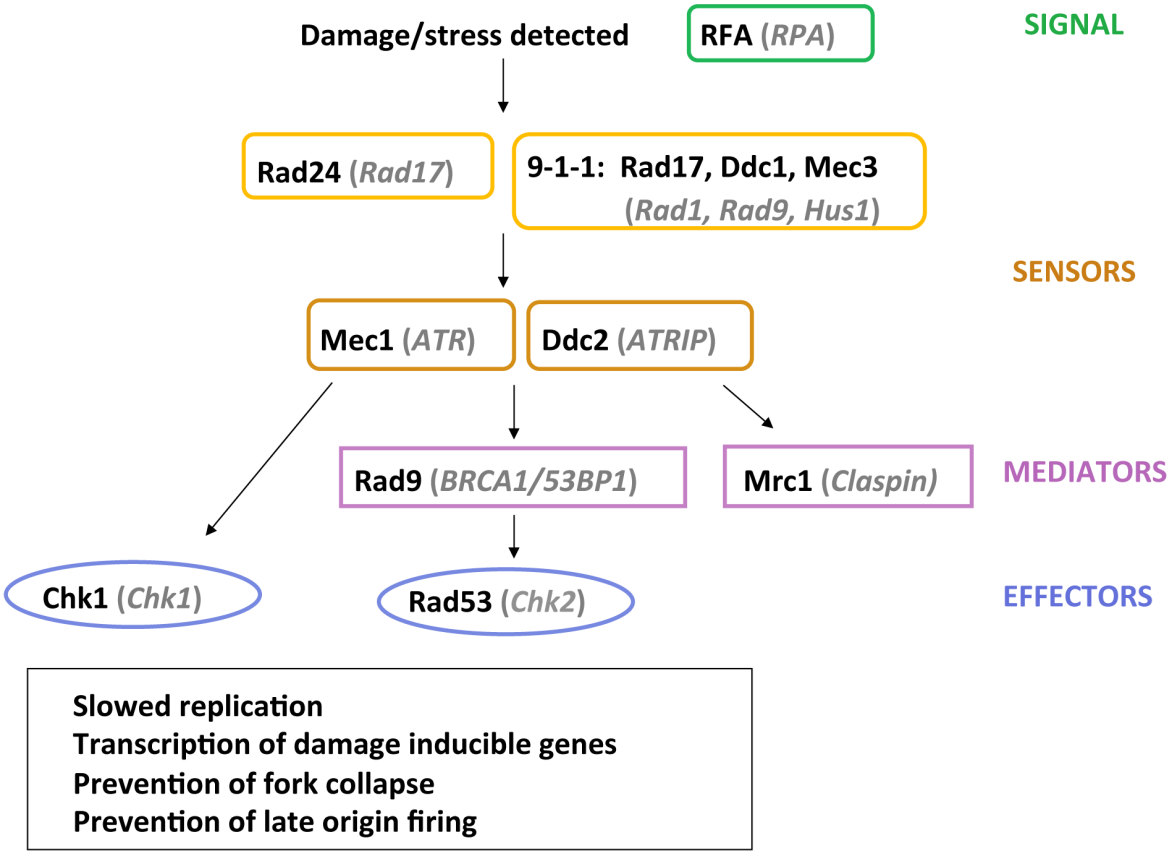

Figure 1.4 The S phase checkpoint pathway.
The S phase checkpoint cascade in budding yeast. The human homologs are shown in grey.

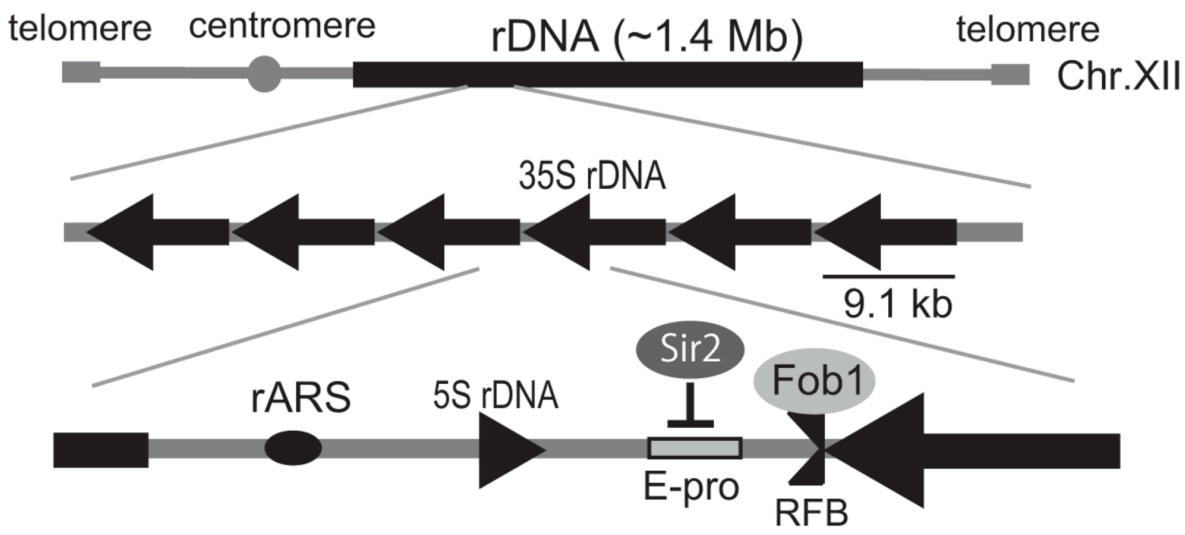

Figure 1.5 The rDNA locus in budding yeast.
The rDNA consists of around 150 repeating units that are clustered together on Chromosome XII in budding yeast. Each unit contains a 35S, 5S, rDNA origin (rARS), and a replication fork block (RFB), which is bound by Fob1. Sir2 is also found at the rDNA and is necessary to silence the E-pro promoter, which gives rise to a noncoding RNA (ncRNA) important for regulating homologous recombination (HR) at the rDNA locus. Figure from Ide, S. et al. *PLoS Genetics* (2013).

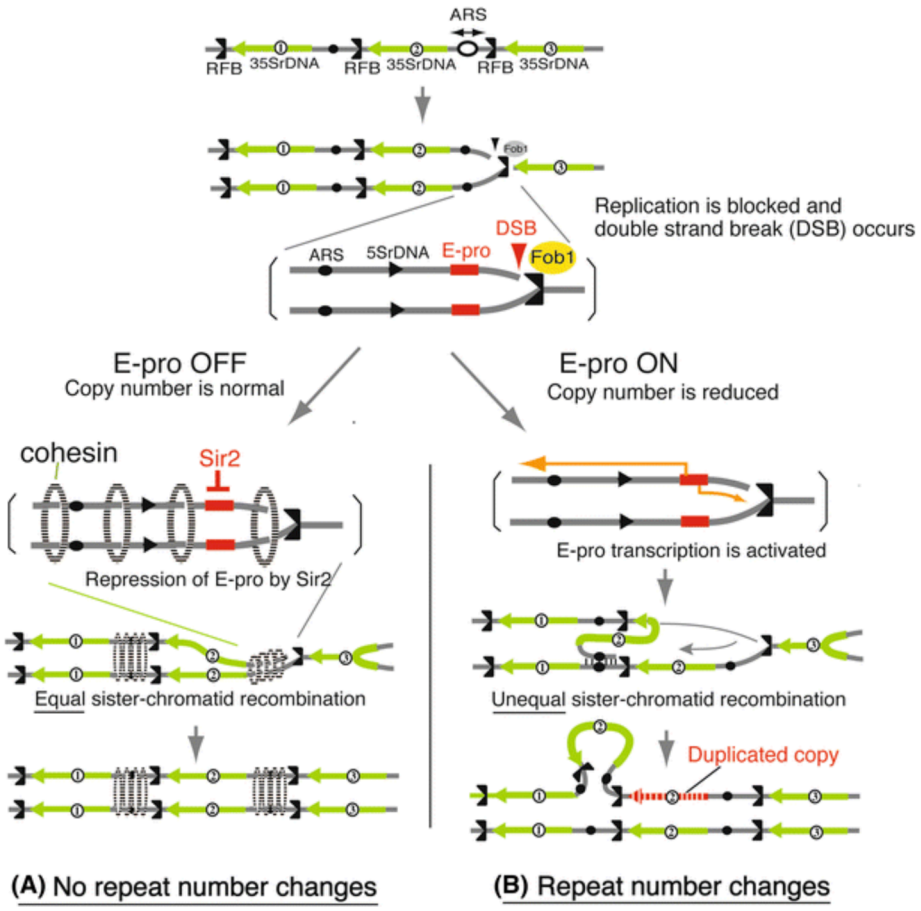

Figure 1.6 Homologous recombination at the rDNA.
During replication, the RFB is bound by Fob1, which results in blocking replication and inducing a double strand break (DSB). The DSB triggers HR to occur. When rDNA copy number is normal, Sir2 is at the rDNA and silences the E-pro promoter. Cohesion allows for sister chromatids to pair and equal sister-chromatid recombination occurs, which does not alter copy number. However, when cells sense that copy number is low, Sir2 is displaced and the E-pro ncRNA is transcribed. E-pro removes cohesion from the rDNA, which results in uneqal sister chromatid recombination and changes in rDNA copy number. Figure from Kobayashi, *T. Proc Jpn Acad Ser B Phys Biol Sci* (2014).

CHAPTER 2

Chromatin remodeling factors Isw2 and Ino80 regulate checkpoint activity and chromatin structure in S phase

Modified from submitted manscript.

Lee, L., Rodriguez, J., and Tsukiyama, T.

Summary

When cells undergo replication stress, proper checkpoint activation and deactivation are critical for genomic stability and cell survival, and therefore must be highly regulated. Although mechanisms of checkpoint activation are well studied, mechanisms of checkpoint deactivation are far less understood. Previously, we reported that chromatin remodeling factors Isw2 and Ino80 attenuate the S phase checkpoint activity, especially during recovery from hydroxyurea in *Saccharomyces cerevisiae* (Au et al., 2011). In this study, we found that Isw2 and Ino80 have a more pronounced role in attenuating checkpoint activity during late S phase in the presence of methyl methanesulfonate (MMS). We therefore screened for checkpoint factors required for Isw2 and Ino80 checkpoint attenuation in the presence of MMS. Here we demonstrate that Isw2 and Ino80 antagonize checkpoint activators and attenuate checkpoint activity in S phase in MMS either through a currently unknown pathway or through RPA. Unexpectedly, we found that Isw2 and Ino80 increase chromatin accessibility around replicating regions in the presence of MMS, through a novel mechanism. Furthermore, through growth assays, we provide additional

evidence that Isw2 and Ino80 partially counteract checkpoint activators specifically in the presence of MMS. Based on these results, we propose that Isw2 and Ino80 attenuate S phase checkpoint activity through a novel mechanism.

Introduction

For proper propagation of cells, DNA must be faithfully copied during replication in S phase. However, during replication, cells are prone to encountering nucleotide depletion or DNA damage, which generates replication stress and induces replication fork stalling. Upon replication stress, cells trigger a mechanism called the S phase checkpoint to allow for proper completion of replication before exit out of S phase. Because this pathway is essential for genomic stability as evidenced by the development of cancer or cell death in checkpoint mutants (Zeman and Cimprich, 2014) and strict conservation in eukaryotic cells, mechanisms of S phase checkpoint activation have been extensively studied (Branzei and Foiani, 2009).

When replication forks stall in budding yeast cells, excess single-stranded DNA (ssDNA) is produced, which is bound by Replication Protein A (RPA). Accumulation of the ssDNA-RPA complex recruits a central kinase Mec1 (ATR in mammalian cells) with its interacting partner Ddc2 (ATRIP), which activates the downstream effector kinases Rad53 (Chk2) and Chk1 (Chk1) to stabilize replication forks, up-regulate damage-inducible genes, and slow S phase progression through the delay of origin firing until DNA is correctly replicated (Friedel et al., 2009; Rouse and Jackson, 2002; Zou and Elledge, 2003). The S phase checkpoint can be activated through two different pathways, the DNA damage checkpoint (DDC) and/or the DNA replication checkpoint (DRC), depending on the type of damage recognized by the cell (Crabbe et al., 2010). In the DDC of budding yeast, the clamp loader RFC^{Rad24} (RFC^{Rad17}) and subsequently the PCNA-

like 9-1-1 clamp, Rad17-Ddc1-Mec3 (Rad9-Hus1-Rad1), are recruited to ssDNA-dsDNA junctions to facilitate activation of the checkpoint along with Dpb11 (TopBP1) and Rad9 (Gilbert et al., 2001; Kondo et al., 2001; Majka et al., 2006; Navadgi-Patil and Burgers, 2008). In the DRC, Tof1 (TIM), Mrc1 (Claspin), and Dna2 are recruited to replication forks to facilitate activation of the checkpoint (Katou et al., 2003; Kumar and Burgers, 2013).

In contrast to S phase checkpoint activation mechanisms, mechanisms that regulate checkpoint deactivation are far less understood. The best-characterized mechanism of checkpoint deactivation is through Rad53 phosphatases Pph3 and Ptc2. Deletion of Pph3 and Ptc2 results in elevated sensitivity to replication inhibitors and complete replication fork arrest (Szyjka et al., 2008). This result demonstrates that proper control of the amplitude and inactivation of the S phase checkpoint are also essential for DNA replication control in the presence of replication stress. It has also been shown that other modes of checkpoint deactivation exist that have yet to be identified, highlighting the need for more studies on checkpoint deactivation mechanisms (Travesa et al., 2008).

We have recently proposed that the highly conserved chromatin remodeling factors Isw2 and Ino80 play roles in S phase checkpoint attenuation (Au et al., 2011). Chromatin remodeling factors use the energy of ATP hydrolysis to alter chromatin structure, and have been implicated in many DNA-dependent processes including transcription, DNA replication, DNA repair, and checkpoint regulation (Morrison and Shen, 2009). Isw2 has been demonstrated to slide nucleosomes *in vivo* (Fazzio and Tsukiyama, 2003). Functionally, Isw2 has been shown to repress transcription of genes by sliding nucleosomes over transcriptional start sites (Goldmark et al., 2000; Whitehouse et al., 2007). Ino80 can replace the histone variant Htz1 within nucleosomes with canonical histone H2A (Papamichos-Chronakis et al., 2011). Ino80 is required

for proper DNA damage response after DNA double strand breaks (Shen et al., 2000; van Attikum et al., 2004), as well as replication stress responses such as maintaining fork stability and promoting recovery of stalled forks (Papamichos-Chronakis and Peterson, 2008; Shimada et al., 2008). However, how this complex performs these functions remains largely unknown.

We previously reported that Isw2 and Nhp10, a subunit of Ino80 complex, function together to attenuate the S phase checkpoint after transient exposure to the DNA replication inhibitor hydroxyurea (HU) (Au et al., 2011). In this study, we show that Isw2 and Nhp10 exhibit a much stronger effect in attenuating checkpoint activity in the presence of the DNA alkylating agent MMS throughout late S phase. Through systematic genetic tests, we show that Isw2 and Nhp10 antagonize checkpoint activators and facilitate checkpoint attenuation in MMS either through a currently unknown pathway or through the single stranded DNA binding protein RPA. In investigating changes in chromatin structure in *isw2 nhp10* during replication stress, we unexpectedly found that Isw2 and Ino80 increase chromatin accessibility around replicating regions, through a mechanism unrelated to their known biochemical activities. Consistent with checkpoint activity control, growth assays in the presence of MMS reveal that Isw2 and Ino80 partially oppose checkpoint activators specifically in the presence of MMS. Based on these results, we propose that Isw2 and Ino80 alter chromatin structure at replicating regions and attenuate the S phase checkpoint through currently unknown mechanism(s).

Results

Isw2 and Ino80 attenuate the checkpoint upon MMS treatment in mid-late S phase

Saccharomyces cerevisiae Isw2p is the ATPase subunit of the Isw2 chromatin remodeling factor involved in gene repression (Goldmark et al., 2000; Whitehouse et al., 2007).

Nhp10p is a subunit of Ino80 that is known to exclusively exist within the Ino80 complex and facilitates interactions with chromatin (Morrison et al., 2004). We previously reported that the *isw2 nhp10* mutant exhibits two phenotypes in the presence of replication inhibitors: 1) slow growth due to a prolonged S phase without an increase in cell death, and 2) over-activation of the checkpoint during S phase (Au et al., 2011; Vincent et al., 2008). Previously, we reported that *isw2 nhp10* elevates and prolongs checkpoint activity during S phase in the presence of replication inhibitors, especially after transient exposure to HU (Au et al., 2011). Our Rad53 *in situ* auto-phosphorylation assay (ISA) revealed rapid loss of the checkpoint activity in wild type (WT) cells, but not in *isw2 nhp10* cells, after transient treatment with HU (Au et al., 2011). However, upon examining Rad53 checkpoint activity by Western blot, we noticed that Rad53 protein could no longer be detected in later time points when samples were prepared according to the protocol used in our previous report (Au et al., 2011) (Figure 2.1A). Importantly, Rad53 protein was lost at much earlier time points in WT than in *isw2 nhp10* (Figure 2.1A). We found that the loss of Rad53 protein could be attributed to an increase in cell volume as the time course went on, which we did not previously adjust for, causing inefficient TCA precipitation of proteins. Due to slower S phase progression in *isw2 nhp10* cells, Rad53 is lost later in *isw2 nhp10* compared to WT (Figure 2.1A). Thus, the apparent checkpoint hyperactivity in *isw2 nhp10* after HU treatment detected by ISA could be attributed to inefficient recovery of Rad53 protein in WT cells (Figure 2.1A and Figure 2.1B). We therefore prepared protein samples adjusting for the differences in cell numbers between WT and *isw2 nhp10* cells (see Materials and Methods for details) and repeated the ISA assay. This procedure revealed that, although Rad53 protein is still slightly more phosphorylated based on Western blotting in *isw2 nhp10*

compared to WT cells after HU treatment (Figure 2.1B), the difference in phosphorylation is not to the same degree as what we previously reported using ISA (Figure 2.1A).

These results prompted us to re-examine checkpoint activity of WT and *isw2 nhp10* cells under various conditions using both Western blotting and Rad53 ISA while accounting for cell volume. These tests revealed that the difference in Rad53 checkpoint activity between WT and *isw2 nhp10* is much more robust upon MMS treatment, as compared to HU treatment (Figure 2.1B and Figure 2.1C). To investigate how Isw2 and Ino80 attenuate checkpoint activity in MMS, we sought to determine when, during S phase, Isw2 and Ino80 perform their roles by defining the kinetics of checkpoint activity. To this end, we performed a time course experiment in which cells were arrested in G1 and released into S phase into rich medium containing MMS and we monitored cell-cycle progression and checkpoint activity by flow cytometry and Rad53 ISA, respectively (Figure 2.1D and Figure 2.2A). Consistent with our previous report (Vincent et al., 2008), *isw2 nhp10* has a delay in S phase progression, which is not a result of incomplete replication as shown by DNA profiles (Figure 2.1D and Figure 2.2B). The delay is associated with stronger and prolonged checkpoint activity in the presence of MMS (Figure 2.1E). This experiment revealed that the biggest difference in checkpoint activity occurs during mid-late S phase (Figure 2.1E). Consistent with the fact that early origin firing is not greatly affected in *isw2 nhp10* (Vincent et al., 2008), these results suggest that Isw2 and Ino80 function after replication has already been initiated. Once checkpoint activity is more strongly triggered in S phase, activation remains elevated through transition into G2/M phase in *isw2 nhp10* (Figure 2.1C). Taken together, our results suggest that Isw2 and Ino80 prevent hyperactivation of the checkpoint activity in mid to late S phase in the presence of MMS to allow for efficient replication progression and transition into G2/M phase.

Isw2 and Ino80 function outside of DNA repair or fork protection pathways

Because checkpoint activity is much more strongly activated in *isw2 nhp10* by MMS than HU, we next tested whether *ISW2* and *NHP10* could function through DNA repair or replication fork protection pathways. We have previously showed, by genetic tests, that *ISW2* and *NHP10* do not function through several genes involved in replication fork protection and DNA repair pathways (Vincent et al., 2008), leading to a conclusion that they do not function through these pathways (Au et al., 2011). However, these tests were not very quantitative and additional genes involved in DNA damage response and replication fork protection were identified after our previous tests (Crabbe et al., 2010; Engels et al., 2011; Gonzalez-Prieto et al., 2013; Hegnauer et al., 2012; Kubota et al., 2013). We therefore performed more comprehensive genetic tests to determine whether *ISW2* and *NHP10* function in these pathways. *ISW2* and *NHP10* were deleted in a given mutant to create a triple mutant, and the single and triple mutant growth phenotypes were compared on gradient plates of rich media with increasing concentrations of MMS (Figure 2.3A). If *ISW2* and *NHP10* function through a pathway in which a DNA damage response or replication fork protection gene plays a central role, the single and the triple mutant should exhibit similar MMS sensitivity. In contrast, if *ISW2* and *NHP10* function independently of a DNA damage response or replication fork protection gene, the phenotypes should be additive and the triple mutant should be more sensitive than the single mutant. *CTF18*, *ELG1* and *SGS1* all influence checkpoint activity (Crabbe et al., 2010; Hegnauer et al., 2012; Kanellis et al., 2003). All of the triple mutants within these mutant backgrounds show additive MMS sensitivity, suggesting that these genes are not required for *ISW2* and *NHP10* function (Figure 2.3A). Other genes involved in fork protection (lavender), replication (grey) and different DNA damage

response pathways (teal) also show that Isw2 and Ino80 act independently of these pathways (Figure 2.3B). DNA polymerase ε (Pol ε) associates with Dpb11 to facilitate DNA replication and the S phase checkpoint (Masumoto et al., 2000), and the Dpb4 subunit of Pol ε also exists in the Isw2 complex (Iida and Araki, 2004; McConnell et al., 2004). Therefore, to test genetic interactions of Pol ε with Isw2 and Nhp10, we used a *pol2-12* mutant, which attenuates S phase checkpoint activity (Li et al., 2008). However, the *pol2-12 isw2 nhp10* mutants exhibited extreme growth defects and readily picked up suppressor mutations (data not shown). While we were not able to measure MMS sensitivity of this mutant, the additive effect even in the absence of replication stress suggests that Isw2 and Nhp10 have functions independent from Pol ε. Together, these results reinforce the conclusion that Isw2 and Ino80 do not function through a single DNA damage response or replication fork protection pathway.

Isw2 and Ino80 antagonize checkpoint activators and attenuate checkpoint activity independently of any single checkpoint factor downstream of RPA

The results above are consistent with our model that Isw2 and Ino80 play a direct role in attenuating the S phase checkpoint activity. Thus to gain insight into the mechanism of checkpoint attenuation by Isw2 and Ino80 we performed systematic genetic tests to screen for checkpoint factors required for Isw2 and Ino80 checkpoint function using the Rad53 ISA assay. Based on a similar reasoning as above, if a checkpoint protein is required for Isw2 and Ino80 to attenuate checkpoint activity, we would expect deletion of *ISW2* and *NHP10* to not increase checkpoint activity in the relevant mutant background. Alternatively, if a given checkpoint protein is not required for Isw2 and Ino80 function, then deletion of *ISW2* and *NHP10* would still increase the deficient checkpoint activity in the checkpoint mutants. Through these analyses, we

aimed to identify the most upstream checkpoint factor by which Isw2 and Ino80 attenuate checkpoint activity. We screened all major checkpoint factors known to be required for robust S phase checkpoint activity (Figure 2.4A). Unless otherwise indicated, the checkpoint mutants tested were null mutations. The S phase checkpoint cascade has two partially overlapping pathways (Figure 2.4A), the DRC and DDC, that both function to activate the S phase checkpoint. Although the DDC, in blue, is primarily activated in the presence of MMS, the DRC, in pink, can redundantly function to partially activate the S phase checkpoint in the absence of DDC factors (Branzei and Foiani, 2009). Checkpoint components in yellow function in both the DDC and DRC, and thus are the most critical for proper activation. Complete deletion of a DRC component resulted in severe MMS sensitivity because they are also involved in DNA replication, in addition to the DRC (Figure 2.3B). Therefore, for checkpoint factors that also have roles in DNA replication, we used *mrc1-aq* (Szyjka et al., 2005)*, dpb11-600* (Pfander and Diffley, 2011)*, and dna2-WY-AA* (Kumar and Burgers, 2013), which are alleles that were previously shown to be specifically deficient in checkpoint activation. Unexpectedly, we found that *isw2 nhp10* mutation partially rescued checkpoint activity in all the checkpoint-deficient mutants tested, for both DRC and DDC mutants, as indicated by a checkpoint activity ratio (see Materials and Methods) significantly higher than one upon *ISW2 and NHP10* deletion (Figure 2.4B). These results suggest that Isw2 and Ino80 antagonize checkpoint activators in affecting S phase checkpoint activity. Mec1 plays central roles in S phase checkpoint activation, and absence of the Mec1 kinase severely abrogates the S phase checkpoint (Branzei and Foiani, 2010). Perhaps most surprisingly, even in *mec1 sml1* cells, where checkpoint activity is mostly depleted, the deletion of *ISW2* and *NHP10* still results in higher checkpoint activity during S phase, indicating that Isw2 and Ino80 function independently of Mec1 (Figure 2.4C and 2.4D).

Residual checkpoint activity in the *mec1 sml1* mutant is due to the partially redundant function of Tel1 (Mantiero et al., 2007). The mode of Tel1 activation in S phase is not well understood, but in the absence of Mec1, Tel1 can activate the checkpoint to a much lesser degree (Zou, 2013). We attempted to examine the effects of Isw2 and Ino80 when the S phase checkpoint is completely abolished by making a *mec1 tel1 sml1 isw2 nhp10* mutant. However, *tel1* deletion alone causes strong synthetic growth defects with *isw2 nhp10* mutation independent of S phase checkpoint function (see Figure 2.8A below). Because of this genetic interaction, the quintuple mutant had extreme growth defects and readily picked up suppressors (data not shown), making phenotype analyses impossible. The *dna2-WY-AA ddc1* mutant, which abolishes Mec1 activation through both the DRC and DDC pathways (Kumar and Burgers, 2013), also displayed higher checkpoint activity upon *ISW2* and *NHP1*0 deletion (Figure 2.4B). This result is consistent with the partial rescue of the checkpoint activity of *mec1* mutant by *isw2 nhp10*. These findings suggest that Isw2 and Ino80 deactivate checkpoint activity independently of both DRC and DDC pathways. We were unable to test RPA due to the lack of an *rpa* mutant allele that solely affects checkpoint activity. Because RPA is essential for viability and has various roles in DNA replication, checkpoint activation, DNA damage response, and recombination, deleting *ISW2* and *NHP10* in *rpa* mutant backgrounds, *rfa1-degron* and the *rfa1-t11* (Lisby et al., 2004; Umezu et al., 1998), causes severe growth defects (data not shown). While the strong synthetic growth defects of *rpa isw2 nhp10* were not unexpected, it made measuring the checkpoint activity in the mutant impossible. Nevertheless, our data demonstrate that no known S phase checkpoint factor downstream of RPA is required for Isw2 and Ino80 to attenuate checkpoint activity. These results collectively suggest that Isw2 and Ino80 function either through currently unidentified checkpoint activator(s) or through RPA, which feeds into multiple independent checkpoint

activation pathways. For *MRC1*, *DPB11* and *DNA2*, we cannot rule out the possibility that the alleles we used did not inactivate their relevant checkpoint activation function.

Isw2 and Ino80 do not affect abundance of checkpoint factors

We envision that Isw2 and Ino80 attenuate checkpoint activity through at least two possible mechanisms. One possibility is that Isw2 and Ino80 may facilitate removal of a checkpoint protein from replication forks. Alternatively, they may down-regulate the activity of a checkpoint protein. We first tested whether Isw2 and Ino80 alter the abundance of chromatin-bound RPA by chromatin fractionation from cells in G1 and S phase with 0.02% MMS (Figure 2.5A), followed by Western blotting. This analysis revealed that relative levels of chromatin-bound RPA were similar in both WT and *isw2 nhp10* in G1 and S phase, indicating that higher checkpoint activity in the mutant is not a result of RPA accumulation on bulk chromatin (Figure 2.5B). Consistent with this result, overexpression of Rad51 and Rad52, proteins involved in displacement of RPA from double strand break sites (Sugiyama and Kowalczykowski, 2002), did not affect MMS sensitivity of *isw2 nhp10* cells (data not shown). In order to test whether Isw2 and Ino80 affect the abundance of other checkpoint proteins bound to chromatin, we performed stable Isotope Labeling by Amino Acids in cell culture (SILAC) mass spectrometry to compare differences in global levels of chromatin bound proteins in WT and *isw2 nhp10*. This method was successfully used to find an abnormal increase in chromatin bound replisome components in Δ*ctf18* (Kubota et al., 2011). This analysis revealed no notable difference in the abundance of the vast majority of chromatin-bound proteins between WT and *isw2 nhp10* in the presence of MMS ($r^2 = 0.92$), including DNA replication, replication checkpoint, and DNA repair proteins (Figure 2.5C). The outliers that increase the most in abundance in *isw2 nhp10* are Sen34p (~20 fold), a

subunit of the tRNA splicing endonuclease, Hsp26p (~20 fold), a small heat shock protein, and Gpx2 (~7 fold), a phospholipid hydroperoxide glutathione peroxidase that is normally induced upon replication stress (Tkach et al., 2012). Outliers that correspond to the most reduced abundance in *isw2 nhp10*, include Sts1p (~1/8-fold), which is involved in protein transport and ribosomal RNA stability, Ptc2p (~1/5-fold), a Rad53 phosphatase, and not surprisingly other Ino80 subunits like Ies1 (~1/4-fold). Other than Ptc2p, no outliers have been previously described to have a function in the S phase checkpoint. No other Rad53 phosphatases were found to have different protein abundance in the SILAC data, and due to the redundancy of the Rad53 phosphatases, Ptc2 alone plays only a minor role in checkpoint recovery after MMS treatment (Szyjka et al., 2008). Furthermore, we have previously shown that Isw2 and Ino80 clearly function independently of the Rad53 phosphatases (Au et al., 2011). Taken together, our results show that Isw2 and Ino80-dependent checkpoint attenuation cannot be explained by changes in the abundance of chromatin bound proteins, at least at the bulk level.

Chromatin accessibility around replication forks is decreased in *isw2 nhp10* in the presence of MMS

Previously, we (Vincent et al., 2008) and others (Papamichos-Chronakis and Peterson, 2008; Shimada et al., 2008) showed that both Isw2 and Ino80 are enriched at stalled replication forks. Therefore we considered the possibility that Isw2 and Ino80 may affect chromatin structure around replication forks, thereby altering checkpoint activity. Ino80 functions in opposition to Swr1 and exchanges nucleosomal H2A.Z/H2B dimers for H2A/H2B dimers (Papamichos-Chronakis et al., 2006; Papamichos-Chronakis et al., 2011). Meanwhile, Isw2 alters chromatin structure by sliding nucleosomes away from coding regions or toward gene promoters

(Fazzio and Tsukiyama, 2003; Yadon et al., 2010). We sought to determine whether these known biochemical activities might be required for S phase functions of Isw2 and Ino80. If the important role of Nhp10 is in Htz1 exchange, we can expect to see partial rescue of the MMS sensitivity of *isw2 nhp10* cells by deleting *HTZ1*. However, *htz1* mutation not only showed no rescue but increased the MMS sensitivity of *isw2 nhp10*, suggesting that Htz1 exchange is not the relevant activity of Isw2 and Nhp10 in MMS (Figure 2.6A). To confirm that the genetic interaction with Htz1 was representative of Ino80 complex rather than Nhp10 alone, we tested another subunit of Ino80, Ies5. The *isw2 ies5 htz1* displayed an even stronger additive growth defect in the presence of MMS (Figure 2.7A). Deleting *swr1* in *isw2 nhp10* also resulted in a stronger growth defect in the presence of MMS compared to either *swr1* or *isw2 nhp10* (Figure 2.7B). These results collectively suggest that Htz1 deposition is not the relevant biochemical activity for growth in MMS.

We also mapped nucleosome positions around replicating regions in WT and *isw2 nhp10* in both G1 and S phase in MMS. For this experiment, harvesting cells in early S phase was necessary to achieve the best possible synchrony of replication forks. We first confirmed that nucleosome positions at known Isw2 targets shift in *isw2 nhp10* as anticipated. However, we did not detect significant changes in nucleosome positioning at replicating regions either in G1 or early S phase in MMS (data not shown). Although this negative result has caveats that replication forks are not completely synchronous within cell population, and that the resolution of our nucleosome mapping may not be high enough, it does not support a model that regulation of nucleosome positions account for the mechanism behind checkpoint regulation by Isw2 and Ino80.

We next tested whether chromatin accessibility might be altered in *isw2 nhp10* around

replication forks. We have recently developed a method to measure chromatin accessibility to micrococcal nuclease (MNase) in a way normalized for nucleosome occupancy, called Normalized Chromatin Accessibility to MNase (NCAM) (Rodriguez et al., 2014; Rodriguez and Tsukiyama, 2013). To measure NCAM, we digest chromatin with MNase, purify monoucleosomal DNA, and hybridize the nucleosomal DNA to high-density tiled microarrays. We then quantify nucleosome signals, which can be affected by both nucleosome occupancy and sensitivity of nucleosomes to MNase at any given site (Rodriguez and Tsukiyama, 2013; Weiner et al., 2010). At the same time, we perform chromatin immuno-precipitation using anti histone H3 antibody to measure nucleosome occupancy. By normalizing the strength of MNase signals to nucleosome occupancy, we can calculate NCAM, which measures the relative amount of MNase digestion per nucleosome (Rodriguez and Tsukiyama, 2013). As expected for both WT and *isw2 nhp10*, overall NCAM increases compared to genome average at regions of active replication, which is depicted near early origins that have fired in most cells at this time point. However, NCAM is significantly reduced in *isw2 nhp10* compared to WT (Figure 2.6B and 2.6C). It is unlikely that the lower NCAM at this time point is caused by inefficient replication initiation in the mutant, as we have shown previously that *isw2 nhp10* do indeed efficiently fire early origins similarly to WT (Vincent et al., 2008). Indeed, WT and *isw2 nhp10* cell exhibit similar levels of DNA synthesis around early-firing origins at this time point (Figure 2.6B). In contrast, non-replicating regions, which are represented by chromatin surrounding late origins that have not fired at this time point, are overall less accessible compared to the rest of the genome as expected (Figure 2.6B and 2.6C). We did detect minor decreases in NCAM in *isw2 nhp10* compared to WT at these non-replicating regions, which is most likely attributed to passive replication occurring at these sites (Figure 2.6C). Taken together, these results suggest

that Isw2 and Ino80 complexes affect NCAM around actively replicating regions. Furthermore, the reduction in NCAM of *isw2 nhp10* is not a result of global reduction in NCAM signal because NCAM is very similar or even slightly increased in the mutant at transcriptional start sites, both in G1 and in S phase in MMS (Figure 2.6D). These results collectively show that Isw2 and Ino80 increase chromatin accessibility specifically around replication forks in the presence of MMS. Although the decrease in NCAM in *isw2 nhp10* at actively replicating regions can be partially attributed to differences in nucleosome occupancy, the changes are mainly driven by a decrease in nucleosome signal (Figure 2.7C and 2.7D). We have confirmed the genome-wide decrease in nucleosome signals around replication forks in *isw2 nhp10* cells by deep sequencing nucleosomal DNA (data not shown).

***isw2 nhp10* partially rescues MMS sensitivity of severe checkpoint deficient mutants**

Because *isw2 nhp10* can stimulate checkpoint activity even in the absence of the known checkpoint activators, we sought to determine whether deletion of *isw2 nhp10* in checkpoint deficient mutants could also rescue cell growth in the presence of MMS. The DRC checkpoint specific mutations yielded WT-like MMS sensitivity, consistent with previous reports that the DRC checkpoint components are dispensable for the checkpoint in MMS (Alcasabas et al., 2001; Crabbe et al., 2010) (Figure 2.8A). Deletion of *ISW2* and *NHP10* in these backgrounds did not cause detectable genetic interactions. On the other hand, the DDC mutants were more sensitive to MMS than WT cells as expected (Hustedt et al., 2013), and unexpectedly, deletion of *ISW2* and *NHP10* did not yield an additive phenotype despite a rescue in checkpoint activation shown earlier (Figure 2.8A and 2.8B). These results showed, for the first time, that checkpoint over-activation and growth in MMS are genetically separable, as checkpoint over-activation does take place without affecting MMS sensitivity in DDC mutants (Figure 2.8A and 2.8B). However, in

the mutants that could not activate either the DRC or the DDC in S phase, *isw2 nhp10* partially rescued MMS sensitivity, which is consistent with the partial rescue in checkpoint activity (Figure 2.8A and 2.8C). We previously failed to detect the rescue of the MMS sensitivity of *mec1* mutant by *isw2 nhp10* mutation (Au et al., 2011), because the rescue is slight and can be detected only after an extended period of time, due to very slow growth of the mutant. While the rescue of the *mec1* phenotype by *isw2 nhp10* was modest, we saw a more prominent rescue in *ddc1 dna2-WY-AA* (Figure 2.8A and 2.8C). Because sensitivity of *mec1* to MMS is a result of both an abrogated checkpoint and replication fork protection defect, it is not surprising that *isw2 nhp10* only slightly rescues MMS sensitivity. In contrast, *isw2 nhp10* dramatically rescues *ddc1 dna2-WY-AA*, which has been shown to be sensitive to replication inhibitors solely due to its defect in activating the checkpoint. To determine whether the rescue was specific to MMS, we also tested genetic interactions on other replication inhibitors, including HU and camptothecin (CPT) (Figure 2.9A and 2.9B). Both CPT and HU exposure yielded either minimal or additive sensitivity when *ISW2* and *NHP10* were deleted in the checkpoint deficient mutants (Figure 2.9A and 2.4B). These results are consistent with the observation that Isw2 and Ino80 only minimally affect checkpoint activity upon HU treatment (Figure 2.1B). While growth sensitivity to MMS does not always directly reflect the changes in checkpoint regulation, a partial rescue of the severe MMS sensitivity of these checkpoint deficient mutants by *isw2 nhp10* is consistent with the notion that Isw2 and Ino80 oppose checkpoint activators in the presence of MMS.

Discussion

We had previously shown that Isw2 and Ino80 are important for attenuation of the S phase checkpoint, especially after transient HU treatment (Au et al., 2011). However, in this

study, we discovered that the previous method of protein preparation resulted in the loss of Rad53 protein. Using a method that can efficiently retain Rad53 protein, we found that Isw2 and Ino80 play much bigger roles in attenuating the S phase checkpoint activity in the presence of MMS than in HU. Consistent with this finding, growth assays also show that Isw2 and Ino80 antagonize checkpoint activators more profoundly in the presence of MMS compared to other replication inhibitors. Although *isw2 nhp10* is sensitive to other replication inhibitors (Vincent et al., 2008), our results suggest that Isw2 and Ino80 may play distinct roles in the presence of different replication inhibitors.

Based on previous findings (Au et al., 2011; Vincent et al., 2008) and this study, we believe that *isw2 nhp10* cells do not have increased replication fork problems or DNA damage response defects, leading to our model that they directly attenuate checkpoint activity. We cannot completely exclude the possibility that there is an increased uncoupling of the replicative helicase to DNA polymerase (Byun et al., 2005) in *isw2 nhp10* cells in MMS, which could be the cause of stronger checkpoint activation and slower S phase progression. However, we do not favor this model. As we have shown previously (Au et al., 2011) and here, the dissociation of replicative helicase and DNA polymerases in the presence of MMS is detrimental in the absence of replication fork protection by S phase checkpoint. For example, we previously reported that deletion of *CTF4* or *TOF1*, which are implicated in coupling MCM helicase with DNA polymerase during replication (Katou et al., 2003; Tanaka et al., 2009), in the *mec1* background lead to strongly additive MMS sensitivity (Au et al., 2011). In contrast, *isw2 nhp10* mutations cause no increase but partially rescue the MMS sensitivity of severe checkpoint mutants such as *mec1* and *ddc1 dna2-WY-AA*.

How do Isw2 and Ino80 complexes function? We do not believe Isw2 and Ino80 function by affecting transcription because there were no significant differences in transcription between MMS-treated WT and *isw2 nhp10* cells (Vincent et al., data not shown). Our checkpoint activity assays suggest that Isw2 and Ino80 attenuate checkpoint activity independently of all major checkpoint activators outside of RPA. Therefore, we propose that they function either through a currently unidentified checkpoint regulator(s) or through RPA. We show here that Isw2 and Ino80 do not affect the amounts of chromatin-bound checkpoint proteins including RPA at the bulk level, but it is possible that they affect the location of checkpoint proteins on chromatin. Isw2 has the ability to translocate on ssDNA (Fischer et al., 2009). Furthermore, chromatin remodeling factors have been shown to interact with non-histone proteins, and Mot1, an ATPase highly related to chromatin remodeling factors, can displace TBP, a non-histone protein, from DNA (Au et al., 2011; Auble et al., 1994; Moreau et al., 2003; Sugimoto et al., 2011). Because Isw2 and Ino80 physically interact with RPA (Au et al., 2011), we initially considered the possibility that they may be able to directly remove RPA from ssDNA template using DNA translocase activity. However, the results of the direct test for this possibility *in vitro* have been negative so far (data not shown). We have also attempted RPA ChIP-chip and ChIP-seq, which have yet to yield any conclusive results due to the difficulty of capturing RPA peaks on replication forks that are moving with imperfect synchrony (data not shown). While it is still possible that Isw2 and Ino80 could be affecting RPA localization at sites of stalled replication, we currently do not have the adequate tools to address this scenario. Although it seems unlikely based on biochemical activities of chromatin remodeling factors, it is also possible that Isw2 and Ino80 directly affect the activity of a checkpoint kinase rather than localization of checkpoint proteins.

Most intriguingly, we demonstrate for the first time that Isw2 and Ino80 promote chromatin accessibility around actively replicating regions. Together with the fact that both Isw2 and Ino80 are enriched at stalled replication forks (Vincent et al., 2008), this observation is consistent with a model that the chromatin remodeling factors function at stalled replication forks. Multiple reports suggested that chromatin remodeling factors can alter chromatin structure to facilitate replication fork progression (Fyodorov et al., 2004; Poot et al., 2004; Shimada et al., 2008; Vincent et al., 2008). Moreover, we previously showed that chromatin accessibility increases around replication forks to promote replication (Rodriguez and Tsukiyama, 2013). Therefore, one possibility is that Isw2 and Ino80 may attenuate checkpoint activity by changing the way checkpoint protein(s) interact with chromatin at stalled forks, which in turn affects replication progression and checkpoint dynamics. Because we found that Isw2 and Ino80 likely do not function through their known biochemical activities, we speculate that Isw2 and Ino80 function in a currently unknown manner. This can be either by modifying how DNA and core histones interact, or by changing histone turnover rate, which may influence other factors to bind and potentially affect checkpoint factor localization or activity. For example, weakening histone-DNA interactions around stalled replication forks could cause an increase in accessibility to recruit checkpoint repressors to facilitate removal of checkpoint factor(s) and promote resumption of DNA replication. Indeed another ATP-dependent chromatin remodeling factor, Fun30 and its mammalian counterpart SMARCAD1, were both found to be recruited to sites of DSBs to promote resection, presumably by removing Rad9 from DSB ends (Chen et al., 2012; Costelloe et al., 2012). Alternatively, checkpoint hyper-activation in the chromatin remodeling factor mutant may be the cause of the observed decrease in chromatin accessibility. Interestingly, we have previously shown that a mutation in *mec1* also results in decreased chromatin

accessibility at replicating regions in S phase in HU (Rodriguez and Tsukiyama, 2013). However, because Mec1 facilitates chromatin accessibility around stalled replication forks (Rodriguez and Tsukiyama, 2013), it is difficult to explain the increased checkpoint activity in *isw2 nhp10* cells as the direct cause of the decreased chromatin accessibility in the mutant. Whether these changes in chromatin structure are related to the phenotypes of *isw2 nhp10* in MMS remains to be explored and will be investigated in future work. Finally, it is also possible that the changes in chromatin accessibility are separable from checkpoint activation.

Our findings suggest that Isw2 and Ino80 likely function through currently unknown mechanisms to regulate both chromatin accessibility and S phase checkpoint attenuation. In the future, understanding the molecular mechanisms underlying Isw2- and Ino80-dependent chromatin accessibility at replication forks will be crucial in defining new biochemical activities of chromatin remodeling factors as well as elucidating a currently unknown mechanism of checkpoint control.

Materials and Methods

Yeast Strains and culture

All yeast strains are MAT**a** and congenic to W303-1a with a correction for the weak *rad5* allele in the original W303 (Thomas and Rothstein, 1989; Zhao et al., 1998). Strains used for SILAC mass spectrometry were in a Δ*lys2* Δ*arg4 CAN1+* background. Strains were constructed using standard gene knockout protocols and genetic crosses (Table 2.1).

Cell synchronization and Flow Cytometry (FACS)

All yeast strains were grown at 30°C to early log phase to a density of OD_{660} = 0.2-0.25, then arrested in G1 phase with a final concentration of 5µg/mL alpha factor. Cells were filtered on a 0.45-mm nitrocellulose membrane, washed twice with YPD, and released into half the volume of pre-warmed YPD containing 0.02% MMS. Cells were harvested at each time point and stored in a final concentration of 66.7% (v/v) ethanol, then processed for flow cytometry as described previously (Vincent et al., 2008).

Rad53 In Situ Autophosphorylation Assay (ISA) and Rad53 Western

Cells were arrested in G1 by alpha factor (5µg/ml) and released into rich media (YPD) containing 0.02% MMS as described in the text. In the initial protein preparation method, about 25 mL of cells were harvested for each time point. However, in the modified method accounting for cell density, 10^8 cells were harvested at each time point. Cells were washed once with water, then with 20% trichloroacetic acid (TCA). Protein samples were prepared as described previously and run on a 8% sodium dodecyl sulfate (SDS)-polyacrylamide gel (Pellicioli et al., 1999). Rad53 autophosphorylation was normalized by autophosphorylation of non-specific proteins within the same sample that served as a loading control. For Rad53 western blotting, goat polyclonal Rad53 (yC-19) antibody (Santa Cruz Biotech, sc-6749) was used. The checkpoint activity was quantified by taking the ratio of Rad53 autophosophorylation signal to the other kinases with ISA signal.

Chromatin Fractionation and SILAC

Strains were grown in either YC media with 15mg/L L-arginine and 30mg/L L-lysine or 15mg/L [$^{13}C_6$]L-arginine and 30mg/L [$^{13}C_6$, $^{15}N_2$]L-lysine. 4 x 10^9 cells were harvested at mid-S

phase in 0.02% MMS and chromatin was prepared as described previously (Kubota et al., 2012). The chromatin pellet was resuspended in 1.5x Tris-glycine SDS sample buffer. A H2B Western blot using the H2B C-term antibody (Active Motif) was used for normalization. RPA polycolonal antibody (Agrisera, AS07 214) was used to detect Rfa1. Equivalent amounts of protein were loaded onto a 8-16% Tris-glycine gel (Thermoscientific), washed in sterile water, stained with GelCode Blue Safe Protein Stain (Thermoscientific), then destained in water. The lane was cut into 10 slices and subjected for mass spectrometry.

LC-MS/MS and Data Analysis

The 10 gel pieces were destained with 50% methanol 5% acetic acid and washed consecutively with water twice and 50% acetonitrile. After rinsing once more with 100 mM ammonium bicarbonate in water, the gel pieces were dehydrated using acetonitrile. The protein was digested over-night at 37°C with 12.5 ng/µL trypsin (Promega Corporation) in 50 mM ammonium bicarbonate. After transferring excess solutions to separate vials, the peptides were first extracted using 0.1% trifluoroacetic acid in water for 30 min, then acetonitrile was added to make 50% acetonitrile, 0.1% trifluoroacetic acid. The pooled extracts were dried in a speed vac and cleaned using ZipTip™ C18 (Millipore Corporation) before the subsequent MS analysis following manufacture's protocols. LC-MS/MS analysis was performed with an Easy-nLC 1000 (Thermo Scientific) coupled to an Orbitrap Elite mass spectrometer (Thermo Scientific). The LC system configured in a vented format (Licklider et al., 2002) consisted of a fused-silica nanospray needle (PicoTip™ emitter, 50 µm ID, New Objective) packed in-house with Magic C18 AQ 100Å reverse-phase media (Michrom Bioresources Inc.) (25 cm), and a trap (IntegraFrit™ Capillary, 100 µm ID, New Objective) containing Magic C18 AQ 200Å (2 cm).

The peptide sample was diluted in 10 µL of 2% acetonitrile and 0.1% formic acid in water and 8 µL was loaded onto the column and separated using a two-mobile-phase system consisting of 0.1% formic acid in water (A) and 0.1% acetic acid in acetonitrile (B). A 90-minute gradient from 7% to 35% acetonitrile in 0.1% formic acid at a flow rate of 400 nL/minute was used for chromatographic separations. The mass spectrometer was operated in a data-dependent MS/MS mode over the m/z range of 400-1800. The mass resolution was set at 120,000. For each cycle, the 15 most abundant ions from the scan were selected for MS/MS analysis using 35% normalized collision energy. Selected ions were dynamically excluded for 30 seconds. Data analysis was performed using Proteome Discoverer 1.4 (Thermo Scientific). The data were searched against *Saccharomyces cerevisiae* strain S288C protein sequences that were updated on February 3, 2011 from Saccharomyces Genome Database (SGD, http://www.yeastgenome.org/), which included common contaminants. Trypsin was set as the enzyme with maximum missed cleavages set to 2. The precursor ion tolerance was set to 10 ppm, and the fragment ion tolerance was set to 0.6 Da. Variable modifications were set to methionine oxidation (+15.995 Da), 6 x ^{13}C (+6.020 Da) on arginine, and 6 x ^{13}C and 2 x ^{15}N on lysine. Sequest (Eng et al., 1994) was used for search, and search results were run through Percolator (Kall et al., 2007) for scoring. The ratio between heavy and light amino acids was normalized to an average of all histone proteins detected by mass spectrometry.

Genomic DNA Profiles, Microarray Hybridization and Data Analysis

DNA samples were amplified, fragmented and labeled as previously described (Rodriguez and Tsukiyama, 2013). S phase DNA samples were competitively hybridized to G1 DNA for replication profiling to custom tiled arrays, as described previously (Rodriguez and

Tsukiyama, 2013). The data was smoothed using a previously established pseudomedian method (Royce et al., 2007) with a 50-bp moving window. Relative RPA levels were ranked based on increasing amounts of genomic DNA content for both WT and *isw2 nhp10* samples, where the average amounts of RPA were further smoothed with a 100-bp sliding window. The rDNA locus and outliers from either extremely low or saturated DNA signal were left out of the analysis.

NCAM (normalized chromatin accessibility to MNase) assay

Cells were harvested from G1 and at an early time point S phase in 0.02% MMS, where FACS profiles were similar between WT and *isw2 nhp10*. Sample harvest, preparation and analysis were performed as described previously (Rodriguez et al., 2014; Rodriguez and Tsukiyama, 2013). Z-score normalization was performed as described previously (Rodriguez and Tsukiyama, 2013), but based on digestion patterns at the +2 to +6 nucleosomes within ORFs genome-wide rather than transcriptional start sites (TSSs), because promoter regions tend to be targets for Isw2 and Ino80 remodeling (Papamichos-Chronakis et al., 2011; Whitehouse et al., 2007). The NCAM graphs were generated by integrating the signal over 40kb regions surrounding three classes of origins: early high (n=11), early low (n=12), and late (n=37). To determine S phase specific changes, NCAM from G1 was subtracted from S phase. NCAM was averaged over a 40kb region surrounding the origin or 3kb region surrounding TSSs to quantitate relative NCAM signal.

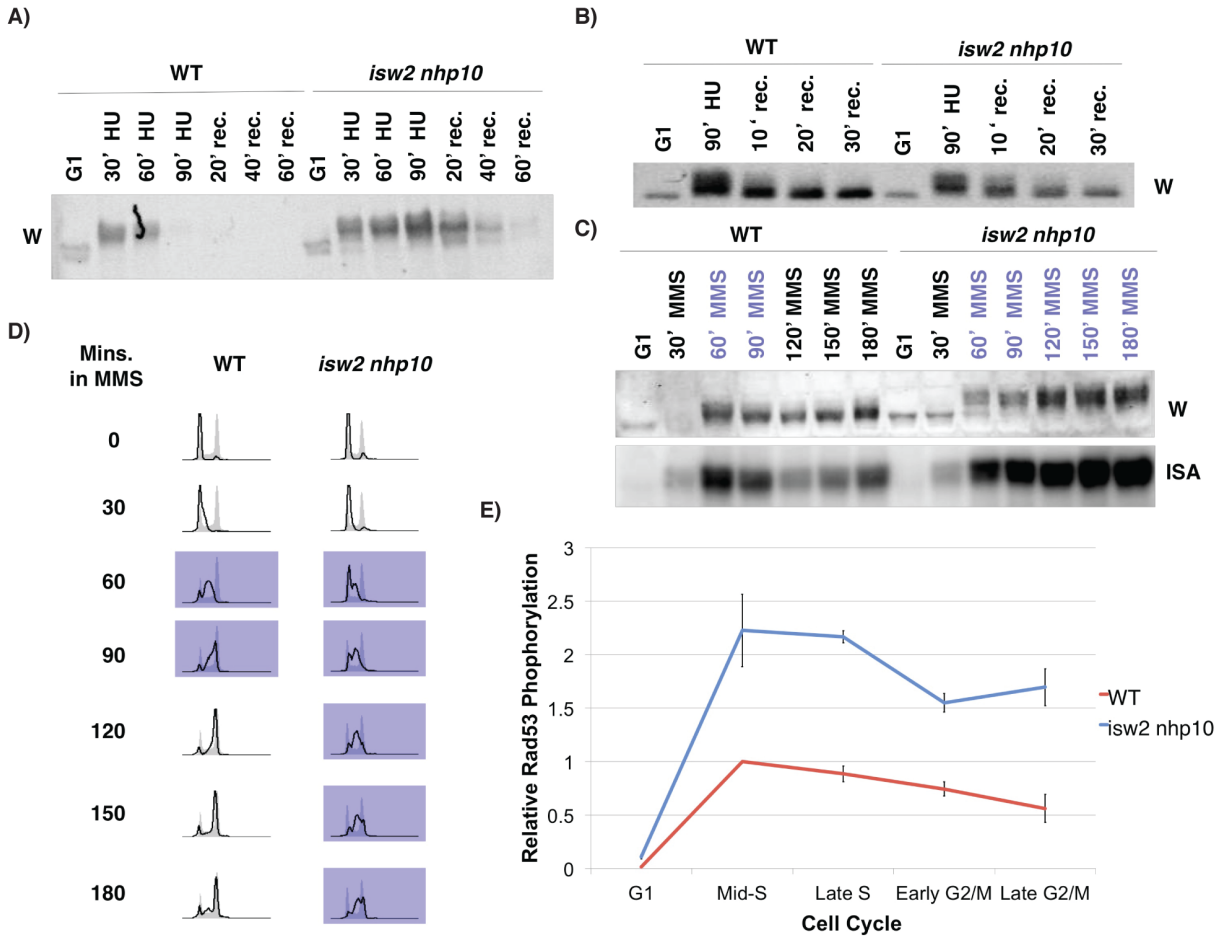

Figure 2.1 *isw2 nhp10* displays stronger checkpoint activity throughout S phase and into G2/M phase in the presence of MMS.
A) Rad53 Western blot of WT and *isw2 nhp10* using the protein preparation methods in our previous report (Au et al. 2011). Cells were arrested in G1 with α-factor for 90 minuets, released into 200mM HU for 90 minutes, then HU was washed out. "rec" denotes recovery time in minutes. B) Rad53 Western blot of protein preparations that used amounts of TCA that had been normalized for differences in cell volumes. C) A Western blot (W) and in situ auto-phosphorylation assay (ISA) of Rad53 of samples taken from indicated time points. Time points indicated in purple represent when cells are in S phase. D) Cell cycle profiles of WT and *isw2 nhp10* cells after release from α-factor into media containing MMS. Asynchronous profiles are shown in grey. FACS profiles shown in purple indicate time points in S phase. E) Quantitation of Rad53 ISA time course. WT checkpoint activity was measured at 60 min for mid-S, 90 min for late S, 120 min for early G2/M, and 150 min for late G2/M. *isw2 nhp10* checkpoint activity was measured at 120 min for mid-S, 180 min for late S, 240 min for early G2/M and 300 min for late G2/M. The error bars denote the standard errors of the mean from two experiments using independently created strains.

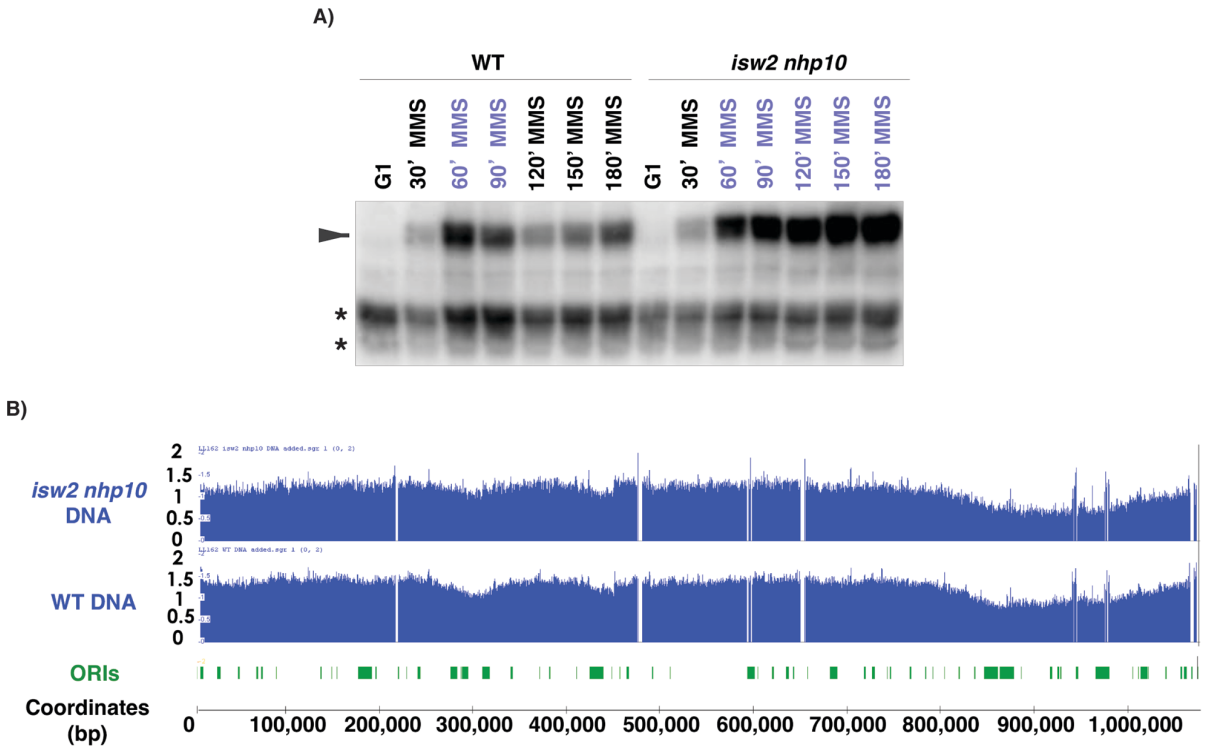

Figure 2.2 Checkpoint hyperactivation is not a result of insufficient replication in *isw2 nhp10*.
(A) The Rad53 ISA shown in Figure 1C with nonspecific bands. WT and *isw2 nhp10* were arrested in G1 and released into S phase in the presence of 0.02% MMS. Phosphorylation of Rad53 is depicted by the arrow and phosphorylation of two nonspecific bands are indicated by the asterisks. The nonspecific bands were used as loading controls to normalize and quantitate Rad53 phosphorylation. The times in purple denote times in S phase. (B) A snap shot of DNA profiles from Chromosome XII for WT (bottom) and *isw2 nhp10* (top) in S phase as shown in blue. The DNA profiles represent S phase DNA that was competitively hybridized against G1 DNA. Cells with similar flow cytometry profiles were taken at a late time point in S phase, 90 min. in WT cells and 150 min. in *isw2 nhp10* cells, but at this time point the checkpoint was more highly activated in *isw2 nhp10* as shown in A. The green boxes indicate origins of replication (ORIs) and in black depicts the chromosomal coordinates.

A)

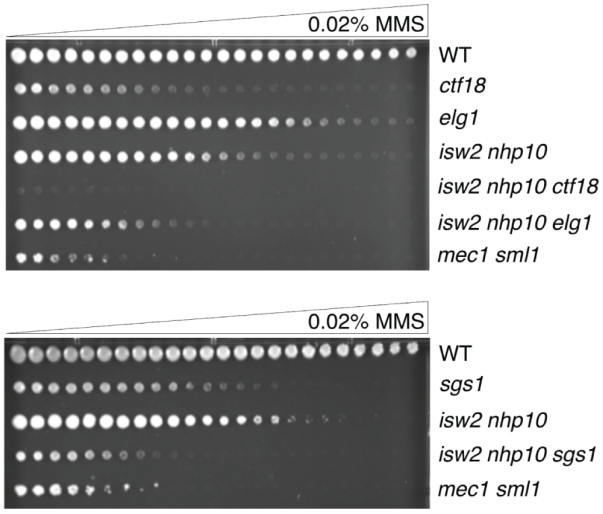

B)

Strain Background	—	*isw2 nhp10*
WT	1	3
exo1	2	4
sgs1	4	5
rad50	5	6
slx4	4	5
rad51	4	5
rad52	5	6
yku70	2	4
elg1	2	4
dpb11-1	3	6
orc2-1	3	4
mrc1	2	4
tof1	2	5
ctf18	4	6

Figure 2.3 Isw2 and Ino80 function is independent of DNA damage response or fork protection pathways.
A) Representative results of the spot tests on 0.02% MMS gradient plates performed as previously described (Au et al. 2011). The top panel shows that deletion of replication components such as *ELG1* or *CTF18* results in additive MMS sensitivity with *isw2 nhp10*. The bottom panel shows deletion of a DNA resection factor *SGS1* is additive with *isw2 nhp10* as well. *mec1 sml1* serves as a control to determine the severity of sensitivity on MMS. B) A summary of the spot test results with genes involved in DNA repair and replication fork protection. MMS sensitivity is ranked on a scale of 1-6, with 1 being the least sensitive (WT level) and 6 being the most sensitive. Repair genes are shown in teal, replication fork protection genes are shown in lavender, and other genes involved in replication are shown in grey.

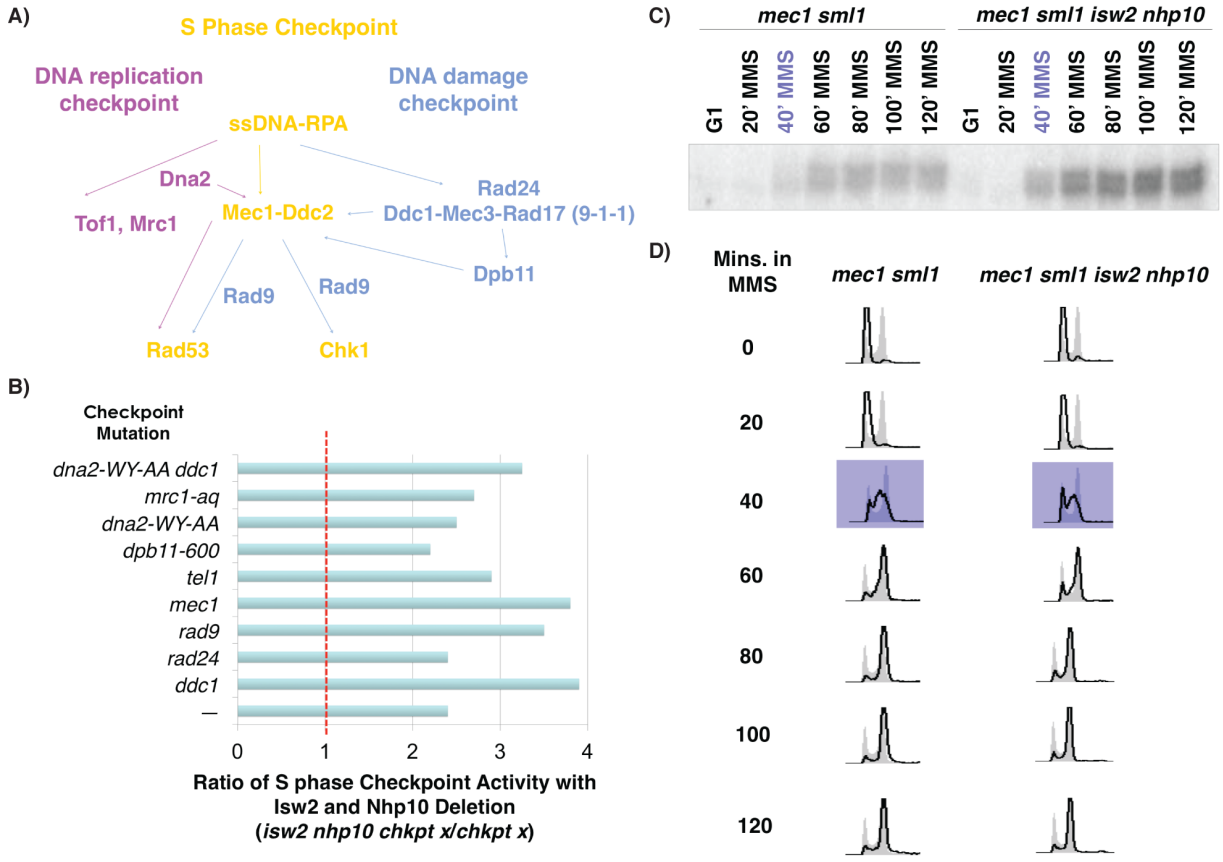

Figure 2.4 Isw2 and Ino80 function are independent of any single checkpoint factor downstream of RPA.
A) A schematic drawing of S phase checkpoint pathway, which is divided into the DNA replication checkpoint (DRC) in pink, DNA damage checkpoint (DDC) in blue, and factors present in both pathways in yellow. B) A bar graph showing the ratio of S phase checkpoint activity in checkpoint mutants in the absence of *ISW2* and *NHP10* compared to the checkpoint mutant alone. The dashed red line indicates the expected S phase checkpoint ratio if a given checkpoint protein is required for Isw2 and Ino80 function. C) Rad53 ISA of *mec1 sml1* and *mec1 sml1 isw2 nhp10* cells released from G1 into S phase containing 0.02% MMS. Time points in S phase are denoted in purple. D) Corresponding flow cytometry profiles of time points from the ISA with profiles in purple denoting time points in S phase.

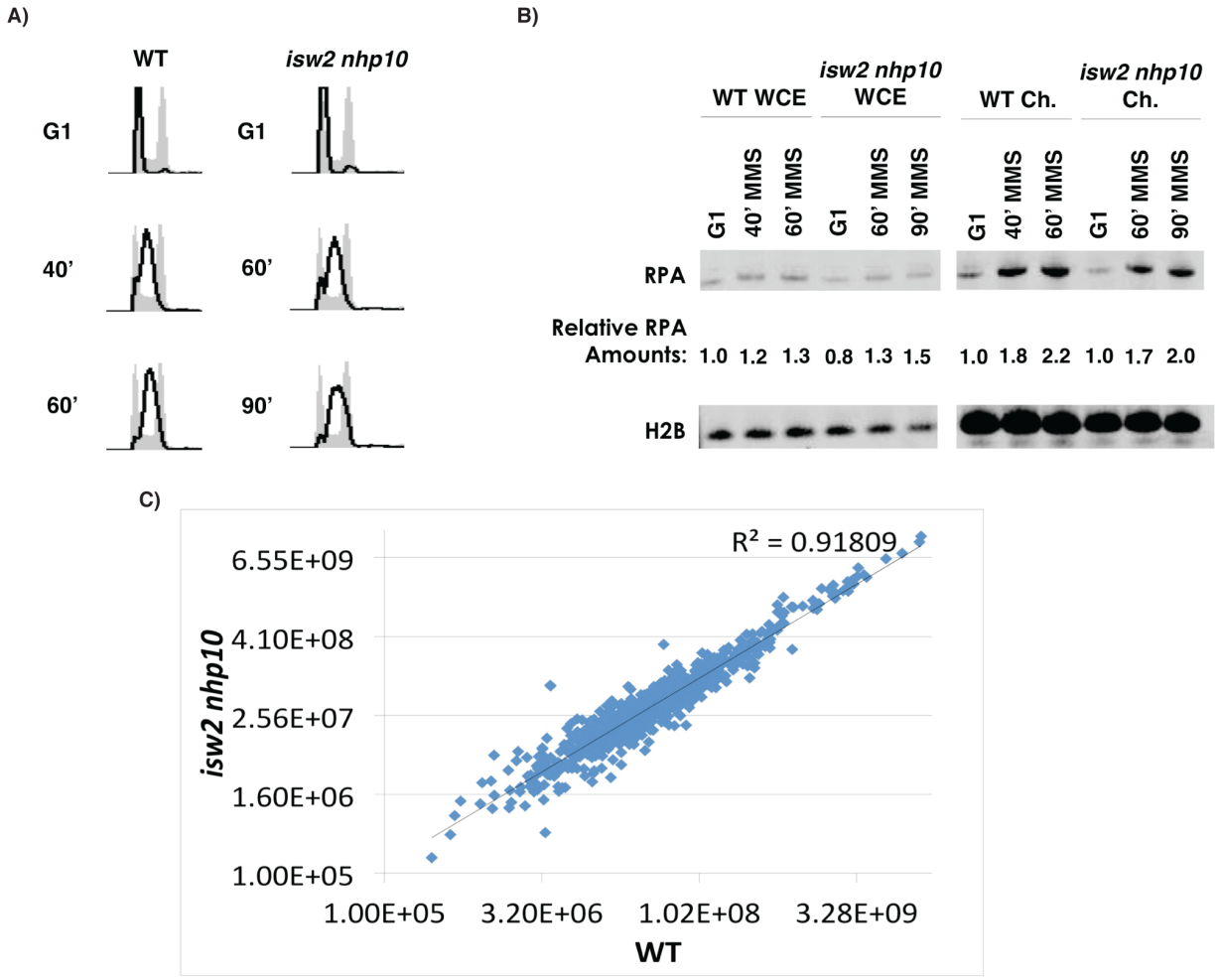

Figure 2.5 Bulk levels of chromatin-bound checkpoint proteins are largely unchanged between WT and *isw2 nhp10*.
A) FACS profiles of samples used for chromatin preparation in B) during G1 and S phase in 0.02% MMS. B) A Western blot of RPA and H2B levels from whole cell extracts and fractionated chromatin of WT and *isw2 nhp10*. Levels of RPA were normalized to H2B and the quantitation is shown. C) A chart graphing the SILAC mass spectrometry data of nuclear proteins from WT vs. *isw2 nhp10* in mid-S phase in 0.02% MMS. Total protein was normalized based on total amount of histones.

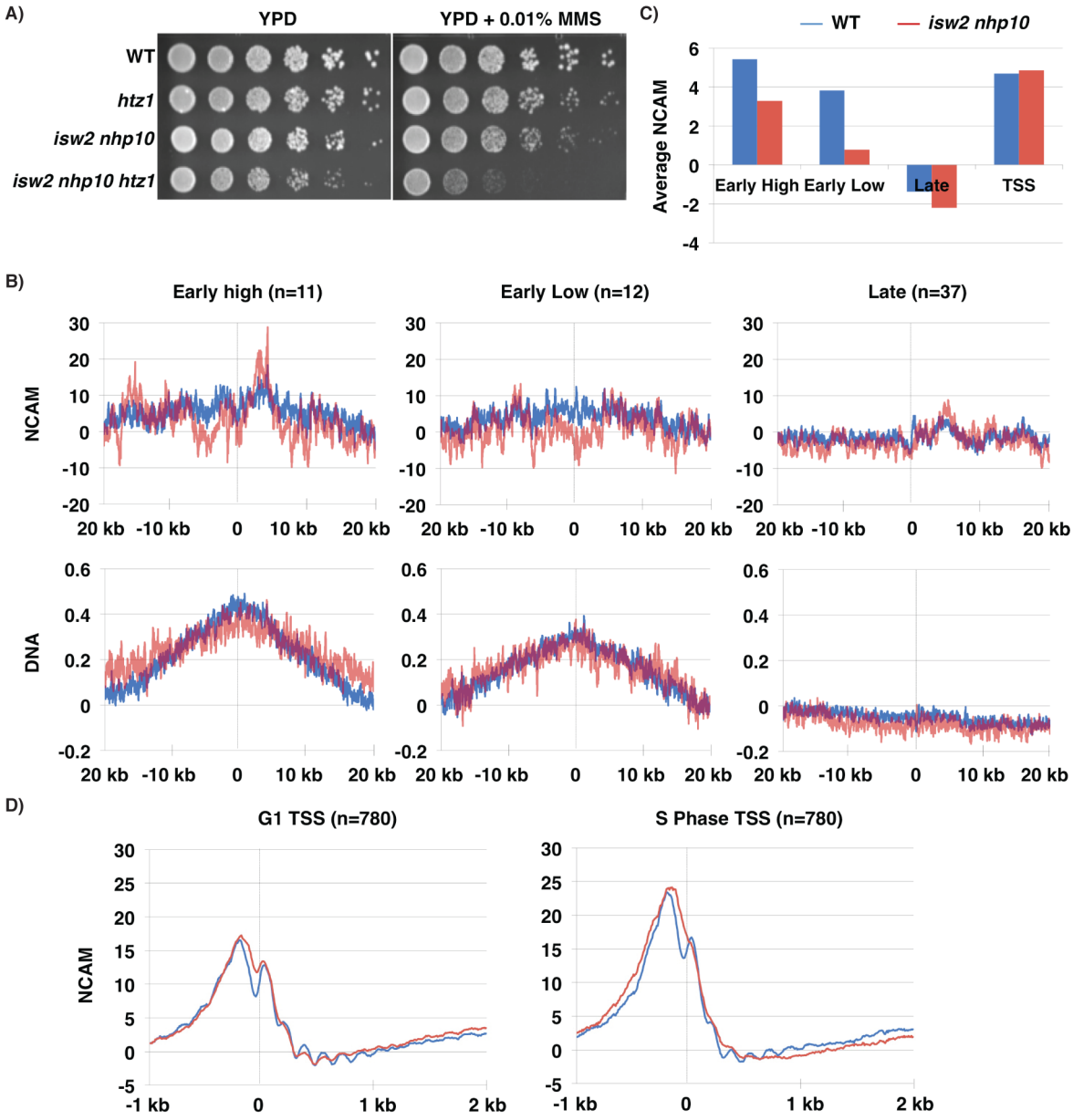

Figure 2.6 Isw2 and Ino80 increase chromatin accessibility at replicating regions.
A) Spot assay of *htz1* and *htz1 isw2 nhp10* grown at 30°C as previously described (AU et al. 2011) on YPD and YPD with 0.01% MMS. B) Graphs represent NCAM and DNA profiles over a 40kb window from three classes of origins on chromosomes III, VI and XII: early, high-efficiency (n=11), early, low-efficiency (n=12) and late (n=37). The dashed lined indicates the origin midpoint. C) Measurement of NCAM around replication origins in WT and *isw2 nhp10*. WT is depicted in blue, while *isw2 nhp10* is in red. NCAM has been Z-score normalized by the +2 to +6 ORF nucleosomes. To visualize S phase specific changes, S phase NCAM was subtracted from G1 NCAM. The bar graph quantitates the average S phase specific differences in NCAM from 40kb around origins in C and 3kb around transcriptional start sites (TSSs) in D. D) NCAM signal from all TSSs (n=780) at G1 and S phase in MMS in a 3kb window. The dashed line indicates the TSS midpoint.

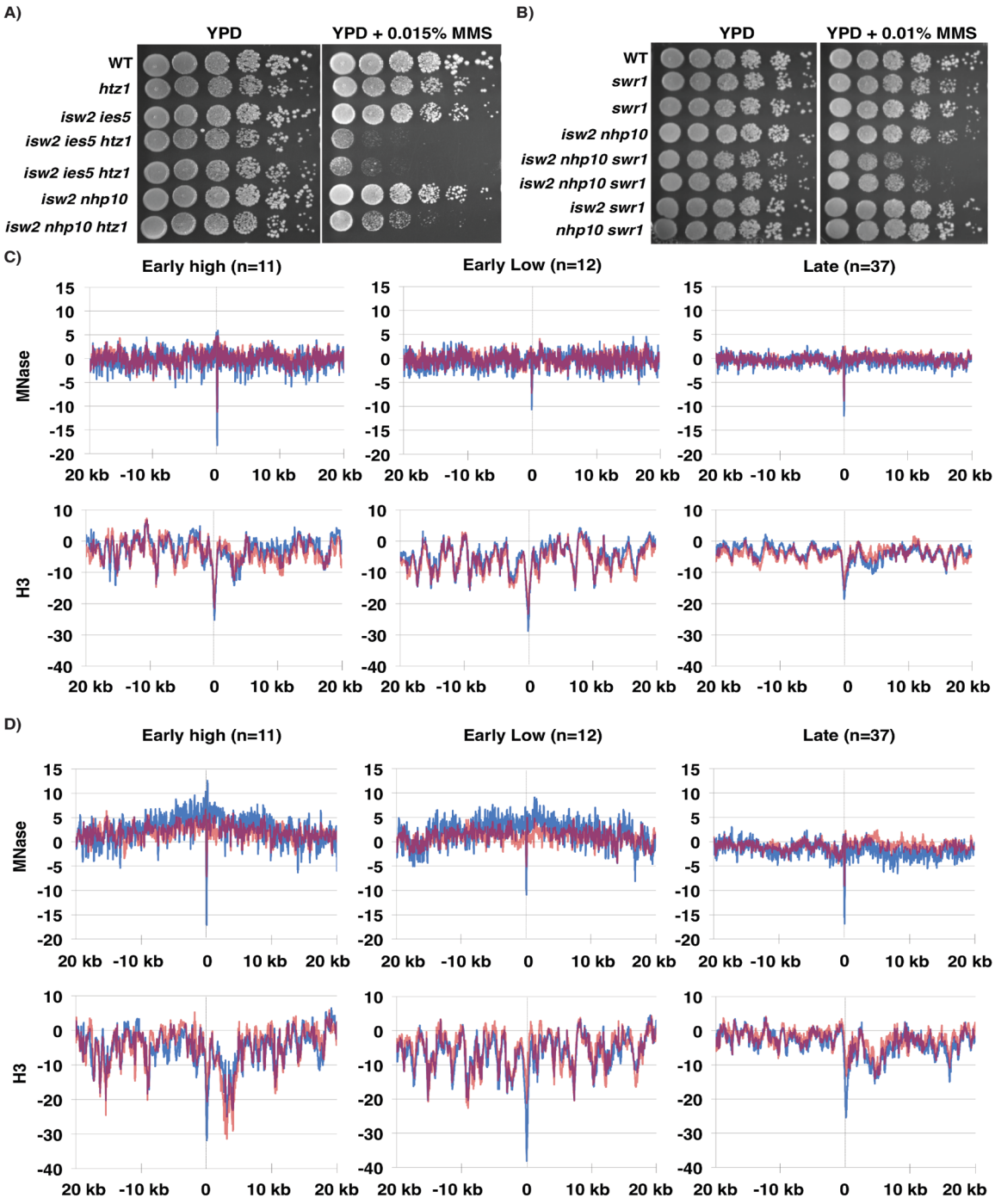

Figure 2.7 Isw2 and Ino80 function in S phase using novel mechanisms.
A) A spot assay of *htz1* and *htz1 isw2 ies5* on YPD and YPD with 0.015% MMS. B) Spot assay of *swr1* and *isw2 nhp10 swr1* on YPD and YPD with 0.01% MMS. C) Graphs represent Z-score normalized MNase and H3 ChIP profiles from cells in G1 over a 40kb window from 3 classes of origins on chromsomes III, VI and XII: early high (n=11), early low (n=12) and late (n=37). WT is in shown in blue and *isw2 nhp10* is shown in red, with the dashed line indicating the origin midpoint. D) Z-score normalized MNase and H3 ChIP profiles from cells in early S phase.

A)

= DRC = DDC = DRC + DDC

Strain Background	MMS sensitivity	
	—	*isw2 nhp10*
WT	1	3
mrc1	2	5
mrc1-AQ	1	3
tof1	2	5
dna2-WY-AA	1	3
ddc1	3	3
dpb11-600	1	3
ddc1 dpb11-600	3	3
rad17	3	3
rad24	3	3
rad9	1	3
ddc1 dna2-WY-AA	5	4
rad9 mrc1-AQ	5	4
mec1 sml1	5	4
tel1	1	4
chk1	1	3
rad53-21	3	5

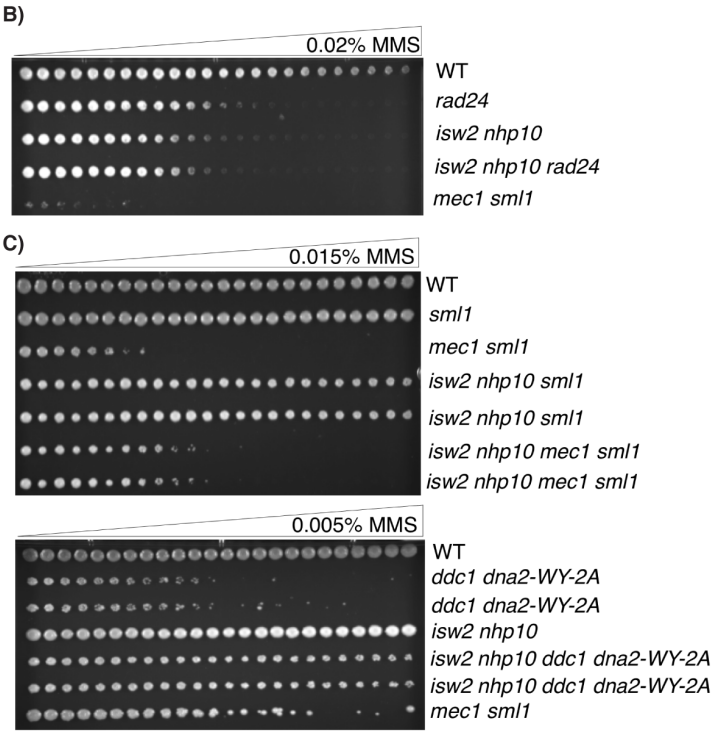

Figure 2.8 Isw2 and Nhp10 antagonize checkpoint activators.
A) A summary of the spot test results with checkpoint proteins. MMS sensitivity is ranked on a scale of 1-6, with 1 being the least sensitive (WT level) and 6 being the most sensitive. Mutated genes are grouped into colored boxes with pink representing the DRC genes, blue representing the DDC genes and yellow present- ing components of both the DRC and DDC. Results are color-coded with blue indicating additive sensitivity, red indicating similar sensitivity and green indicating a partial rescue in sensitivity with the deletion of *ISW2* and *NHP10*. The mutations in black did not show detectable MMS sensitivity as single mutants and exhibited no genetic interactions with *isw2 nhp10*. B) The gradient plate shows the lack of genetic interactions between *ISW2*, *NHP10* and *RAD24*. C) Both gradient plates show a partial rescue of varying degrees to MMS sensitivity of either *mec1 sml1* (top panel) mutant or *ddc1 dna2-WY-2A* (bottom panel) by *isw2 nhp10* mutation.

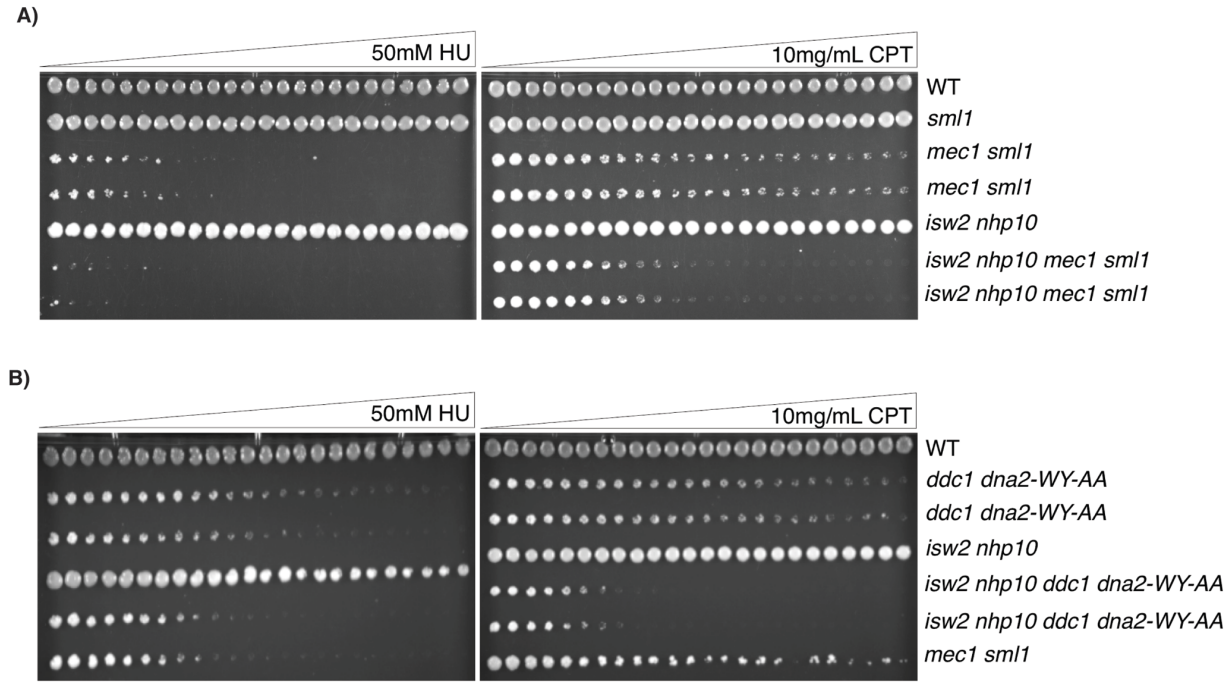

Figure 2.9 Checkpoint deficient mutants show additive MMS sensitivity with *isw2 nhp10*. A) Gradient plates comparing *mec1 sml1* and *mec1 sml1 isw2 nhp10* with increasing amounts of 10mg/mL CPT and 5mM HU. B) Gradient plates comparing *ddc1 dna2-WY-AA* and *ddc1 dna2-WY-AA isw2 nhp10* with increasing amounts of 10mg/mL CPT and 50mM HU.

Table 2.1 Chapter 2 yeast strains

Strain	Genotype	Source
W1588-4c	*MAT***a** *ade2-1 can1-100 his3-11,15 leu2-3,112 trp1-1 ura3-1 RAD5+*	(Thomas and Rothstein, 1989; Zhao et al., 1998)
YTT3777	*MAT***a** *Δisw2::NatMX Δnhp10::Hyg*	(Au et al., 2011)
YTT4960	*MAT***a** *Pol1-3FLAG-KanMX*	(Rodriguez and Tsukiyama, 2013)
YTT5031	*MAT***a** *Pol1-3FLAG-KanMX Δisw2::NatMX Δnhp10::Hyg*	This study
YTT5787	*MAT***a** *Δexo1::KanMX*	This study
YTT5805	*MAT***a** *Δexo1::KanMX Δisw2::NatMX Δnhp10::Hyg*	This study
YTT5822	*MAT***a** *Δsgs1::KanMX*	This study
YTT5852	*MAT***a** *Δsgs1::KanMX Δisw2::NatMX Δnhp10::Hyg*	This study
YTT2616	*MAT***a** *Δrad50::KanMX*	(Vincent et al., 2008)
YTT2653	*MAT***a** *Δrad50::KanMX Δisw2::NatMX Δnhp10::Hyg*	(Vincent et al., 2008)
YTT5969	*MAT***a** *Δslx4::KanMX*	This study
YTT5931	*MAT***a** *Δslx4::KanMX Δisw2::NatMX Δnhp10::Hyg*	This study
YTT5277	*MAT***a** *Δelg1::KanMX*	This study
YTT5279	*MAT***a** *Δelg1::KanMX Δisw2::NatMX Δnhp10::Hyg*	This study
YTT3203	*MAT***a** *Δmrc1::KanMX*	(Vincent et al., 2008)
YTT3224	*MAT***a** *Δmrc1::KanMX Δisw2::NatMX Δnhp10::Hyg*	(Vincent et al., 2008)
Ssy072	*MAT***a** *Δmrc1::HIS5 pRS405-mrc1aq::LEU2*	(Szyjka et al., 2005)
YTT5860	*MAT***a** *Δmrc1::HIS5 pRS405-mrc1aq::LEU2 Δisw2::NatMX Δnhp10::Hyg*	This study
YTT5952	*MAT***a** *Δrad9::KanMX Δmrc1::HIS5 pRS405-mrc1aq::LEU2*	This study
YTT5956	*MAT***a** *Δrad9::KanMX Δmrc1::HIS5 pRS405-mrc1aq::LEU2 Δisw2::NatMX Δnhp10::Hyg*	This study
YTT3394	*MAT***a** *Δtof1::KanMX*	(Vincent et al., 2008)
YTT3409	*MAT***a** *Δtof1::KanMX Δisw2::NatMX Δnhp10::Hyg*	(Vincent et al., 2008)
YTT5986	*MAT***a** *dna2-WY-AA*	Modified (Kumar and Burgers, 2013)
YTT5990	*MAT***a** *dna2-WY-AA Δddc1::KanMX*	This study
YTT5994	*MAT***a** *dna2-WY-AA Δisw2::NatMX Δnhp10::Hyg*	This study
YTT5996	*MAT***a** *dna2-WY-AA Δddc1::KanMX Δisw2::NatMX Δnhp10::Hyg*	This study
YTT3759	*MAT***a** *Δctf18::KanMX*	This study

YTT5275	*MAT***a** *Δctf18::KanMX Δisw2::NatMX Δnhp10::Hyg*	This study
YTT2883	*MAT***a** *Δddc1::KanMX*	(Vincent et al., 2008)
YTT2904	*MAT***a** *Δddc1::KanMX Δisw2::NatMX Δnhp10::Hyg*	(Vincent et al., 2008)
YBP82	*MAT***a** *dpb11-600::Hyg*	(Pfander and Diffley, 2011)
YTT5831	*MAT***a** *dpb11-600::Hyg Δisw2::NatMX Δnhp10::KanMX*	This study
YTT5943	*MAT***a** *dpb11-600::Hyg Δddc1::URA3*	This study
YTT5948	*MAT***a** *dpb11-600::Hyg Δddc1::URA3 Δisw2::NatMX Δnhp10::KanMX*	This study
YTT2953	*MAT***a** *Δrad17::KanMX*	(Vincent et al., 2008)
YTT2958	*MAT***a** *Δrad17::KanMX Δisw2::NatMX Δnhp10::Hyg*	(Vincent et al., 2008)
YTT2938	*MAT***a** *Δrad24::KanMX*	(Vincent et al., 2008)
YTT2943	*MAT***a** *Δrad24::KanMX Δisw2::NatMX Δnhp10::Hyg*	(Vincent et al., 2008)
YTT2885	*MAT***a** *Δrad9::KanMX*	(Vincent et al., 2008)
YTT2909	*MAT***a** *Δrad9::KanMX Δisw2::NatMX Δnhp10::Hyg*	(Vincent et al., 2008)
YTT4976	*MAT***a** *Δmec1::KanMX Δsml1::NatMX*	(Au et al., 2011)
YTT4967	*MAT***a** *Δmec1::KanMX Δsml1::NatMX Δisw2::LEU2 Δnhp10::Hyg*	(Au et al., 2011)
YTT4560	*MAT***a** *Δtel1::KanMX*	This study
YTT4584	*MAT***a** *Δtel1::KanMX Δisw2::NatMX Δnhp10::Hyg*	This study
YTT5327	*MAT***a** *Δchk1::KanMX*	This study
YTT5329	*MAT***a** *Δchk1::KanMX Δisw2::NatMX Δnhp10::Hyg*	This study
RDKY2218	*MAT***a** *rfa1-t11*	(Umezu et al., 1998)
YTT6113	*MAT***a** *rfa1-t11 Δisw2::NatMX Δnhp10::Hyg*	This study
YTT5293	*MAT***a** *ADE2 URA3::CUP1-Ub-Rfa1-8ala-CFP*	Modified (Lisby et al., 2004)
YTT5683	*MAT***a** *ADE2 URA3::CUP1-Ub-Rfa1-8ala-CFP Δisw2::NatMX Δnhp10::Hyg*	This study
YTT3621	*MAT***a** *Δhtz1::KanMX*	This study
YTT3636	*MAT***a** *Δhtz1::KanMX Δisw2::NatMX Δnhp10::Hyg*	This study
YTT6083	*MAT***a** *Δlys2 Δarg4::HIS3 CAN1+ Δisw2::NatMX Δnhp10::Hyg*	This study
YTT6080	*MAT***a** *Δlys2 Δarg4::HIS3 CAN1+*	This study
YTT6184	*MAT***a** *Δrad51::KanMX*	This study
YTT6192	*MAT***a** *Δrad51::KanMX Δisw2::NatMX Δnhp10::Hyg*	This study

YTT6188	*MAT***a** *Δrad52::KanMX*	This study
YTT6196	*MAT***a** *Δrad52::KanMX Δisw2::NatMX Δnhp10::Hyg*	This study
YTT5323	*MAT***a** *dpb11-1*	(Masumoto et al., 2000)
YTT5325	*MAT***a** *dpb11-1 Δisw2::NatMX Δnhp10::Hyg*	This study
YTT6277	*MAT***a** *yku70::KanMX*	This study
YTT6282	*MAT***a** *yku70::KanMX Δisw2::NatMX Δnhp10::Hyg*	This study
YTT6115	*MAT***a** *rad52-21*	(Miles et al., 2013)
YTT6117	*MAT***a** *rad52-21 Δisw2::NatMX Δnhp10::Hyg*	This study
YTT6355	*MAT***a** *orc2-1*	This study
YTT6357	*MAT***a** *orc2-1 Δisw2::NatMX Δnhp10::KanMX*	This study
YTT2612	*MAT***a** *Δswr1::Hyg*	This study
YTT6363	*MAT***a** *Δswr1::Hyg Δnhp10::KanMX*	This study
YTT6365	*MAT***a** *Δswr1::Hyg Δisw2::NatMX*	This study
YTT6367	*MAT***a** *Δswr1::Hyg Δisw2::NatMX Δnhp10::KanMX*	This study
YTT3122	*MAT***a** *Δhtz1::Hyg*	This study
YTT2189	*MAT***a** *Δisw2::NatMX Δies5::KanMX*	This study
YTT6371	*MAT***a** *Δisw2::NatMX Δies5::KanMX Δhtz1::Hyg*	This study
06328	*MAT***a** *pol2-12*	(Li et al., 2008)

CHAPTER 3

Functions of chromatin remodeling factors Isw2 and Ino80 at telomeres and ribosomal DNA

Summary

Vast portions of eukaryotic genomes are made up of non-protein coding and highly repetitive DNA, and these elements are integral in maintaining genome stability. Both the ribosomal DNA (rDNA) and telomeres have been shown to have significant roles in cellular senescence and aging. To prevent genome instability, these elements must maintain strict regulation of the cellular processes that occur at these loci. Chromatin structure has been shown to be a key regulator in controlling these cellular processes. Both the rDNA and telomeres have distinct chromatin structures that change during cellular growth, however, it is not well understood which factors are responsible for establishing and maintaining these chromatin structures. Here we show that chromatin remodeling factors Isw2 and Ino80 have roles at the rDNA and telomeres. Isw2 and Ino80 genetically interact with rDNA and telomere maintenance genes and contribute to proper structural integrity and transcription. Interestingly, Isw2 and Ino80 localize and alter chromatin structure at the rDNA, but are absent at telomeres. Despite their absence at telomeres, we found that Isw2 and Ino80 affect the distribution of Sir histone deacetylases, which are targeted to both the rDNA and telomeres to repress transcription. Furthermore, Isw2 and Ino80 interact with Sirs to regulate DNA-dependent processes. Taken

together our results show novel roles for chromatin remodeling factors at these repetitive elements that are important for genome stability.

Introduction

Once perceived as "junk DNA", non-protein coding, highly repetitive DNA has shown to be extremely important in maintaining genome integrity, and thus highly conserved across eukaryotes (Postepska-Igielska and Grummt, 2014). These large repetitive regions make up a vast amount of the genome and are located at telomeres, centromeres and ribosomal DNA (rDNA). Because of their repetitive nature, they tend to be hot spots for homologous recombination (HR) and vulnerable for chromosomal aberrations. Therefore mechanisms to strictly regulate cellular processes at these loci are necessary to prevent genome instability. While structurally telomeres, centromeres and rDNA share similar features, they vary diversely in function (Postepska-Igielska and Grummt, 2014). Recent studies have suggested that both rDNA and telomeres act as "sensors" for aging. Indeed, as cells age, both the rDNA and telomeres become unstable resulting in cell senescence (Kobayashi, 2011).

The rDNA locus gives rise to the ribosomal RNAs (rRNAs), which are required for ribosome biogenesis. Because robust production of ribosomes is required during cell growth, the rDNA is the most transcriptionally active region in the genome, making up about 80% of total RNA in the cell (Warner, 1999). In order to transcribe rRNAs at such high levels, multiple copies of the rDNA unit cluster together in the nucleolus. In *Saccharomyces cerevisiae*, wild type cells have about 150 copies of a 9.1kb rDNA unit, which resides on Chromosome XII (Figure 1.5). Each rDNA unit has a 35S gene, which is transcribed by Pol1 and processed into the 25S, 5.8S and 18S RNAs. Pol III transcribes a separate 5S gene within the unit. The 35S and 5S are separated by a spacer region, which contains a replication fork block (RFB), an origin of

replication (rARS) and a noncoding RNA promoter (E-pro). Interestingly, rDNA copy number can vary in cells. As mentioned, rDNA is highly recombinogenic and is prone to recombinational deletions. Recombination can occur within rDNA repeats of the rDNA locus leading to loss of repeats and formation of extra chromosomal rDNA circles (ERCs). To maintain rDNA copy number, cells have a system to amplify the rDNA (Kobayashi and Ganley, 2005) (Figure 1.6). The mechanism entails Fob1 binding to RFBs and an induction of a double stand break (DSB), which triggers HR at the rDNA (Burkhalter and Sogo, 2004; Kobayashi et al., 2004). In cells with normal rDNA copy number, histone deacetylase Sir2 binds to the E-pro promoter to silence transcription of a noncoding RNA (ncRNA) (Kobayashi et al., 2004). In the absence of the ncRNA, sister chromatids at the rDNA are held together in register by cohesion; if there is recombination between the sisters, there is no change in copy number (Kobayashi and Ganley, 2005). However, when rDNA copy number is low, Sir2 is released from the rDNA and the ncRNA is expressed, resulting in displacement of cohesion, which allows unequal sister chromatid recombination and expansion or reduction of rDNA repeats (Kobayashi and Ganley, 2005). Continued unequal sister chromatid recombination results in rDNA copy number variation, genomic instability, and subsequently cell senescence (Kobayashi, 2014).

Despite the demand for abundant transcription of rRNAs, not all rDNA units behave the same transcriptionally. Studies show that rDNA exists in two structurally distinct chromatin populations (Dammann et al., 1993). About half of the copies are nucleosome free copies and actively transcribed, while the other half are nucleosome dense and transcriptionally inactive (Dammann et al., 1993). What is the biological significance of this phenomenon? A study has shown that in a strain where all rDNA copies are active, cells are more sensitive to DNA damaging agents and genetically unstable (Ide et al., 2010). It was postulated that if the

transcription machinery occupies all the rDNA units, then factors involved in proper recombination repair are unable to access the rDNA, resulting in genomic instability (Ide et al., 2010). Therefore both HR and transcription at the rDNA must be tightly regulated and chromatin structure has a significant role in regulating these processes. As indicated, HDACs like Sirs participate in silencing of unequal sister chromatin recombination (Kobayashi et al., 2004). In mammals, the ATP-dependent chromatin remodeling factor nucleolar remodeling complex (NoRC), a member of the ISWI family of proteins, is a key component for silencing rRNA genes and maintaining rDNA stability (Postepska-Igielska and Grummt, 2014). NoRC slides rDNA promoter nucleosome downstream of the transcription start site (TSS) and recruits other factors involved in heterochromatin formation (Li et al., 2006; Santoro et al., 2002). In yeast remodeling factors Chd1, Isw1 and Isw2 have also been shown to localize to active rDNA units and affect transcription termination of rRNAs (Jones et al., 2007).

Like the rDNA, telomeres are also highly repetitive heterochromatic structures in the genome. Telomeres are defined as the ends of chromosomes, and while all telomeres share some similarities, each telomere can vary in structure and sequence (Wellinger and Zakian, 2012). Telomere maintenance is extremely important for genome stability and cellular senescence. Telomere capping protects DNA ends from degradation and improper fusion events with other chromosomal ends (Wellinger and Zakian, 2012). In addition, telomere length regulates cellular senescence and aging. Studies suggest that aged cells have shorter telomeres, and that lengthening telomeres increase lifespan (Joeng et al., 2004; Lundblad and Szostak, 1989). Telomeres shorten progressively after every replication cycle because the 3’ end of telomeres cannot be replicated, since the last RNA primer cannot be replaced with DNA. To preserve telomere ends, an enzyme called telomerase lengthens telomeres (Greider and Blackburn, 1985).

Furthermore, telomere silencing is necessary for telomere length maintenance, as derepression of genes close to telomeres can also result in telomere shortening (Maicher et al., 2012). Like the rDNA, many of these processes are regulated by chromatin structure. Interestingly, Sir2, which associates with the rDNA, also localizes to telomeres (Moretti et al., 1994; Roy et al., 2004). At telomeres, Sir2, in collaboration with Sir3 and Sir4, form heterochromatin to promote telomeric silencing (Kueng et al., 2013). Similarly, NoRC was found to establish heterochromatin at telomeres in mammals (Postepska-Igielska et al., 2013). In addition, budding yeast chromatin remodeling factors were suggested to have roles at telomeres. Ino80 was suggested to establish Sir boundaries at telomeres (Xue et al., 2015), while SWI/SNF was proposed to evict Sir3 from telomeres (Manning and Peterson, 2014).

Multiple reports highlight the presence of chromatin regulators at the rDNA and telomeres, and having functional roles in the processes that maintain genomic stability at these loci. However, chromatin structure is highly dynamic and complex, and we have only scratched the surface of chromatin regulation at these highly structured elements. The downstream outcomes of changing chromatin structure and their associated mechanisms at the rDNA and telomeres need to be further elucidated to provide insight in the pathways that regulate genome stability and aging. Therefore in this study we sought to further explore the effects of chromatin structure at these repetitive regions and characterize the functional consequences. We have found that chromatin remodeling factors, Isw2 and Ino80 have previously unknown roles at the telomere and rDNA. We show that *ISW2* and *NHP10,* an Ino80 subunit, interact with rDNA and telomere maintenance genes. Moreover, we demonstrate that Isw2 and Ino80 are important for maintaining proper telomere length and rRNA transcription. Surprisingly, while Isw2 and Ino80 only localized to the rDNA and not telomeres, Sir distribution was altered at both of these

regions in *isw2 nhp10*. Finally, we found that Isw2 and Ino80 function with Sirs to regulate rRNA transcription and telomere maintenance.

Results

ISW2 and *NHP10* genetically interact with rDNA and telomere maintenance genes

The eukaryotic genome is comprised of constitutively heterochromatic and repetitive regions, such as the rDNA, telomeres and centromeres that are highly conserved and important for maintaining genomic integrity. Chromatin regulators have been implicated in regulating DNA-dependent processes at these elements. In mammals, ATP-dependent chromatin remodeling factor NoRC, part of the ISWI family of proteins, has been shown to localize to both the rDNA and telomeres to form heterochromatin. However the budding yeast counterpart of NoRC and other chromatin regulators that establish chromatin structure at these regions remain unknown. Previously, we showed that deletion of *ISW2* and *NHP10*, a subunit of Ino80, resulted in sensitivity to replication inhibitors, such as DNA alkylating agent methyl methanesulfonate (MMS) (Vincent et al., 2008). In attempting to discover the pathways that Isw2 and Ino80 participate in, we screened for genes that interacted with *ISW2* and *NHP10* in the presence of MMS. Interestingly, we found that *ISW2* and *NHP10* genetically interacted with many genes known to affect rDNA biology (Figure 3.1A-C). Sir2 is known to silence replication and homologous recombination (HR) at the rDNA, while Fob1, which localizes to the replication fork block (RFB), is known to promote HR. Deletion of *SIR2* rescued the sensitivity of *isw2 nhp10*, indicating that Sir2 functions in opposition to Isw2 and Ino80 to promote growth on MMS (Figure 3.1A). Similarly, overexpression of *FOB1*, using a plasmid with galactose inducible promoter fused to *FOB1* (GAL-FOB1), also rescued *isw2 nhp10* (Figure 3.1B). In

contrast, deletion of FOB1 showed no growth phenotype (data not shown). Histone deacetylase Rpd3 also acts at the rDNA to counter Sir2 and promote rDNA replication (Yoshida et al., 2014). The *isw2 nhp10 rpd3* exhibited stronger growth defects both in the absence and presence of MMS (Figure 3.1C). However because Rpd3 has roles outside of rDNA replication, this genetic interaction may not be due to defects in rDNA pathways. We also tested interactions of *ISW2* and *NHP10* with telomere mutants. Surprisingly, in mutating telomere genes in an *isw2 nhp10* background, we found that *ISW2* and *NHP10* strongly interacted with telomere mutants (Figure 3.1D). Even in the absence of MMS, an additional telomere mutation in *isw2 nhp10* resulted in severe growth sensitivity or cell death (Figure 3.1D). Taken together these results suggest that Isw2 and Ino80 may have roles at the rDNA and telomeres.

Isw2 and Ino80 affect rDNA and telomere structure

Because of the striking genetic interactions with rDNA and telomere genes, we next tested whether Isw2 and Ino80 could affect structural integrity at these regions. Previous studies have observed nucleolus structure by imaging Fob1-GFP tagged cells (Defossez et al., 1999). Microscopy of live cells showed brighter and more discrete Fob1-GFP foci in the *isw2 nhp10* compared to wild type, suggesting that nucleolar structure is more condensed in the mutant (Figure 3.2A). To determine whether changes in nucleolar structure could cause rDNA instability, we performed a Southern blot to test for ERC production. ERCs accumulate over time and are prevalent in aged cells (Sinclair and Guarente, 1997). However mutants that have an unstable rDNA, like *sir2*, accumulate ERCs much earlier (Pasero et al., 2002). In *isw2 nhp10,* there was no indication of early ERC accumulation, suggesting that Isw2 and Ino80 do not contribute to ERC formation (Figure 3.2B). We also examined telomere structure using telomere

length assays. Previously it was shown that Tel1 regulates telomere length and in *tel1* mutants, telomeres are stable but short (Greenwell et al., 1995). Like the rDNA, we found that telomeres also have structural changes, with *isw2 nhp10* displaying shorter telomeres in comparison to wild type (Figure 3.2C). These results suggest that Isw2 and Ino80 are required for proper maintenance of rDNA and telomere structures.

Isw2 and Ino80 affect rDNA but not telomere transcription

Transcriptional regulation at rDNA and telomeres has been shown to affect genome stability (Ide et al., 2010; Maicher et al., 2012). Around half the rDNA copies are transcriptionally silent, and loss of these silent copies result in genome instability (Ide et al., 2010). At telomeres, transcriptional depression can cause telomere shortening and cell senescence (Maicher et al., 2012). To address whether Isw2 and Ino80 have roles in transcriptional regulation at these repetitive regions, we performed RNA-seq analysis in cycling wild type and *isw2 nhp10* cells. Averaging all RNA transcripts from the end of the DNA to 15kb into the centromere shows low levels of overall transcription at telomeres for both WT and *isw2 nhp10* (Figure 3.3A). Furthermore, levels of RNA transcripts do not change in *isw2 nhp10,* indicating that Isw2 and Ino80 do not regulate transcription at telomeres (Figure 3.3A). In contrast, rDNA transcription is significantly reduced in *isw2 nph10* (Figure 3.3B and 3.3C). Equal amounts of total RNA were loaded on a gel and stained with ethidium bromide, which shows that the stable 35S, 5.8S and 18S transcripts are down regulated in *isw2 nhp10* compared to wild type cells (Figure 3.3B). The data suggest that Isw2 and Ino80 could be involved in either rRNA processing or transcription. Thus to directly determine whether Isw2 and Ino80 had roles in transcription, we performed a northern blot probing for the nascent 35S transcript. The

northern showed that transcription of the nascent 35S rRNA is indeed dampened in *isw2 nhp10* (Figure 3.3C). We next determined whether the changes in transcription at the rDNA were an indirect result of the transcriptional changes in *isw2 nhp10*. RNA-seq analysis suggests that overall transcription is very similar between WT and *isw2 nhp10* (Figure 3.3C). The few outliers we found were unrelated as they were mostly RNAs involved in retrotransposition. These results suggest that transcription of rRNAs, but not telomere RNAs, are significantly altered in *isw2 nhp10*.

Isw2 and Ino80 are targeted to the rDNA but not to telomeres

To further validate that Isw2 and Ino80 are functioning directly at the rDNA and telomeres, we performed Isw2 and Nhp10 chromatin immunprecipitation followed by high throughput sequencing (ChIP-seq) to determine whether these factors are targeted to these regions. Sequencing reads were normalized for read count excluding reads from the rDNA locus. In a previous report, wild type Isw2 was shown to be difficult to ChIP because of transient interactions with chromatin, and instead, catalytically inactive Isw2-K215R was established to stabilize interactions and crosslink better (Gelbart et al., 2005). Therefore in this study, Isw2-K215R was used to examine Isw2 targeting. Interestingly, we found that both Isw2 and Nhp10 were enriched at the rDNA in cycling cells (Figure 3.4A). Both factors localized across the 35S gene body. Levels of Nhp10 were reduced around the rDNA origin (rARS) as well as the 5S (Figure 3.4A). However Isw2 was highly enriched at the rARS and 5S (Figure 3.4A). These results suggest that Isw2 and Ino80 directly localize to the rDNA. In contrast, we could not detect enrichment of Isw2 and Nhp10 at any of the telomeres (Figure 3.4B). It is possible that Isw2 and Ino80 are binding to the very ends of the telomeres, a region that is difficult to

sequence due to the highly repetitive DNA nature. Nevertheless, we find that by sequencing there is no evidence for Isw2 and Ino80 being targeted to telomeres.

Chromatin structure at the rDNA locus is altered in *isw2 nhp10*

Chromatin remodeling factors primarily function to alter chromatin structure. Therefore we sought to determine whether Isw2 and Ino80 altered chromatin structure at the rDNA and telomeres. We examined two parameters of chromatin structure: H3 occupancy as measured by H3 ChIP-seq and nucleosome positioning as measured by (micrococcal nuclease) MNase-seq. At the rDNA, there were changes in both nucleosome occupancy and in nucleosome positioning (Figure 3.5A and 3.5B). Consistent with previous findings, on average the rDNA units have low levels of nucleosomes compared to genome average, especially within the promoter and gene bodies of the rRNA genes (Figure 3.5A) (Dammann et al., 1993). In *isw2 nph10* cells, nucleosome occupancy was significantly increased at the rDNA locus, which could be the cause for a more condensed nucleolus in the mutant (Figure 3.2A). Simultaneously, nucleosomes positions are altered specifically shifting towards the promoter regions of the 35S and 5S, and the rARS in *isw2 nhp10* (Figure 3.5B). These results further indicate that Isw2 and Ino80 are important for regulating chromatin structure at the rDNA. In contrast, the results were not as clear for telomeres. While Isw2 and Ino80 did not localize to the telomeres using ChIP-seq, it is still possible that Isw2 and Ino80 could indirectly affect chromatin structure. The data show that Isw2 and Ino80 affect chromatin structure at some telomeres, and not others (Figure 3.5C). In *isw2 nhp10*, some telomeres displayed changes in nucleosome occupancy, whereas at other telomeres did not (Figure 3.5C). However, there was no clear pattern of changes in nucleosome occupancy. On the other hand, nucleosome positions at telomeres did not seem to change much

between WT and *isw2 nhp10* (Figure 3.5C). Meanwhile, chromatin structure is highly similar for the rest of the genome in wild type and *isw2 nhp10* (data not shown). Taken together, these results suggest that Isw2 and Ino80 promote active chromatin structures at the rDNA, whereas their roles in chromatin structure at telomeres still remain undefined.

Isw2 and Ino80 affect Sir localization and function with Sirs

While Isw2 and Ino80 function directly at the rDNA to affect chromatin structure, it is unclear how Isw2 and Ino80 function at telomeres. Normally during DNA replication, only 20% of rARSs fire in a given S phase (Linskens and Huberman, 1988). Previously it was reported that de-repression of rARS firing results in reduced origin firing at other origins in the genome, presumably due to increased competition for limiting initiation factors (Yoshida et al., 2014). This study proposed the idea that the rDNA can act as a sponge to soak up limiting factors (Yoshida et al., 2014). To determine whether the telomere phenotypes were an indirect result of the function of Isw2 and Ino80 at the rDNA, we sought to determine whether Isw2 and Ino80 could affect localization of other factors targeted to both loci. Sir proteins are limiting and known to localize to both the rDNA and telomeres (Kueng et al., 2013). Thus we performed ChIP-seq of Sir proteins in WT and *isw2 nhp10*. First we examined the rDNA locus and found that both Sir2 and Sir3 localized to the rDNA and telomeres, similar to previous findings (Figure 3.6A-D). However in *isw2 nhp10*, we saw a marked reduction in both Sir2 and Sir3 levels at the rDNA (Figure 3.6A and 3.6B). Simultaneously at telomeres we found that both Sir2 and Sir3 levels increased in *isw2 nhp10* (Figure 3.6C and 3.6D). These results suggest that Isw2 and Ino80 regulate Sir localization. Next we sought to determine whether Isw2 and Ino80 functioned through Sirs to regulate rDNA and telomere function. To this end we performed northern blots to

assess nascent rRNA transcription of the 35S rRNA in *sir2* and *sir2 isw2 nhp10* mutants. Interestingly, Sir2 was required for robust rRNA transcription, and transcription of rRNAs by Isw2 and Ino80 was dependent on Sir2 (Figure 3.6E). These results are consistent with the possibility that Isw2 and Nhp10 function through Sirs to regulate rRNA transcription. We also tested whether the change in Sir distribution was responsible for the change in telomere length. However, we found that Sir2 actually acts with Isw2 and Ino80 to maintain telomere length (Figure 3.6F). These results suggest that Isw2 and Ino80 regulate telomere length in parallel with Sir2.

Discussion

Here we show novel roles for chromatin remodeling factors Isw2 and Ino80 in rDNA and telomere functions. While functions of chromatin remodeling factors in transcription have been well characterized, their functions in other biological processes are far less characterized. However, we and others suggest that chromatin remodeling factors have significant roles at constitutively heterochromatic regions, which are required for maintaining genome stability (Dror and Winston, 2004; Manning and Peterson, 2014; Postepska-Igielska and Grummt, 2014; Xue et al., 2015). Chromatin remodeling factors have previously been shown to localize to rDNA telomeres, and centromeres but their functions at these regions are not fully understood. In mammals, chromatin remodeling factor NoRC coordinates the establishment of heterochromatin at telomeres, rDNA and centromeres (Postepska-Igielska and Grummt, 2014). Yeast SWI/SNF and INO80 families of proteins have also been implicated at regulating activities at the rDNA and telomeres (Dror and Winston, 2004; Manning and Peterson, 2014; Xue et al., 2015). Because these structures are highly organized and complex, there are probably numerous chromatin

regulators that are necessary to establish and maintain their unique chromatin structure. Therefore future work to identify the layers of chromatin regulation and their mechanisms will contribute to elucidating regulation of genome stability and aging.

While Isw2 and Ino80 were not found at telomeres by ChIP-seq, we cannot exclude the possibility that Isw2 and Ino80 are binding to the ends of chromosomes. Previously it was shown that subunits of Ino80 bind to telomeres by ChIP PCR (Yu et al., 2007), but we could not reproduce this result by either ChIP PCR (data not shown) or ChIP-seq. One possibility is that Isw2 and Ino80 are functioning directly at telomeres through chromosome looping. Indeed DNA looping was shown to facilitate Isw2 targeting (Yadon et al., 2013). Furthermore, heterochromatin is known to form close domains with each other allowing for interactions based on close proximity. However, it is also entirely possible that Isw2 and Ino80 do not function directly at telomeres. Rather the effect of Isw2 and Ino80 on the rDNA could result in redistribution of factors involved in telomere homeostasis. While the change in Sir binding does not seem to be the reason for shorter telomeres, there could be redistribution of other factors that would result in downstream consequences for telomeres. Many HR proteins also function at telomeres and the changes in chromatin structure likely alter interactions with many of these factors. Therefore more mechanistic work will be needed to determine how chromatin regulates these factors and their downstream effects.

An interesting result is that Isw2 and Ino80 seem to promote transcription of rRNAs and this occurs in a Sir-dependent manner. While it is well documented that Sirs have roles in silencing Pol II transcription (Kueng et al., 2013), it has not been shown that Sirs are required for Pol I transcription. Transcription has been linked to rDNA stability (Ide et al., 2010). Cells that have only active rDNA copies have defects in sister chromatid cohesion, which results in

unstable rDNA (Ide et al., 2010). While heavily transcribed rDNA is detrimental to cells, there have been no reports exploring how rDNA stability is affected in cells that have too many inactive copies. Presumably, not enough rRNAs will be made to keep up with cell growth. Indeed, we do see slower growth in *isw2 nhp10* in the presence of rapamycin, which mimics a cell starvation response (data not shown). While ERC production does not change in logarithmically growing *isw2 nhp10*, it is still possible that rDNA stabllity is affected. Recent reports suggest the ERC accumulation is a downstream effect of rDNA instability, but rDNA still occurs in the absence of ERCs as well (Ganley et al., 2009).

This work establishes novel roles for chromatin remodeling factors in new and important biological processes. While we establish important functions for Isw2 and Ino80 at these constitutively heterochromatic regions, future work will be needed to investigate whether they directly affect genome stability and cellular aging. Furthermore, in this study we did not characterize their functions at centromeres. While we do not have any evidence that Isw2 and Ino80 are targeted to centromeres, we have yet to explore whether they affect centromere functions. Characterizing the chromatin regulators in genome stability will help us elucidate their function in aging and cancer.

Materials and Methods

Yeast Strains and culture

All yeast strains are MAT**a** and congenic to W303-1a with a correction for the weak *rad5* allele in the original W303 (Thomas and Rothstein, 1989; Zhao et al., 1998). Strains were constructed using standard gene knockout protocols and genetic crosses.

Chromatin Immunprecipitation (ChIP)

Cells were fixed and harvested, and chromatin was prepped as previously described (Rodriguez and Tsukiyama, 2013). 30 µl of Protein G beads (Invitrogen) as conjugated to 4 µl of FLAG polyclonal antibody (Sigma). Bead conjugation and the ChIP protocol can be found at http://www.fhcrc.org/science/labs/tsukiyama.

Sequencing

ChIP and input sequencing libraries were prepared using the manufacturer's protocol from the NuGEN Ovation Ultralow System v2 (Nugen). Libraries were deep sequenced, aligned and normalized as previously described (McKnight and Tsukiyama, 2015).

Spot Tests

Yeast were grown and plated on MMS as previously described (Au et al., 2011).

Flourescence Microscopy

Fob1-GFP cells were grown mid log phase and 1 ml of cells were harvested. 2ul of the cells and 2ul of 1.4% agarose was pipetted onto a microscope slide and live cells were imaged.

Southern Blot

DNA isolation and Southern blot was performed as previously described (Fazzio and Tsukiyama, 2003). DNA digestions and probes were designed as previously described for telomeres (Singer et al., 1998), and rDNA (Sinclair and Guarente, 1997).

Northern Blot

10ug of total RNA was loaded and Northern blots were performed as previously described (Alcid and Tsukiyama, 2014). ACT1 and ITS1 RNA probes were generated with T7 polymerase as described (Alcid and Tsukiyama, 2014; Kuhn et al., 2009).

MNase-seq

DNA was isolated and digested with MNase as previously described (Rodriguez and Tsukiyama, 2013). The resulting DNA was run on a 1.8% low melt agarose gel (GeneMate) and mono-nucleosomes were size selected for library construction. Libraries were prepared using the manufacturer's protocol from the NuGEN Ovation Ultralow System v2 (Nugen). Sequencing and analysis were performed as previously described (McKnight and Tsukiyama, 2015).

RNA-seq

RNA was isolated, sequenced, and analyzed as previously reported (McKnight and Tsukiyama, 2015).

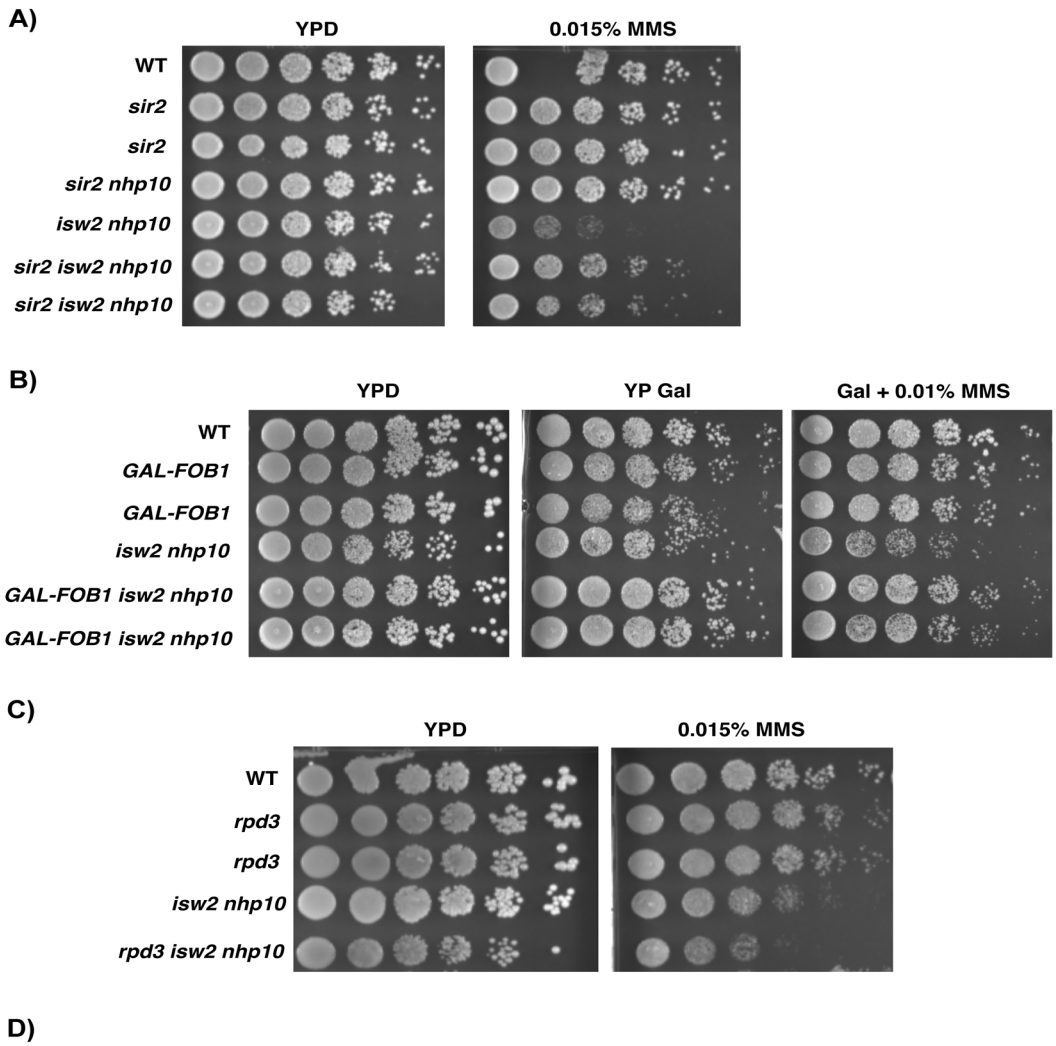

D)

Mutant *(isw2 nhp10* background*)*	Growth Sensitivity
tel1	Sick
yku70	Synthetic Lethal
yku80	Synthetic Lethal
est	Sick
rif1	Synthetic Lethal
pif1	Synthetic Lethal
mre11	Sick

Figure 3.1 *ISW2* and *NHP10* genetically interact with rDNA and telomere genes.
A) Spot assay to assess genetic interactions between *ISW2* and *NHP10* with *SIR2*. Yeast strains were grown to saturation and 1:5 serial dilutions were spotted on YPD and YPD with 0.015% MMS. B) Same as in A) to observe interactions between *ISW2* and *NHP10* with overexpression of *FOB1,* which was fused to the GAL promoter and induced by addition of galactose. Spots were plated on YPD, YP with galactose, and YP with galactose and 0.01% MMS. C) Same as in A) to observe interactions between *ISW2* and *NHP10* with *RPD3.* D) A table of genetic interactions of *ISW2* and *NHP10* with telomere genes.

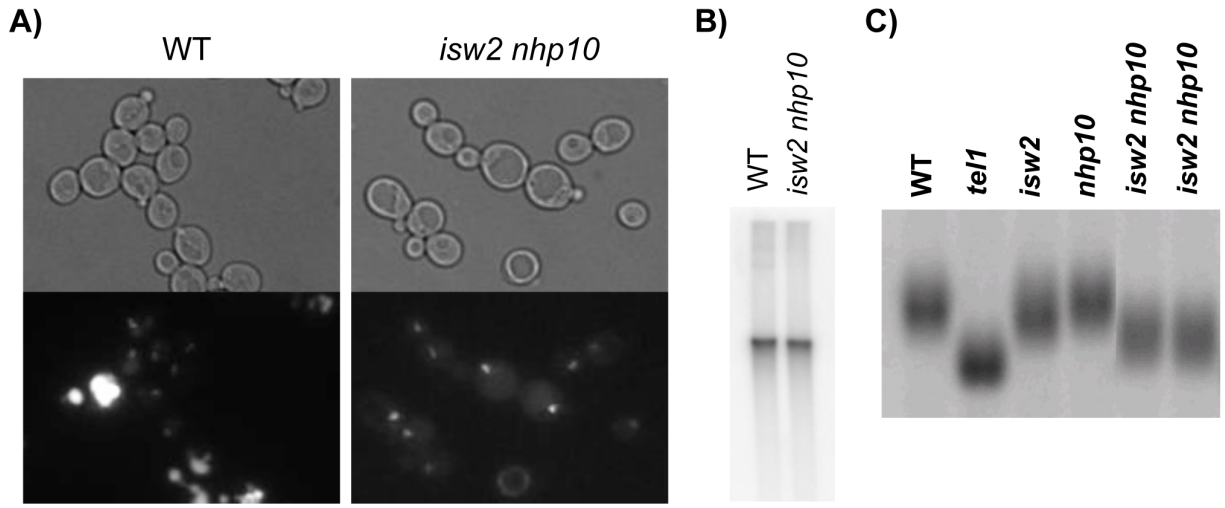

Figure 3.2 Isw2 and Ino80 alter rDNA and telomere structure.
A) Microscopy images of the nucleolus, indicated by Fob1-GFP, from live WT and *isw2 nhp10* cells. B) Southern blot of 9.1kb rDNA unit to examine ERC production. The band corresponds to the endogenous rDNA locus. C) Southern blot of Y' element in the subtelomeric region of chromosomes. Telomere length is assessed WT, tel1, isw2, nhp10, and two independent isolates of isw2 nhp10.

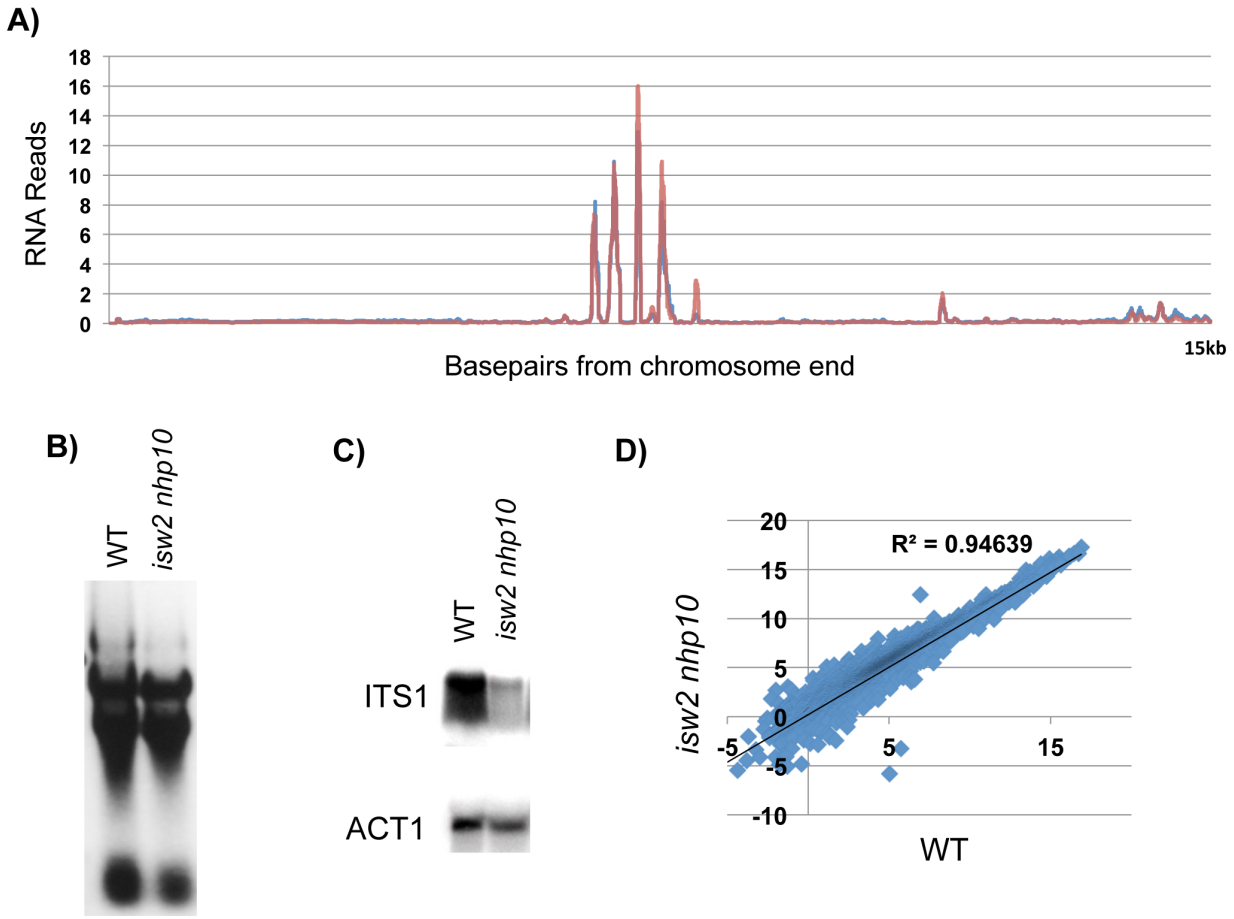

Figure 3.3 Isw2 and Ino80 regulate rRNA transcription.
A) Averaged RNA-seq transcripts in WT (blue) and *isw2 nhp10* (red) at all telomeres from the end of the chromosome to 15kb towards the centromere. B) Log phase cells were counted on a hemocytometer and RNA was purified and quantified. 1ug of total RNA was loaded on a 0.8% agarose gel and stained with ethidium bromide. C) Northern analysis of ITS1, which corresponds to the 35S nascent transcript, and ACT1, which was used as a loading control. D) WT RNA transcripts (x-axis) plotted against *isw2 nhp10* RNA transcripts (y-axis) from RNA-seq data. The correlation coefficient is shown as the R^2 value.

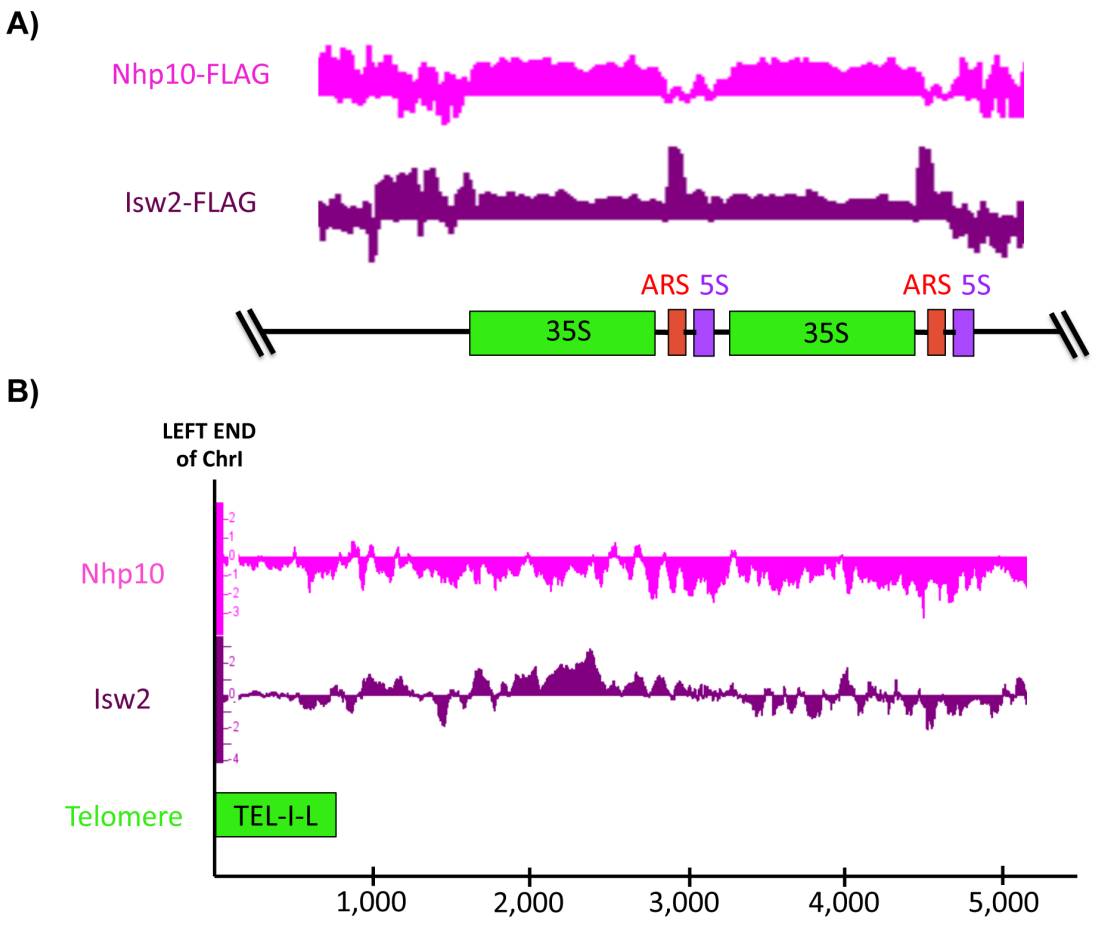

Figure 3.4 Isw2 and Ino80 are targeted to the rDNA.
A) ChIP-seq of Nhp10-3FLAG (pink) and Isw2-3FLAG (maroon) read mapped to two units of the rDNA on Chromosome XII. B) The same as in A), but at a representative telomere on the left end of Chromosome I.

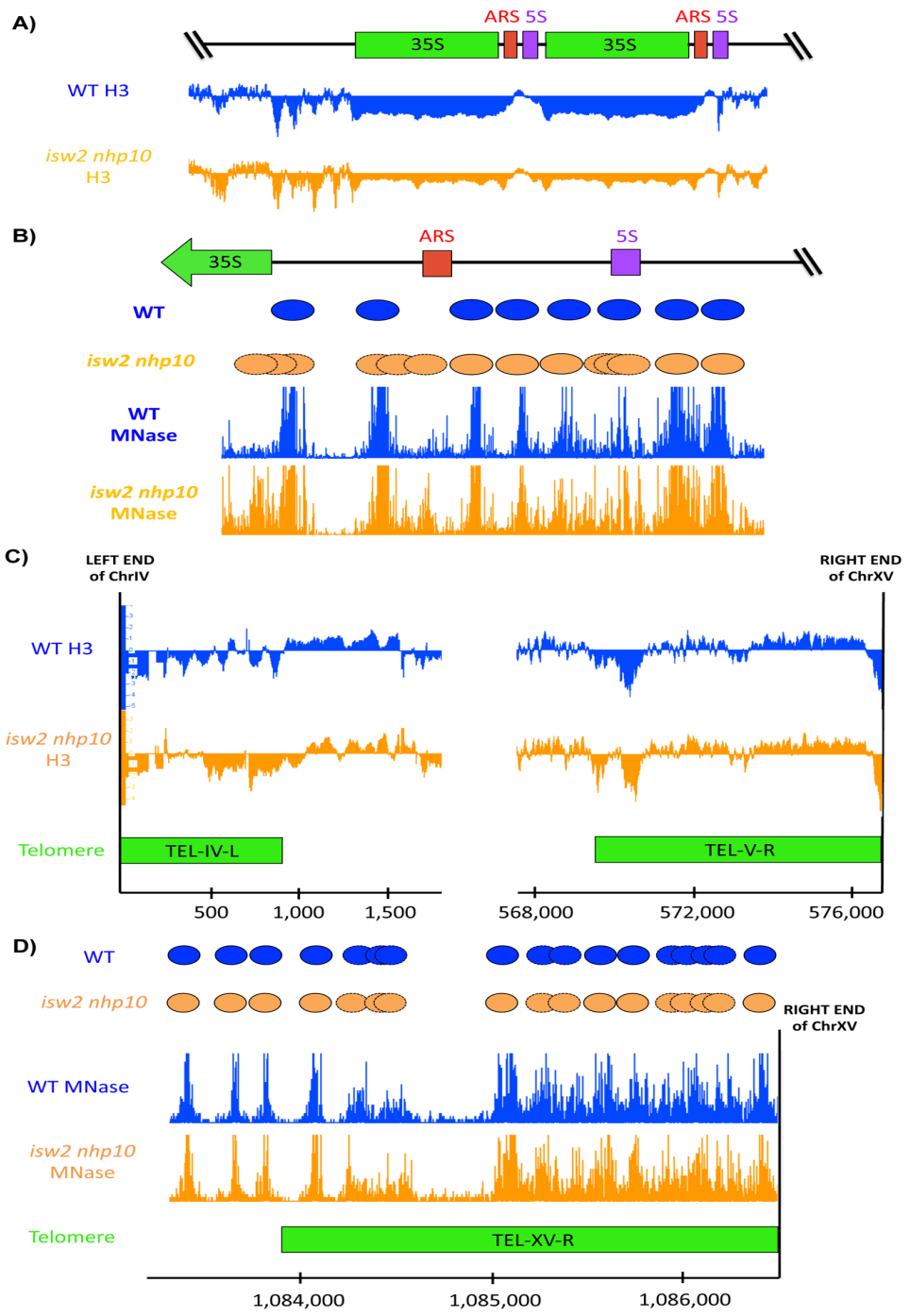

Figure 3.5 Isw2 and Ino80 alter chromatin structure at rDNA and telomeres.
A) ChIP-seq of H3 in WT (blue) and *isw2 nhp10* (orange) at the rDNA. B) MNase-seq of WT and *isw2 nhp10* at the spacer region of the rDNA. A nucleosome map corresponds to the nucleosome positions. C) Same as in A) but at telomeres. The telomere at the left end of chromosome IV, and the telomere at the right end of chromosome XV are shown. D) Same as in B) but for the telomere at the right end of Chromosome XV.

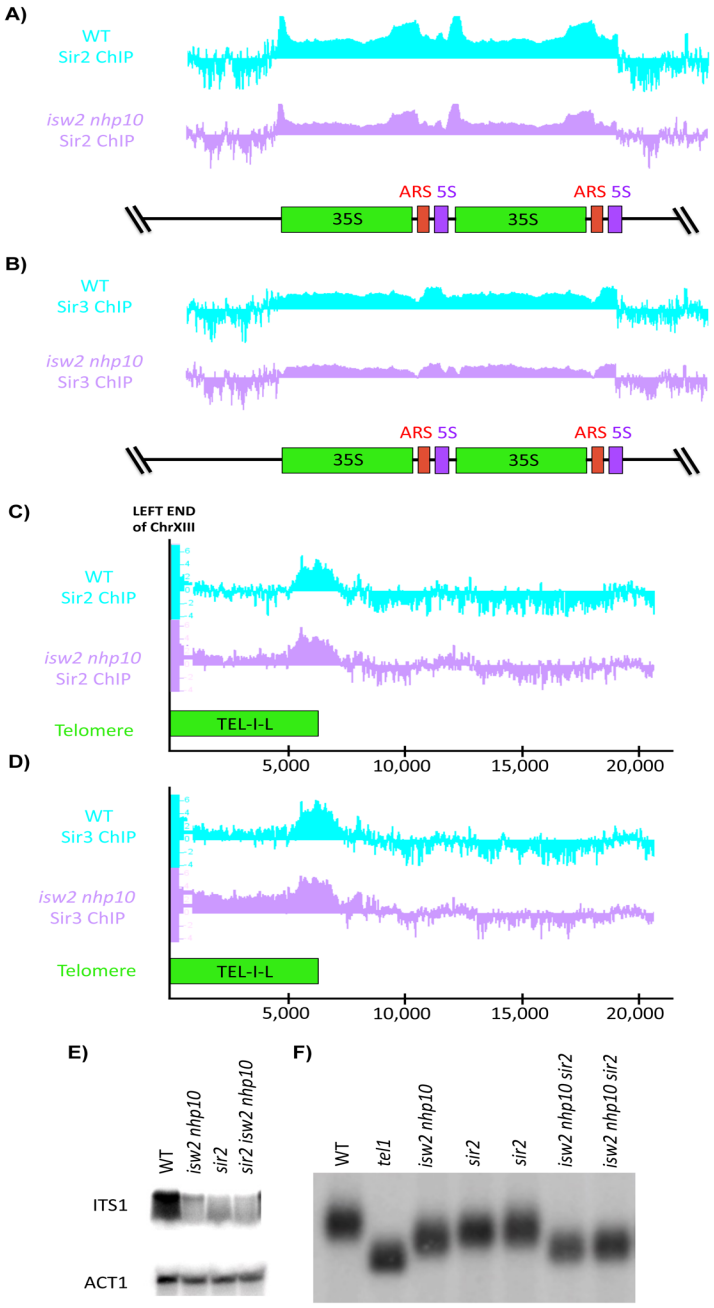

Figure 3.6 Isw2 and Ino80 redistribute Sir proteins and interact with Sirs to regulate rDNA and telomere functions.
A) ChIP-seq of Sir2-3FLAG at the rDNA in WT (light blue) and *isw2 nhp10* (lavender). B) Same as in A) but Sir3-3FLAG ChIP. C) ChIP-seq of Sir2-3FLAG at the left end of telomere XIII in WT and *isw2 nhp10.* D) Same as in C) except Sir3-3FLAG ChIP. E) On the left, a northern blot of ITS1, which corresponds to the 35S nascent transcript, in WT, *sir2*, *isw2 nhp10*, and *sir2 isw2 nhp10*. ACT1 is used as a loading control. On the right, a Southern blot of the Y' element in the subtelomeric region in WT, *tel1, isw2, nhp10, isw2 nhp10*, and two independent isolates of *isw2 nhp10 sir2*.

Table 3.1 Chapter 3 yeast strains

Strain	Genotype	Source
W1588-4c	*MAT***a** *ade2-1 can1-100 his3-11,15 leu2-3,112 trp1-1 ura3-1 RAD5+*	(Thomas and Rothstein, 1989; Zhao *et al.* 1998)
YTT3337	*MAT***a** *Δisw2::NatMX Δnhp10::Hyg*	(Au *et al.*, 2011)
YTT3339	*MAT***a** *Δisw2::NatMX Δnhp10::Hyg*	(Au *et al.*, 2011)
YTT3320	*MAT***a** *Δisw2::NatMX*	(Vincent *et al.*, 2008)
YTT3333	*MAT***a** *Δnhp10::Hyg*	(Vincent *et al.*, 2008)
YTT6168	*MAT***a** *Δsir2::KanMX*	This study
YTT6121	*MAT***a** *Δsir2::KanMX Δisw2::NatMX Δnhp10::Hyg*	This study
YTT6122	*MAT***a** *Δsir2::KanMX Δisw2::NatMX Δnhp10::Hyg*	This study
YTT4560	*MAT***a** *Δtel1::KanMX*	This study
YTT6441	*MAT***a** *Sir2-2L-3FLAG-KanMX*	This study
YTT6445	*MAT***a** *Δisw2::NatMX Δnhp10::Hyg Sir2-2L-3FLAG-KanMX*	This study
YTT6443	*MAT***a** *Sir3-2L-3FLAG-KanMX*	This study
YTT6446	*MAT***a** *Δisw2::NatMX Δnhp10::Hyg Sir3-2L-3FLAG-KanMX*	This study
YTT1996	*MAT***a** *Isw2K215R-3FLAG-KanMX*	(Gelbart *et al*., 2005)
YTT3426	*MAT***a** *Nhp10-3FLAG-KanMX*	(Vincent *et al*., 2008)

*All strains are MATa and congenic to W1588-4c with a correction for the weak *rad5* allele

CHAPTER 4

Nucleosome occupancy as a novel chromatin parameter for replication origin functions

Modified from submitted manuscript.

Rodriguez, J.*, Lee, L.*, Lynch, B., and Tsukiyama, T.

Summary

Eukaryotic DNA replication initiates from multiple discrete sites in the genome termed origins of replication (origins). Prior to S phase multiple origins are bound by the pre-replicative complex (pre-RC) and are ready to initiate replication. Origin activation must be tightly regulated, but not all the parameters that control origin activation have been elucidated. Many studies have suggested chromatin to be an important determinant in regulating origin initiation. To explore the role of chromatin structure in regulating origin properties, we used H3 chromatin immunoprecipitation followed by deep sequencing to comprehensively analyze nucleosome occupancy around origins. We show that nucleosome occupancy in G1 varies greatly among all origins. Classification of origins by nucleosome occupancy shows that the nucleosome occupancy around origins correlates with many properties of origins. We further demonstrate that nucleosome occupancy around origins in G1 is established during transition from G2/M to G1, and this cell cycle dependent change in nucleosome occupancy is contingent upon pre-RC assembly. Importantly, the loss of changes in nucleosome occupancy around origins in *orc1-161*

mutant is associated with misregulation of origin initiation. We propose that nucleosome occupancy contributes along with other factors to regulate origin activation.

Introduction

DNA replication is an essential process in all organisms, and faithful completion of replication is required for proper cell division, differentiation and the maintenance of genome integrity (Bell and Dutta, 2002). Eukaryotic DNA replication initiates from multiple discrete sites called origins of replication (hereafter origins). In *Saccharomyces cerevisiae*, origins have an AT-rich DNA sequence known as an autonomously replicating sequence (ARS) (Marahrens and Stillman, 1992). However, the ARS consensus sequence (ACS) alone is not sufficient for defining origins because many ACSs do not initiate replication (Brewer and Fangman, 1991; Dubey et al., 1991). A six subunit origin recognition complex (ORC) binds to a limited number of ACSs throughout the cell cycle (Bell and Stillman, 1992; Diffley and Cocker, 1992). Then in G1, double hexamers of the mini chromosome maintenance (MCM) complex are subsequently recruited to origins to form the pre-replicative complex (pre-RC) (Remus et al., 2009). Once the pre-RC is formed, origins are licensed to fire. However, to prevent re-replication and maintain genomic integrity, origin activation must be tightly regulated and thus limiting replication factors are distributed to only a subset of origins to initiate in a given S phase (Fragkos et al., 2015).

Each budding yeast origin has distinct properties. Some origins tend to initiate replication (fire) early in S phase while others tend to fire late in S phase. Moreover, in a given population of cells, each origin has a distinct probability of activation, which is defined as origin efficiency. Although population studies have demonstrated that each origin has distinct timing and efficiency properties (Alvino et al., 2007; McCune et al., 2008; McGuffee et al., 2013; Muller et al., 2014; Raghuraman et al., 2001; Yabuki et al., 2002), molecular combing experiments have

shown that DNA replication occurs stochastically in individual cells, and therefore is not as deterministic as population analyses suggest (Czajkowsky et al., 2008; Patel et al., 2006). These findings can by reconciled by averaging the heterogeneous replication kinetics of a large number of cells, which recapitulates the observed data from population studies (Czajkowsky et al., 2008). This observation has led to the postulation that in yeast, origin firing is a largely stochastic event in which different origins have different probabilities for firing. Importantly, the probable time of firing of a given origin is decided in a cell cycle regulated manner. For instance, the property of origin *ARS501* to fire late in S phase is established at some point between G2/M and G1 (Raghuraman et al., 1997), suggesting that the signal for origin activation takes place prior to a given S phase.

What dictates the probability of origin initiation? The local chromatin environment has been suggested to be one of the key contributors in affecting origin firing. For example, introducing a nucleosome within an ARS resulted in marked reduction of origin activation (Simpson, 1990). In addition, a previous study showed that a late-firing origin *ARS501* fires early when the origin placed on a plasmid, indicating that chromatin context is important (Ferguson and Fangman, 1992). Chromosomal elements like telomeres are also associated with late firing origins (Ferguson and Fangman, 1992; McCarroll and Fangman, 1988), while centromeres are associated with early firing origins (McCarroll and Fangman, 1988; Raghuraman et al., 2001). Because of these reports, many studies have tried to establish the parameters of chromatin that are involved in origin firing. We and others have shown that histone modifications such as acetylation affect origin timing and efficiency (Iizuka et al., 2006; Knott et al., 2009; Unnikrishnan et al., 2010; Vogelauer et al., 2002). Moreover, asymmetric nucleosome positions, determined by ORC, are important for origin activity (Eaton et al., 2010; Lipford and Bell,

2001), and genome-wide MNase mapping further shows that nucleosome positions dictate the association of Mcm2-7 with origins (Belsky et al., 2015). Many of these studies have contributed to comprehending how chromatin can affect origin regulation, but a complete understanding of the chromatin dynamics involved in origin initiation is still lacking. Perhaps one of the most glaring aspects of chromatin structure that has not been thoroughly explored in origin regulation is nucleosome occupancy at origins.

In order to determine how nucleosome occupancy affects origin properties, we performed high-resolution histone chromatin immunoprecipitation followed by deep sequencing (ChIP-seq) to measure nucleosome occupancy around origins. Here we show that nucleosome occupancy in G1 varies greatly among origins, and correlates well with many properties of origins and the level of pre-RC formation. We further found that the nucleosome depleted region (NDR) around origins expands between G2/M and G1, and these cell cycle changes are dependent upon the pre-RC. Finally, we provide evidence supporting the idea that nucleosome occupancy is important for proper origin timing and efficiency. Our work thus establishes nucleosome occupancy as a novel and useful parameter of chromatin structure for proper origin control.

Results

Nucleosome occupancy varies across origins in G1 and is ORC-dependent

It has been long suggested that chromatin structure affects origin activities (Eaton et al., 2010; Knott et al., 2009; Lipford and Bell, 2001; Simpson, 1990), but the chromatin parameters that affect origin properties are not well understood. We therefore sought to determine how the local chromatin environment around replication origins affects their properties. To this end, we systematically analyzed chromatin structure around all 798 predicted origins listed in the OriDB

database (Nieduszynski et al., 2007) in G1 phase. Origins are typically located within nucleosome depleted regions (NDRs), which are surrounded by well positioned nucleosomes (Eaton et al., 2010). However, nucleosome occupancy around origins has yet to be properly analyzed genome-wide. To measure nucleosome occupancy, we performed chromatin immunoprecipitation (ChIP) using antibodies against histone H3 followed by deep sequencing (ChIP-seq). Nucleosome occupancy is often measured by the height of nucleosome signals after micrococcal nuclease (MNase) digestion of chromatin. However, the levels of nucleosome signals after MNase digestion are determined by both the occupancy and the MNase sensitivity of the nucleosome (Rodriguez and Tsukiyama, 2013; Weiner et al., 2010). Therefore, histone ChIP after sonication is a better method to measure nucleosome occupancy. As expected, nucleosomes are depleted around most ARS consensus sequences (ACSs) as shown previously (Belsky et al., 2015; Eaton et al., 2010). However, surprisingly, nucleosome occupancy in G1 varied very significantly around 397 ORC-bound origins (Belsky et al., 2015) (Figure 4.1A and 4.1B, left). As a control, we measured nucleosome occupancy around 401 ORC-unbound ACS sequences (Belsky et al., 2015), which revealed significantly shallower NDRs (Figure 4.1A and 4.1B, right). Because ORC has been shown to position nucleosomes at origins (Eaton et al., 2010; Lipford and Bell, 2001), we tested whether ORC affects NDR formation at origins. The *orc1-161* allele is a temperature sensitive mutation that inhibits ORC from binding DNA at the restrictive temperature (Aparicio et al., 1997). ORC does bind origins at permissive temperatures in *orc1-161*, albeit at slightly reduced levels. H3 ChIP-seq performed in *orc1-161* in G1 at a permissive temperature (25 °C) revealed higher nucleosome occupancy at ORC-bound origins (Figure 4.1B, left). In contrast, nucleosome occupancy was significantly less affected in *orc1-161* mutant at ORC-unbound ACSs (Fig 4.1B, right), as well as transcription start sites (TSSs)

and transcription termination sites (TTSs) (Figure 4.1C). Because H3 levels were similar across TSSs in WT and *orc1-161* (Figure 4.1C), H3 ChIP was z-score normalized at TSSs in the following analyses to account for slight differences in the degree of sonication (see Materials and Methods for details). These results collectively showed that nucleosome occupancy at origins is reduced in an ORC-dependent manner in G1. We classified ORC-bound origins into three classes based on nucleosome occupancy around the ACS, and these classes are used in the subsequent analyses.

Nucleosome occupancy in G1 correlates with origin properties

We next sought to determine whether nucleosome occupancy around origins during G1 correlates with various origin properties. Comparison of origin firing time, defined by origin firing patterns in hydroxyurea (HU) (Belsky et al., 2015), to nucleosome occupancy revealed a statistically significant correlation between low nucleosome occupancy and early firing ($p=0.0057$: χ^2 test) (Figure 4.2A). Global origin firing efficiencies were established from deep sequencing of Okazaki fragments (McGuffee et al., 2013). Lower nucleosome occupancy was associated with higher origin efficiencies, while higher nucleosome occupancy was associated with lower efficiencies ($p=1.02\text{x}10^{-5}$: χ^2 test) (Figure 4.2B). Previously, a systematic comparison of ORC binding properties *in vitro* on naked DNA versus those *in vivo* led to the classification of origins into DNA-dependent, chromatin-dependent and weak ORC binding classes (Hoggard et al., 2013): ORC strongly binds origins both *in vitro* and *in vivo* in the DNA-dependent class, while it binds origins much more strongly *in vivo* than *in vitro* in the chromatin-dependent class. Comparison of nucleosome occupancy around origins with these published ORC binding properties revealed a statistically non-significant correlation ($p = 0.119$: Fisher's exact test).

However, this is likely due to the small number of origins (n=66) that were classified in this manner, as there was a clear trend that DNA-dependent origins were associated with lower nucleosome occupancy and chromatin-dependent origins were associated with higher nucleosome occupancy (Figure 4.2C). It was also recently reported that Forkhead transcription factors, Fkh1 and Fkh2, bind near origins, and their presence can dictate origin timing (Knott et al., 2012). We found no correlation between origins with altered timing in *Δfkh1fkh2* with nucleosome occupancy (p=0.194, χ^2 test) (Figure 4.2D). Taken together, these results support the idea that nucleosome occupancy in G1 correlates well with various properties of origins.

Nucleosome occupancy in G1 correlates with pre-RC formation

As nucleosome occupancy around origins correlated with many origins properties, we next investigated whether it correlated with pre-RC formation. Comparison of Mcm2-7 ChIP-seq signals (Belsky et al., 2015) at all ORC-bound origins in G1 with nucleosome occupancy revealed that Mcm2-7 loading is highest at origins with low nucleosome occupancy (Figure 4.3A). Interestingly, the average MCM ChIP-seq signals at origins with mid and high nucleosome occupancy were virtually indistinguishable (Figure 4.3A). All functional origins are bound by ORC in S phase. While ORC binding is detectable at most origins throughout the cell-cycle by standard ChIP assay (Eaton et al., 2010), ORC footprinting by MNase identified two classes of origins: origins that exhibit ORC footprints at both G2/M and G1, and those that do so only in G1, with the former class enriched for origins that fire earlier and more efficiently (Belsky et al., 2015). We found that origins with lower nucleosome occupancy had a higher frequency of binding to ORC in G2/M, which was statistically significant (p=0.000546: χ^2 test)

(Figure 4.3B). These results suggest the possibility that nucleosome occupancy around origins may be associated with pre-RC formation.

Nucleosome occupancy around ORC bound origins is cell-cycle regulated

It was previously shown that the late firing property of *ARS501* is established between G2/M and G1 (Raghuraman et al., 1997). To determine whether nucleosome occupancy is cell-cycle regulated, we compared nucleosome occupancy around origins in G2/M and G1. This analysis showed that nucleosome occupancy around ORC-bound origins is higher in G2/M, suggesting that nucleosomes around these origins are lost between G2/M and G1 (Figure 4.4A). Subtraction of nucleosome occupancy in G1 from that in G2/M showed that nucleosome occupancy decreases almost 2-fold on average (Figure 4.4B). Interestingly, the strongest loss in nucleosome occupancy takes place immediately adjacent to the ACS, which coincides with MCM ChIP signals in G1 (Figure 4.3A). Ranking origins by the degree of loss in nucleosome occupancy from G2/M to G1 revealed that almost all ORC-bound origins exhibit significant changes in histone levels within the NDR (Figure 4.4C). In contrast, nucleosome occupancy around ORC-unbound ACSs and TTSs did not change significantly between G2/M and G1 (Figure 4.4A-C). To examine how much the nucleosome loss after G2/M contributes to nucleosome occupancy in G1, we correlated the degree of nucleosome occupancy loss with G1 occupancy. This analysis revealed that origins with lower nucleosome occupancy in G1 tend to exhibit higher occupancy loss between G2/M to G1, and *vice versa* (Figure 4.4D). These results suggested that the nucleosome loss between G2/M and G1 plays major roles in determining the occupancy in G1.

Changes in nucleosome occupancy between G2/M and G1 are dependent upon pre-RC components

Based on our results that G1 nucleosome occupancy around origins is partially dependent on ORC, and is strongly affected by nucleosome loss between G2/M and G1, we hypothesized that histone loss around origins may depend on pre-RC formation. To test this model, we first performed H3 ChIP-seq in *orc1-161* in G2/M at a permissive temperature (25°C). We found that nucleosome occupancy in the *orc1-161* mutant in G2/M is much higher that that of wild type cells (Figure 4.5A, left and center). In addition, there is a much smaller degree of loss in nucleosome occupancy between G2/M and G1 in this mutant as compared to wild type cells (Figure 4.5B, left and center). This was the case across all ORC-bound origins, including those that exhibit the biggest loss of histones between G2/M and G1 in wild type cells (Figure 4.5C, left and center). To test whether the MCM complex affects nucleosome occupancy, we constructed an auxin degron (Nishimura et al., 2009) allele of *MCM2* (*mcm2-AID*). To measure G2/M nucleosome occupancy, we arrested cells in G2/M, added auxin to degrade Mcm2, then performed H3 ChIP-seq. For G1 occupancy, we arrested cells in G2/M, added auxin, then released cells into alpha factor in the presence of auxin (see Materials and Methods for details), followed by H3 ChIP-seq. These experiments showed that the loss of MCM during G2/M does not appreciably affect nucleosome occupancy around origins (Figure 4.5A, right). However, the loss of histone occupancy between G2/M and G1 is almost entirely diminished in the absence of Mcm2 (Figure 4.5A and 4.B, right). This was the case across all ORC-bound origins (Figure 4.5C). Together, these results demonstrate that cell-cycle dependent changes in nucleosome occupancy at origins are dependent upon Mcm2-7 complex loading.

The decrease in nucleosome occupancy loss at origins is associated with altered origin activities

We next sought to address whether the change in nucleosome occupancy between G2M and G1 is important for origin activities. To this end, we took advantage of the fact that the *orc1-161* allele causes a significant loss in cell-cycle dependent nucleosome occupancy changes even at the permissive temperature, a condition in which cells do not exhibit severe growth defects. Genome-wide BrdU ChIP experiments (Viggiani et al., 2010) revealed that origin firing is significantly altered in the *orc1-161* mutant (an example shown in Figure 4.6A). At a time point in which cells have undergone similar amounts of replication, some origins that have relatively low activity in wild type cells exhibit higher activity in *orc1-161* mutant, whereas other origins exhibit lower activities in the mutant. Importantly, this pattern is observed across the genome. Although replication profiles are similar between the individual biological replicates for wild type and *orc1-161* (r^2=0.99 and 0.92), they exhibit markedly different origin activities on a global scale (r^2=0.47) (Figure 4.6B). To further analyze the effects of the *orc1-161* mutation, we first ranked origins by timing then efficiency as described (Belsky et al., 2015; McGuffee et al., 2013) (Figure 4.6C and 4.6D, left columns), then examined how this ranking correlates with the effects of the *orc1-161* mutation on origin activity (Figure 4.6C and 4.6D right columns). This analysis revealed that the majority of early firing origins lose activity (Figure 4.6C), whereas efficient late firing origins gain activity (Figure 4.6D) in *orc1-161* mutant. For unknown reasons, some inefficient late firing origins also lose activity in the mutant. To examine whether nucleosome occupancy at origins are associated with changes in origin activities, we compared the effects of *orc1-161* on cell-cycle changes in nucleosome occupancy and origin activities (Figure 4.6E). Origins were ranked by the degree of cell-cycle changes in nucleosome occupancy

(column 1), which was compared to cell-cycle occupancy changes in *orc1-161* mutant (column 2), the effects of *orc1-161* on nucleosome occupancy changes between G2/M and G1 (column 3), and the effects of *orc1-161* on origin activities (column 4). This analysis revealed a slight trend in which origins that lost more nucleosome occupancy between G2M and G1 in wild type cells (higher in ranking) tended to be more strongly affected by *orc1-161* mutation for both nucleosome occupancy changes and origin activities. These results are consistent with the possibility that regulation of nucleosome occupancy at origins partially contributes to the proper control of origin properties.

Discussion

For the first time, we show that origins have varying degrees of nucleosome occupancy in G1, and that the loss of nucleosomes between G2/M and G1 plays a major role in establishing nucleosome occupancy around origins. These results suggest that nucleosome occupancy around origins is reset after S phase, then re-established in every cell-cycle. We also provide evidence supporting the notion that this change in nucleosome occupancy between G2/M and G1 at specific origins is a significant determinant of origin properties. It should be noted that nucleosome occupancy measured by H3 ChIP-seq reflects the fraction of cells within a population that has nucleosomes at any given locus. This means that a large fraction of cells loses nucleosomes around origins between G2/M and G1, and that the fraction that loses nucleosomes varies among origins. This nature of nucleosome occupancy is therefore consistent with findings from single cell analyses that origin firing is stochastic and that origin properties define the probability of origin activation (Czajkowsky et al., 2008).

Our results suggest that there are multiple factors that affect origin properties, and that nucleosome occupancy is one of these factors. For example, Fkh1 and Fkh2 (Knott et al., 2012), and the proximity to telomeres and centromeres are known to affect origin properties, but nucleosome occupancy does not significantly correlate with these parameters. Indeed, while *orc1-161* abolishes major changes in nucleosome occupancy at origins between G2/M and G1 and greatly disrupts proper origin firing, changes in nucleosome occupancy do not perfectly correlate with the changes in origin activities. Although this is likely in part due to the general increase in nucleosome occupancy at all origins even in G2/M in *orc1-161*, which is associated with a global reduction in origin firing, our results suggest the presence of other mechanisms that affect origin properties. Hoggard et al. previously showed that ORC binding, and subsequently origin activation, was dependent upon DNA sequence for only a subset of origins, while the local chromatin environment was more important for other origins (Hoggard et al., 2013). Our analysis revealed that "chromatin-dependent" origins tend to have higher nucleosome occupancy in G1 and tend to lose nucleosomes to a lesser degree between G2/M and G1. We suspect that "chromatin-dependent" origins are regulated by other chromatin factors, which makes these origins rely less on nucleosome occupancy to control their properties. It is not unexpected that origins are regulated by multiple factors, given that strict regulation of origin activation is necessary for proper DNA replication.

What is the molecular basis for the loss of nucleosome occupancy around origins between G2/M to G1? Histone-DNA interactions within nucleosomes are very stable, and active mechanisms are usually used to slide, evict or replace histones at gene promoters for transcriptional regulation (Li et al., 2007). One possibility is that the pre-RC recruits chromatin regulators to facilitate the removal of nucleosomes around origins. The histone chaperone FACT

(facilitates chromatin transcription) was shown to bind histones together with Mcm2-7 and maintain proper levels of nucleosome occupancy at subtelomeric regions (Foltman et al., 2013). The *mcm2-2A* mutation in the amino terminal tail prevents Mcm2-7 from binding histones with FACT, but is dispensable for DNA replication (Foltman et al., 2013). We tested whether Mcm2-7 and FACT could regulate changes in nucleosome occupancy from G2/M to G1 by measuring nucleosome occupancy in the *mcm2-2A* mutant. However, the mutant did not exhibit significant changes in the loss of nucleosome occupancy around origins between G2/M and G1 (Figure 4.7). While this result does not exclude the possibility that the MCM complex collaborates with unidentified factors, it does suggest that the histone binding activity of Mcm2 alone is not sufficient for regulating levels of nucleosome occupancy at origins. Another possibility is that chromatin regulators could affect pre-RC binding, which in turn can alter nucleosome formation at origins. Indeed, nucleosome positions were found to be important for loading Mcm2-7 onto origins in a specific manner (Belsky et al., 2015). We preliminarily screened for potential chromatin regulators, (Rsc, Ser1, Chd, Isw1, Isw2, Snf2 and histone acetylation) using H3 ChIP-seq, but thus far have not found any chromatin regulator responsible for the reduction in nucleosome occupancy around origins at G1. While we cannot exclude the possibility that the change in histone density in G1 is just a consequence of pre-RC binding, this seems highly unlikely because the affinity of ORC to origins alone (Hoggard et al., 2013) cannot explain the nucleosome occupancy in G1. Furthermore, Mcm2-7 ChIP-seq revealed that Mcm2-7 localizes to origins to a similar extent in both mid and high H3 classes of origins, supporting the idea that the changes in nucleosome occupancy is a regulated process and not just a result of pre-RC binding. Given that genetic screens for mutants that alter origin properties are likely difficult to establish, biochemical screens for such factors may be more useful. Recently established *in vitro*

DNA replication systems (Heller et al., 2011; Yeeles et al., 2015), if combined with nucleosomal templates, will likely be a very powerful tool for this purpose.

Thus far, understanding mechanisms of origin regulation has proven to be difficult because of the multiple factors contributing to origin activation. Origin initiation must be strictly controlled but also able to adapt to diverse cellular environments. We propose nucleosome occupancy is an important factor in origin regulation and believe further work will help elucidate how nucleosome occupancy functions, together with other determinants of origin activation, in the regulation of origin activities.

Materials and Methods

Yeast strains

The yeast strains used in this study are listed in S1 Table. All yeast strains are MAT**a** and congenic to W303-1a with a correction for the weak *rad5* allele in the original W303 (Thomas and Rothstein, 1989). Strains used for BrdU profiles had an integrated BrdU vector as previously described (Viggiani and Aparicio, 2006).

Cell synchronization

Yeast strains were grown at 30°C (25°C for *orc1-161*) to early log phase to a density of OD_{660} = 0.2-0.25. Cells were arrested in G1 phase by alpha factor (5µg/mL) or in G2/M phase by nocodazole (15ug/mL). After 2 hours of G2/M arrest in the *mcm2-AID* strain, 500uM of IAA was added for 30 min. Half the culture was taken for the G2/M time point, then the rest of the culture was released into alpha-factor and 500uM IAA for 90 mins.

Chromatin preparation and ChIP

Cells were harvested and chromatin was prepared as previously described (Rodriguez et al., 2014). 30 µl of Protein G beads (Invitrogen) was conjugated to 5ul of H3 C-term rabbit polyclonal antibody (Active Motif). Bead conjugation and the ChIP protocol can be found at http://www.fhcrc.org/science/labs/tsukiyama.

BrdU ChIP

G1 arrested cells filtered on a 0.45-mm nitrocellulose membrane, washed twice with YPD, and released into half the volume of pre-warmed YPD containing BrdU (800ug/mL) for 33 minutes at 24°C. G1 and S phase cells were harvested by adding a 0.1% final concentration of sodium azide. Genomic DNA was prepared and BrdU-labeled DNA was immunoprecipitated as previously described (Viggiani et al., 2010).

Sequencing

ChIP and input sequencing libraries were prepared using the manufacturer's protocol from the NuGEN Ovation Ultralow System v2 (Nugen). Libraries were deep sequenced, aligned and normalized as previously described (McKnight and Tsukiyama, 2015).

Analysis and ranking of nucleosome occupancy

Z-score normalization was performed as described previously using nucleosome occupancy from 1kb upstream and downstream of 4,551 transcription start sites (TSSs) (Nagalakshmi et al., 2008). As a control locus, H3 occupancy was averaged at 5,120 transcription termination sites (TTSs) (Nagalakshmi et al., 2008). H3 occupancy was determined for 798 total origins from

OriDB (Nieduszynski et al., 2007) aligned at the highest scoring ACS (Eaton et al., 2010). Origins were classified into 397 ORC bound and 401 ORC unbound based on ORC footprinting by MNase-seq (Belsky et al., 2015). To calculate the difference in H3 occupancy between G2/M and G1, the log2 ratios were subtracted. H3 occupancy was ranked as low, mid and high based on averaged H3 signal 500bp upstream and downstream from the midpoint of the ACS for 393 ORC bound origins, excluding 4 origins that were too close to the ends of chromosomes or poorly annotated regions.

Analysis of origin properties and pre-RC binding

Origin timing data was obtained from hydroxyurea (HU) experiments (Belsky et al., 2015), and origin efficiency data was determined from deep sequencing of Okazaki fragments (McGuffee et al., 2013) for 393 origins. Origin efficiency was classified as follows: the numerical origin efficiency metric (OEM) of 0.6-1.0 was assigned high efficiency, 0.3-0.6 was assigned mid efficiency, 0-0.3 was assigned low efficiency, and 0 and -1 either detected no firing or were in fork merger zones so they were considered as indeterminable. We correlated H3 occupancy with 66 origins that were classified based on differences in ORC binding properties (Hoggard et al., 2013), and used the Fisher's Exact Test to calculate statistical significance due to the small sample size of origins. A study reported 350 origins that were Fkh1 and Fkh2 dependent (Knott et al., 2012), which was used in our analysis. Mcm2-7 ChIP-seq and ORC footprinting datasets (Belsky et al., 2015) were used for analysis of pre-RC binding. Unless stated otherwise, statistical significance was calculated using the Chi-squared test for all correlations.

Analysis of DNA replication

To compare replication, BrdU ratios of wild type or *orc1-161* biological replicates were linearly correlated. BrdU signal was averaged 1kb upstream and downstream from the midpoint of the ACS, and the difference in replication was calculated by subtracting log2 ratios of *orc1-161* from wild type.

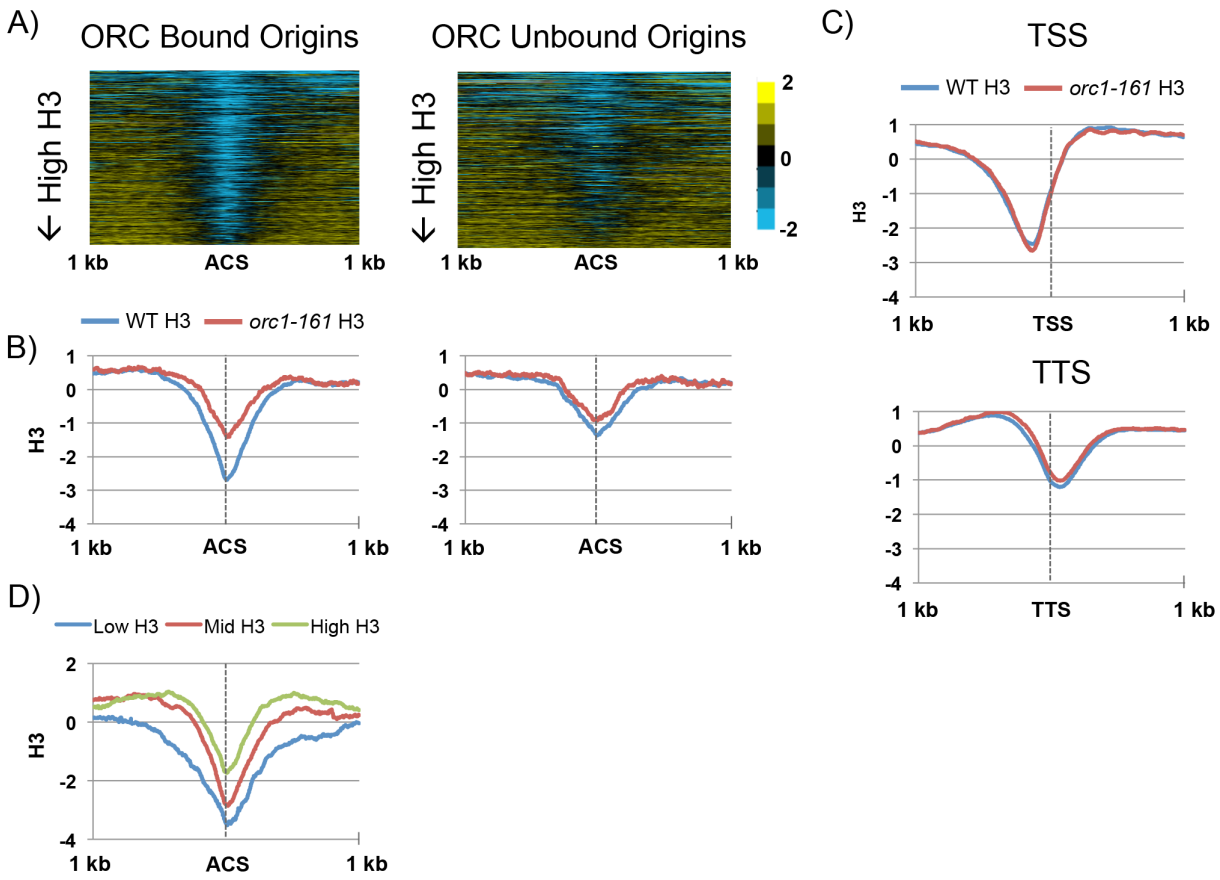

Figure 4.1 Nucleosome occupancy varies across origins in G1 and is Orc-dependent. A) Ranked H3 ChIP-seq signals (log2) in G1 aligned at the ACS for 798 predicted yeast origins from the OriDB database (Nieduszynski et al., 2007). Origins are classified based on ORC binding (397 ORC bound and 401 ORC unbound). B) Average H3 signal after z-score normalization across all ORC bound (left) and ORC unbound origins (right) spanning 1kb upstream and downstream of the ACS. The dotted line represents the midpoint of the ACS. WT H3 is shown in blue and *orc1-161* H3 is in red. C) Average H3 signal 1kb upstream and downstream of 4,551 TSSs and 5,120 TTSs (Nagalakshmi et al., 2008). D) Average H3 signals of ORC bound origins (393) classified based on average H3 levels 500bp upstream and downstream of the ACS: Low H3 includes the bottom 33% (blue), mid H3 includes the middle 33% (red), and high H3 includes top 33% (green).

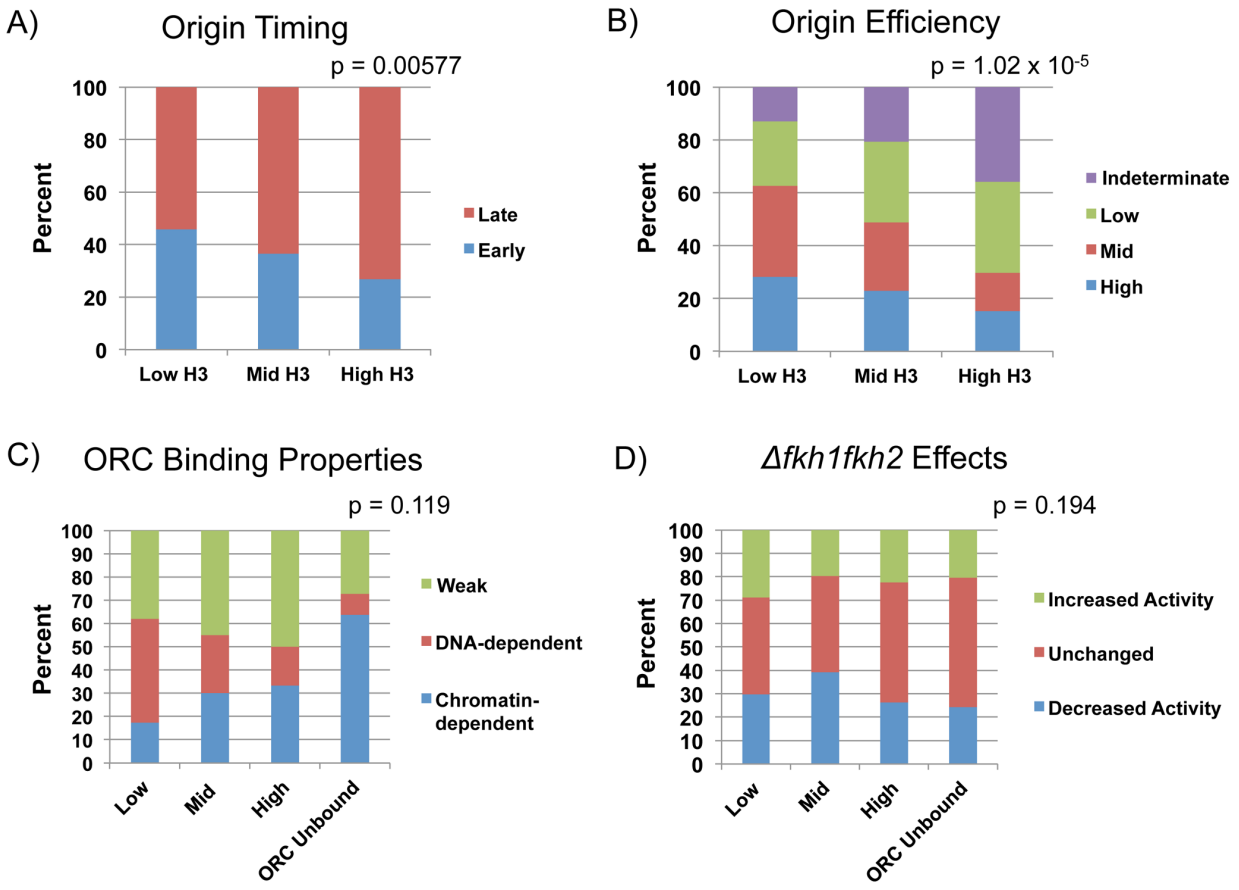

Figure 4.2 Nucleosome occupancy in G1 correlates with origin properties.
A) All origins classified by nucleosome occupancy (n=393) were correlated to origin timing (late or early firing), which was defined from previous BrdU experiments in the presence of HU (Belsky et al., 2015). B) Correlation of nucleosome occupancy with origin efficiency. Previously established values for origin efficiency metric (McGuffee et al., 2013) were used to classify origins as high (blue), mid (red), low (green) or indeterminate (purple) efficiency (see Materials and Methods). C) Nucleosome occupancy correlated to ORC binding for 66 origins, which were previously classified as DNA-dependent (red), chromatin-dependent (blue) or weak (green) (Hoggard et al., 2013). D) Nucleosome occupancy was correlated to origins where activation depended on Forkhead proteins (Knott et al., 2012). Origins that decrease (blue), increase (green) or unchanged (red) in activity in *fkh1fkh2* mutant are shown.

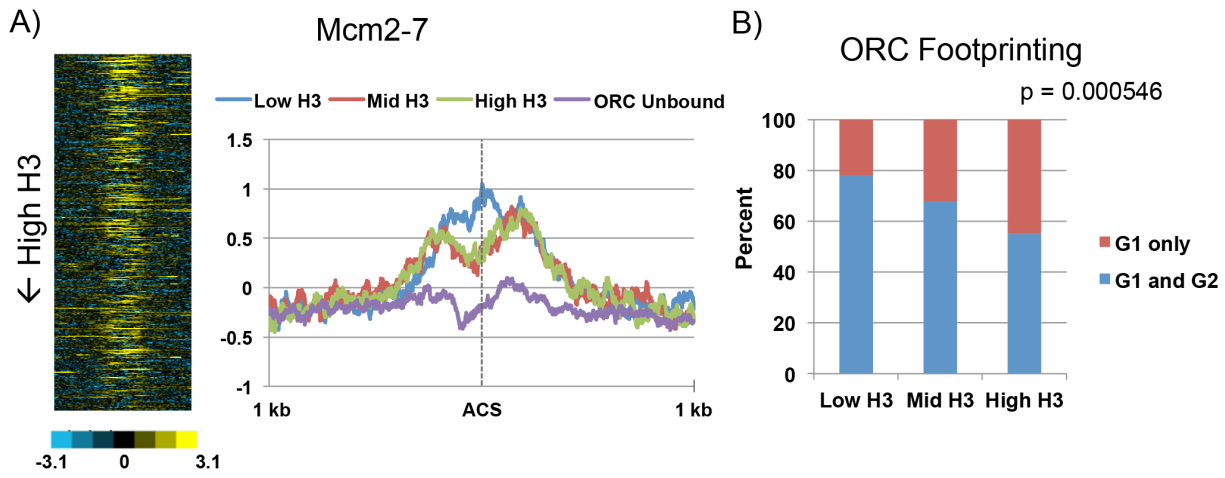

Figure 4.3 Nucleosome occupancy in G1 correlates with pre-RC binding.
A) Mcm2-7 ChIP signals (Belsky et al., 2015) were correlated to nucleosome occupancy. The left panel shows a heat map of Mcm2-7 signals across all ORC bound origins, ranked based on H3 levels. The right panel displays average Mcm2-7 binding aligned at the ACS based on classification by nucleosome occupancy with low H3 in blue, mid H3 in red, high H3 in green and ORC unbound in purple. B) Nucleosome occupancy classes were correlated to cell-cycle ORC footprinting data (Belsky et al., 2015). Blue denotes ORC binding of origins in both G1 and G2, while red denotes ORC binding in G1 only.

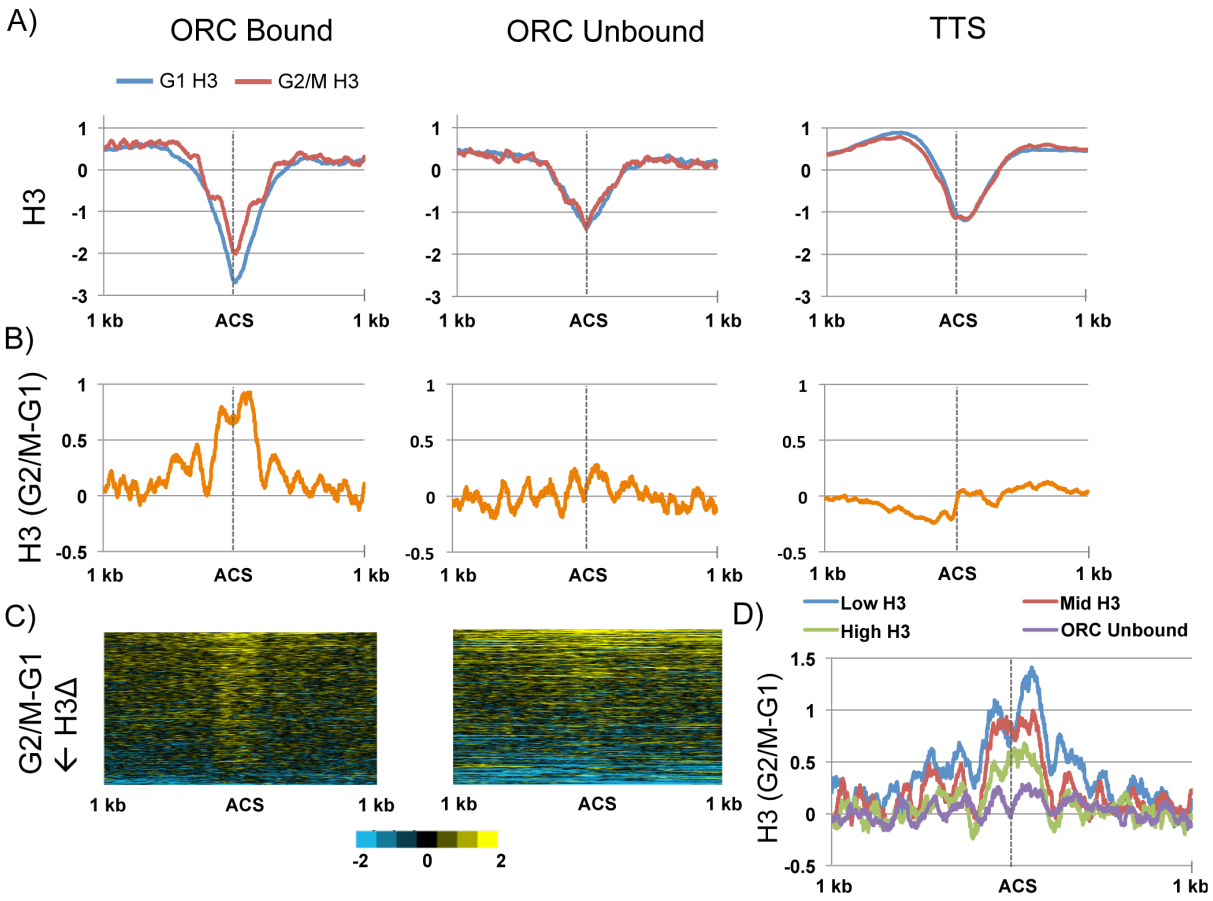

Figure 4.4 ORC bound origins lose nucleosomes during the G2/M to G1 transition.
A) H3 ChIP signals (log2) were averaged within a 2kb window for ORC bound origins (left), ORC unbound origins (center), and TTSs (right) with signals from G1 in blue and G2/M in red. The dotted line represents the midpoint of the ACS. B) The difference in H3 occupancy (log2) between G2/M and G1 (G2M-G1) was plotted in orange for each corresponding group of origins or TSSs. C) Heat maps of the difference in H3 signasl from G2/M to G1 within a 2kb window of the ACS for ORC bound and ORC unbound origins that are ranked based on the difference in nucleosome occupancy. D) The decrease in nucleosome occupancy between G2/M and G1was correlated to origins classified by occupancy in G1. Low H3 is shown in blue, mid H3 is shown in red, high H3 is shown in green and ORC unbound is shown in purple.

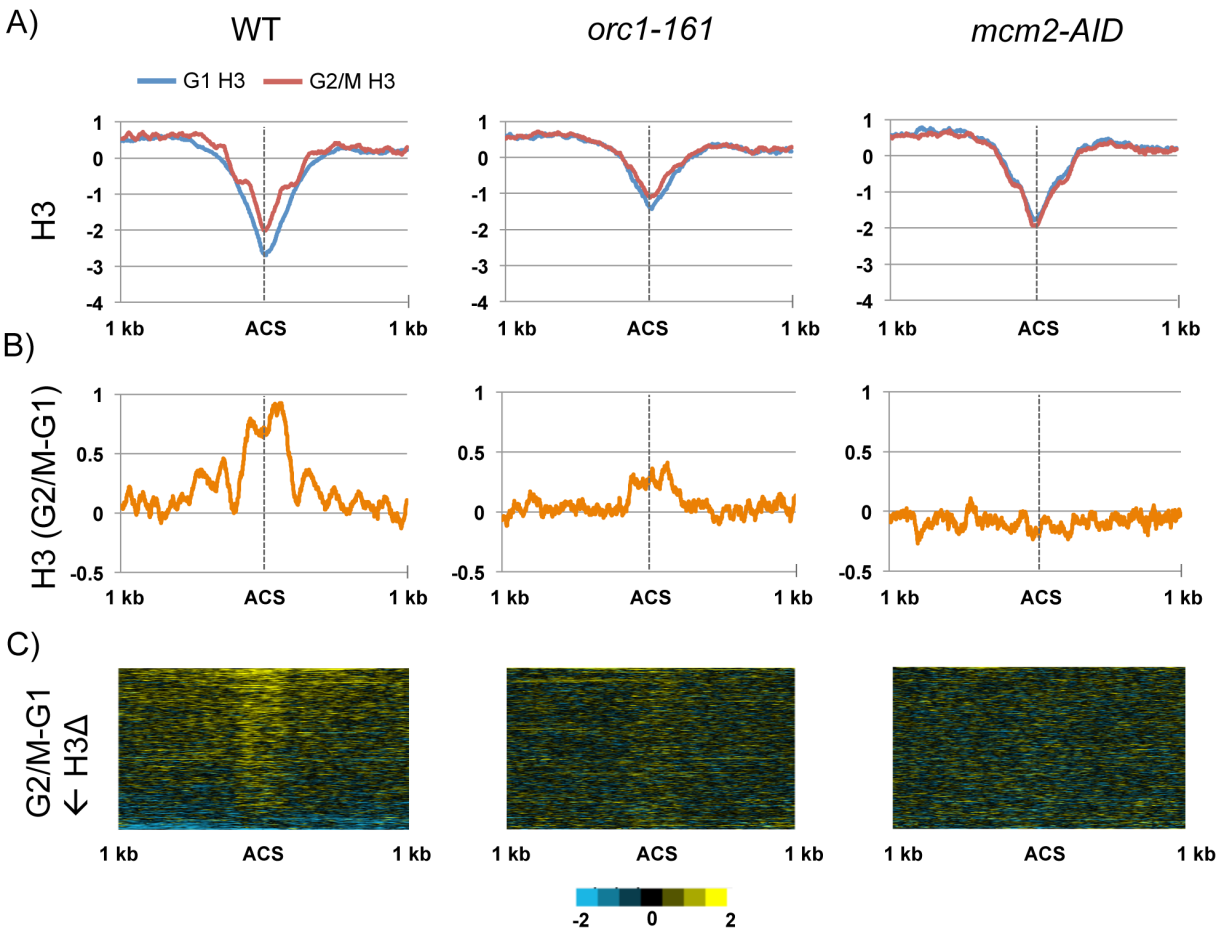

Figure 4.5 The decrease in nucleosome occupancy from G2/M to G1 is pre-RC dependent. A) The average H3 signals around ORC bound origins from wild type (WT), *orc1-161*, and *mcm2-AID* during G1 and G2/M. G1 signals are in blue and G2/M signals are in red. B) The difference in nucleosome occupancy between G2/M and G1 (log 2) is shown in orange. C) Heat maps of H3 ChIP signals at all ORC bound origins that are ranked by the difference in H3 levels between G2/M and G1. For the purposes of comparison, wild type profiles are shown again from Fig 4.

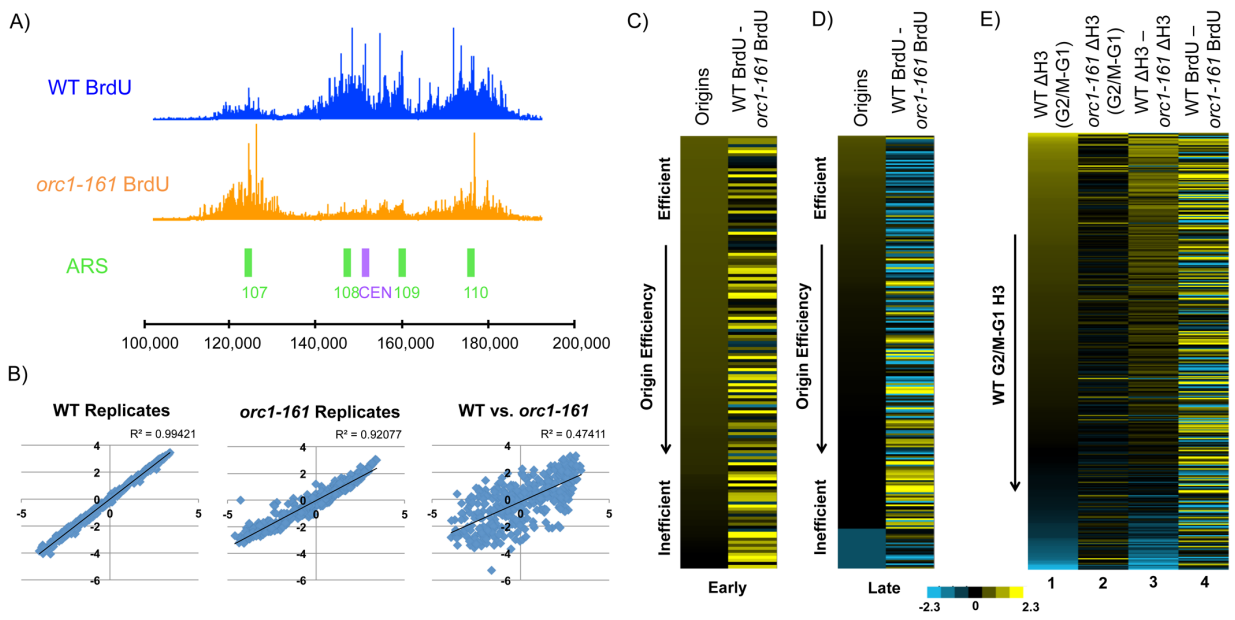

Figure 4.6 Loss of changes in nucleosome occupancy is accompanied with changes in origin usage profiles in *orc1-161*.

A) A snapshot of BrdU profiles for WT in blue and *orc1-161* in orange. The region spans from 100,000 and 200,000 on chromosome I. The green bars indicate annotated ARSs and the purple bar indicates the centromere. B) Graphs correlating averaged BrdU signals from all origins. Biological replicates of BrdU profiles from WT (left) and *orc1-161* (center) were correlated. WT and *orc1-161* profiles (right) were correlated with each other. C) Heat map of the difference in average BrdU signal at early firing origins between WT and *orc1-161*, which is ranked based on efficiency (OEM = -1 to 1) (Belsky et al., 2015; McGuffee et al., 2013). D) Same as C), but for late firing origins. E) Heat maps of the average difference in nucleosome occupancy between G2/M and G1 in wild type (column 1), difference in nucleosome occupancy in *orc1-161* (column 2), difference in nucleosome changes that are caused by *orc1-161* (column 3), and difference in BrdU signal between WT and *orc1-161*. The columns are sorted based on column 1 for all ORC bound origins.

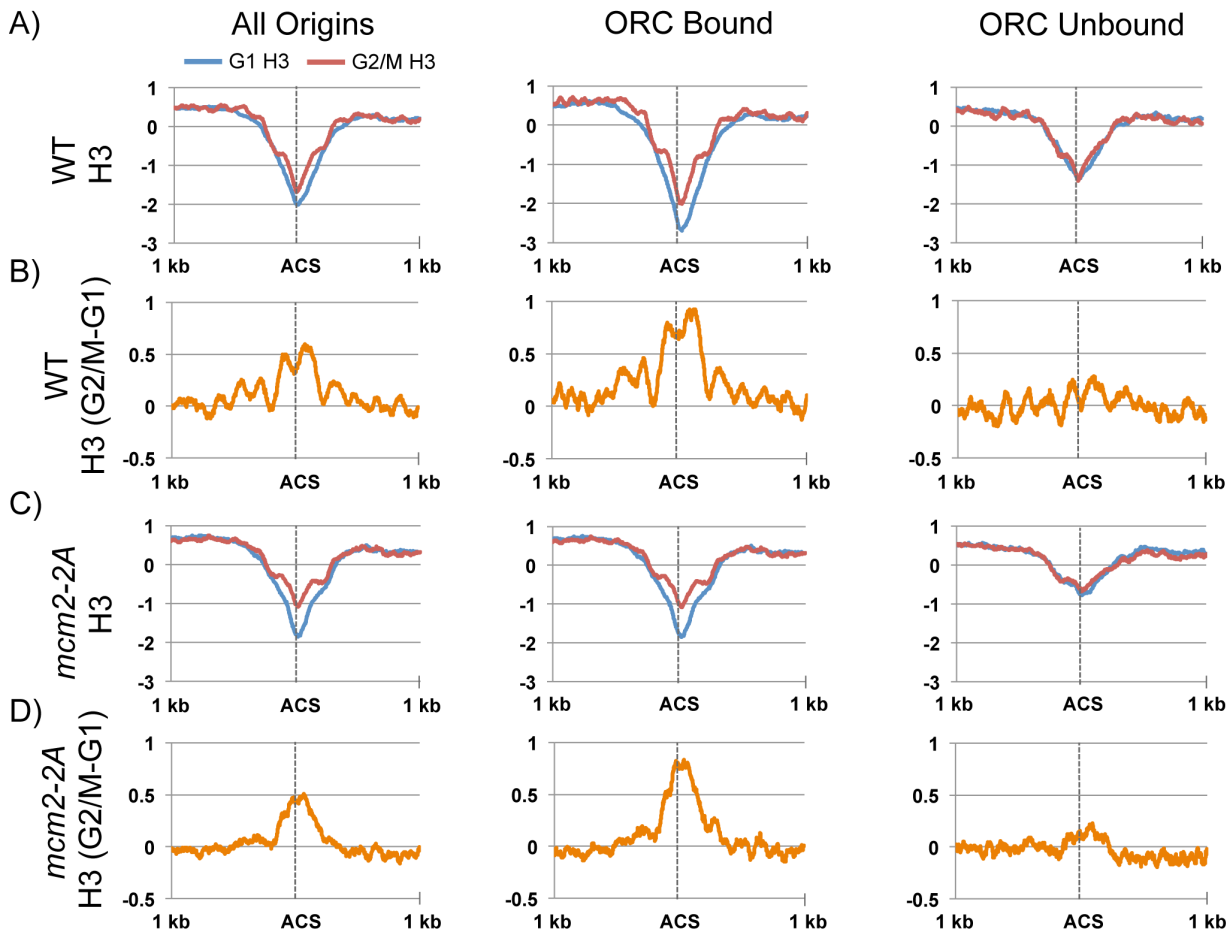

Figure 4.7 Changes in nucleosome occupancy around origins are independent of MCM histone binding activity.

A) Average H3 signals 1kb upstream and downstream of the ACS for all origins, ORC bound origins and ORC unbound origins. H3 signals from G1 are shown in blue and signals from G2/M are shown in red. The dotted lines represent the midpoint of the ACS. B) The difference in H3 from G2/M to G2 is graphed in orange for the corresponding origins. The WT plots are shown here again for the sake of comparison to the *mcm2-2A* mutant. C) Average H3 signals around origins for *mcm2-2A* in G1 and G2/M. D) The difference of average H3 in G2/M and G1 in orange.

Table 4.1 Chapter 4 yeast strains

Strain	Genotype	Source
W1588-4c	*MAT***a** *ade2-1 can1-100 his3-11,15 leu2-3,112 trp1-1 ura3-1 RAD5+*	(Thomas and Rothstein, 1989; Zhao *et al.* 1998)
YTT4709	*Pol1-3FLAG-KanMX*	(Rodriguez and Tsukiyama, 2013)
YTT5095	*Pol1-2L-3FLAG-KanMX*	(Rodriguez and Tsukiyama, 2013)
YTT6270	*URA3::p306-BrdUinc*	This study
YTT6271	*URA3::p306-BrdUinc*	This study
OAy661	*Δbar1:hisG Δorc1:: hisG leu2::orc1-161 (LEU2)*	(Aparicio *et al.*, 1997)
YTT6290	*Δbar1:hisG Δorc1:: hisG leu2::orc1-161 (LEU2) URA3::p306-BrdUinc*	This study
YTT6291	*Δbar1:hisG Δorc1:: hisG leu2::orc1-161 (LEU2) URA3::p306-BrdUinc*	This study
YTT6269	*Mcm2-AID::KanMX ura3-1:OSTIR1-9myc:URA3*	This study
YTT6266	*Mcm2-AID::KanMX ura3-1:OSTIR1-9myc:URA3*	This study
YMP504-13	*mcm2-Y82A-Y91A-9MYC (klTRP1)*	(Foltman *et al.*, 2013)
YMP514	*mcm2-Y82A-Y91A::Hyg (hphNT)*	(Foltman *et al.*, 2013)

*All strains are MATa and congenic to W1588-4c with a correction for the weak *rad5* allele

CHAPTER 5

Conclusions and Perspectives

In this dissertation I showed the importance of chromatin structure on many DNA-dependent processes. Many studies have highlighted the importance of chromatin remodeling factors in transcription (Clapier and Cairns, 2009). However more recent investigations also show their relevance in other pathways (Clapier and Cairns, 2009). My findings reveal novel roles for chromatin regulation, and contribute to elucidating the regulatory mechanisms of a wide variety of processes important for genomic stability. Here, I have shown that chromatin remodeling factors Isw2 and Ino80 oppose functions of checkpoint activators. I also show that Isw2 and Ino80 also have previously unknown roles at the rDNA and telomeres. Specifically, Isw2 and Ino80 are important for regulating structure and activities at the rDNA and telomeres. Finally, in collaboration with Jairo Rodriguez, we show that nucleosome occupancy is a previously underappreciated parameter for origin activation.

In all of these major cellular processes, there are drastic changes in chromatin structure. The major questions going forward are to understand how these changes in chromatin are established and what their functional consequences are. In order to address these questions, it will be important to understand how chromatin regulators are recruited to their targeted loci. Transcription factors were shown to recruit remodeling enzymes, and chromosome looping can facilitate interaction of these remodeling enzymes with other regions in the genome that are within close proximity (Gelbart et al., 2005; Goldmark et al., 2000; Hartley and Madhani, 2009; Yadon et al., 2013). However, the majority of targeting mechanisms for remodeling factors are unknown. Furthermore, it will be important to characterize all of the functional consequences

that occur as chromatin structure changes. Here I discuss some of the potential mechanisms of targeting and subsequent outcomes that occur from the changes in chromatin structure.

Mechanisms of Isw2 and Ino80 in the replication stress response

In our genetic screen, we concluded that Isw2 and Ino80 either function through RPA or an unknown pathway to regulate the S phase checkpoint. Furthermore, it has been shown that Isw2 and Ino80 both can interact with RPA (Au et al., 2011). One possibility is that Isw2 and Ino80 could be targeted to replication forks through RPA and function to displace RPA from stalled forks to deactivate the S phase checkpoint. In mammalian cells, HARP, which is part of the SWI/SNF family of remodeling factors, was shown to rewind RPA-ssDNA (Yusufzai and Kadonaga, 2008). Moreover, other related families of proteins, like Mot1, have been shown to interact with non-histone proteins (Auble et al., 1994). A recent study showed that chromatin remodeling factor SWI/SNF has the ability to interact and activate Mec1, the major budding yeast checkpoint kinase (Kapoor et al., 2015). This study illustrates that a chromatin remodeling factor can indeed act on a non-histone protein. Thus far, most studies have looked at chromatin remodeling factors' function on DNA and histones. However it is possible that chromatin regulators can act on other proteins.

We also examined chromatin structure at replication forks during S phase in MMS and found that chromatin accessibility was significantly reduced in *isw2 nhp10*. One of the major questions going forward is to determine whether this change in chromatin accessibility is a cause or result of the checkpoint phenotype. One possibility is that Isw2 and Ino80 could be targeted by RPA to promote accessibility to checkpoint repressors, which would thereby deactivate the checkpoint. Alternatively, the change in accessibility could be a result of the presence of more

checkpoint factors present at the fork. Further experimentation will be needed to test these models.

Roles for Isw2 and Ino80 at repetitive elements

Increasing evidence suggests that chromatin remodeling factors function at repetitive elements (Dror and Winston, 2004; Manning and Peterson, 2014; Postepska-Igielska and Grummt, 2014; Xue et al., 2015). Ino80 has been implicated in functioning at telomeres to establish boundaries for Sir proteins and interact with telomere components to regulate telomere length and telomere telomere position effect (TPE) (Xue et al., 2015). SWI/SNF has also been implicated in interacting and evicting Sirs at telomeres (Manning and Peterson, 2014), and in silencing Pol II transcription at the rDNA (Dror and Winston, 2004). NoRC is a mammalian SWI/SNF family member that has been shown to be involved in silencing at telomeres, centromeres and the rDNA (Postepska-Igielska and Grummt, 2014). However, while many of these studies show that chromatin remodeling factors have roles at these heterochromatic domains, the mechanisms by which they function are still poorly understood. Isw2 and Ino80 targeting to the rDNA still needs to be determined. Previously our lab showed that Isw2 could localize to Ty elements through Pol III transcription factor TFIIIB subunit Bdp1 (Bachman et al., 2005). Given that Isw2 had minor roles in regulating Ty transposition and transcription, it was puzzling to us as to why Bdp1 recruited Isw2. However, one explanation could be that the primary function of Isw2 recruitment by Bdp1 is to regulate transcription of the 5S rRNA. This raises the question of whether Isw2 and Ino80 can also be targeted by a Pol I transcription factor.

It is interesting that Isw2 and Ino80 have such strong interactions with telomere mutants, yet they do not seem to be targeted to the telomeres. We cannot rule out the possibility that Isw2

and Ino80 still interact with telomeres through looping or binding to the telomere ends. Thus chromosome conformation capture (3C) experiments will be useful to determine whether Isw2 and Ino80 are actually targeted to the telomere through interchromosomal interactions. Alternatively, Isw2 and Ino80 could affect telomeres indirectly by altering factor distribution. At the rDNA, Isw2 and Ino80 seem to be promoting a more open conformation resulting in activation of rRNA transcription. These changes could alter not only Sir distribution but also change localization or activity of other factors to indirectly influence telomere function.

Mechanisms of regulating nucleosome occupancy in origin activation

As mentioned, there are multiple replication origins throughout the genome. However, as replication factors are limited (Mantiero et al., 2011), origin activation must be properly regulated to prevent genome instability. We show that among other factors, nucleosome occupancy is also a key contributor to regulating origin firing. It is clear that nucleosome occupancy varies widely among origins. What establishes the difference in nucleosome occupancy in some origins versus others? The most likely explanation is that a chromatin regulator alters nucleosome occupancy and targeted to origins by pre-RC components. Alternatively, a chromatin regulator could alter pre-RC binding, which would in turn affect nucleosome occupancy because nucleosomes can compete with DNA binding factors. Either way, we believe a chromatin regulator is involved in altering nucleosome occupancy. We preliminarily screened for chromatin remodeling factors that could be affecting nucleosome occupancy between G2/M and G1, and thus far the most promising candidate is remodeling factor SWI/SNF. If SWI/SNF is the factor responsible for nucleosome occupancy at origins, we favor the first model because SWI/SNF was shown to bind to the Orc1 BAH domain (Manning

and Peterson, 2014). Once targeted by ORC, SWI/SNF could evict nucleosomes from origins, resulting in more space for the replication machinery to bind.

One of the other major questions from our findings is how Isw2 and Ino80 affect origin firing in the context that multiple other factors have been shown to affect origin activation (Belsky et al., 2015; Hoggard et al., 2013; Knott et al., 2012; Vogelauer et al., 2002). There are clear instances in which origin activation is not dictated by nucleosome occupancy. Indeed, origins that were affected by Fkh1 and Fkh2 did not correlate with nucleosome occupancy. Chromosomal context also seems to override nucleosome occupancy, as there was no clear trend in occupancy and firing with origins located in telomeres or centromeres (data not shown). Going forward further investigations of which factors are important in which contexts will be needed to better understand origin regulation.

Chromatin structure is integral to genome stability

Many processes in the cell are essential and when they are misregulated, genomic instability occurs. There is emerging evidence that chromatin structure is a key regulatory step in maintaining genome stability. Both here and in other studies, chromatin regulators have increasing roles in DNA repair, chromosome segregation, rDNA stability and telomere homeostasis (Clapier and Cairns, 2009). Moreover, many chromatin regulator mutations result in disease and have emerging roles in cancer (Hargreaves and Crabtree, 2011). However because of their ubiquitous roles in maintaining genomic stability it is currently difficult to understand which mutations are responsible for which disorders. Therefore it will be crucial to understand their mechanisms in all of these pathways so we can specifically determine which mechanisms are clinically relevant. Interestingly, chromatin remodeling factors of all families seem to be

involved in many similar pathways (Clapier and Cairns, 2009). The different families have various activities and functions, so studies showing how all these factors interact and cooperate with each other to regulate chromatin will be significant.

BIBLIOGRAPHY

Alcasabas, A.A., Osborn, A.J., Bachant, J., Hu, F., Werler, P.J., Bousset, K., Furuya, K., Diffley, J.F., Carr, A.M., and Elledge, S.J. (2001). Mrc1 transduces signals of DNA replication stress to activate Rad53. Nature cell biology *3*, 958-965.

Alcid, E.A., and Tsukiyama, T. (2014). ATP-dependent chromatin remodeling shapes the long noncoding RNA landscape. Genes & development *28*, 2348-2360.

Alvino, G.M., Collingwood, D., Murphy, J.M., Delrow, J., Brewer, B.J., and Raghuraman, M.K. (2007). Replication in hydroxyurea: it's a matter of time. Molecular and cellular biology *27*, 6396-6406.

Aparicio, O.M., Weinstein, D.M., and Bell, S.P. (1997). Components and dynamics of DNA replication complexes in S. cerevisiae: redistribution of MCM proteins and Cdc45p during S phase. Cell *91*, 59-69.

Au, T.J., Rodriguez, J., Vincent, J.A., and Tsukiyama, T. (2011). ATP-dependent chromatin remodeling factors tune S phase checkpoint activity. Molecular and cellular biology *31*, 4454-4463.

Auble, D.T., Hansen, K.E., Mueller, C.G., Lane, W.S., Thorner, J., and Hahn, S. (1994). Mot1, a global repressor of RNA polymerase II transcription, inhibits TBP binding to DNA by an ATP-dependent mechanism. Genes & development *8*, 1920-1934.

Bachman, N., Gelbart, M.E., Tsukiyama, T., and Boeke, J.D. (2005). TFIIIB subunit Bdp1p is required for periodic integration of the Ty1 retrotransposon and targeting of Isw2p to S. cerevisiae tDNAs. Genes & development *19*, 955-964.

Bell, S.P., and Dutta, A. (2002). DNA replication in eukaryotic cells. Annual review of biochemistry *71*, 333-374.

Bell, S.P., and Stillman, B. (1992). ATP-dependent recognition of eukaryotic origins of DNA replication by a multiprotein complex. Nature *357*, 128-134.

Belsky, J.A., MacAlpine, H.K., Lubelsky, Y., Hartemink, A.J., and MacAlpine, D.M. (2015). Genome-wide chromatin footprinting reveals changes in replication origin architecture induced by pre-RC assembly. Genes & development *29*, 212-224.

Bernstein, B.E., Liu, C.L., Humphrey, E.L., Perlstein, E.O., and Schreiber, S.L. (2004). Global nucleosome occupancy in yeast. Genome biology *5*, R62.

Biswas, D., Takahata, S., Xin, H., Dutta-Biswas, R., Yu, Y., Formosa, T., and Stillman, D.J. (2008). A role for Chd1 and Set2 in negatively regulating DNA replication in Saccharomyces cerevisiae. Genetics *178*, 649-659.

Boulton, S.J., and Jackson, S.P. (1996). Identification of a Saccharomyces cerevisiae Ku80 homologue: roles in DNA double strand break rejoining and in telomeric maintenance. Nucleic acids research *24*, 4639-4648.

Branzei, D., and Foiani, M. (2009). The checkpoint response to replication stress. DNA Repair (Amst) *8*, 1038-1046.

Branzei, D., and Foiani, M. (2010). Maintaining genome stability at the replication fork. Nature reviews Molecular cell biology *11*, 208-219.

Brewer, B.J., and Fangman, W.L. (1991). Mapping replication origins in yeast chromosomes. BioEssays : news and reviews in molecular, cellular and developmental biology *13*, 317-322.

Burkhalter, M.D., and Sogo, J.M. (2004). rDNA enhancer affects replication initiation and mitotic recombination: Fob1 mediates nucleolytic processing independently of replication. Molecular cell *15*, 409-421.
Byun, T.S., Pacek, M., Yee, M.C., Walter, J.C., and Cimprich, K.A. (2005). Functional uncoupling of MCM helicase and DNA polymerase activities activates the ATR-dependent checkpoint. Genes & development *19*, 1040-1052.
Chen, S.H., Albuquerque, C.P., Liang, J., Suhandynata, R.T., and Zhou, H. (2010). A proteome-wide analysis of kinase-substrate network in the DNA damage response. J Biol Chem *285*, 12803-12812.
Chen, X., Cui, D., Papusha, A., Zhang, X., Chu, C.D., Tang, J., Chen, K., Pan, X., and Ira, G. (2012). The Fun30 nucleosome remodeller promotes resection of DNA double-strand break ends. Nature *489*, 576-580.
Clapier, C.R., and Cairns, B.R. (2009). The biology of chromatin remodeling complexes. Annual review of biochemistry *78*, 273-304.
Costelloe, T., Louge, R., Tomimatsu, N., Mukherjee, B., Martini, E., Khadaroo, B., Dubois, K., Wiegant, W.W., Thierry, A., Burma, S.*, et al.* (2012). The yeast Fun30 and human SMARCAD1 chromatin remodellers promote DNA end resection. Nature *489*, 581-584.
Crabbe, L., Thomas, A., Pantesco, V., De Vos, J., Pasero, P., and Lengronne, A. (2010). Analysis of replication profiles reveals key role of RFC-Ctf18 in yeast replication stress response. Nature structural & molecular biology *17*, 1391-1397.
Czajkowsky, D.M., Liu, J., Hamlin, J.L., and Shao, Z. (2008). DNA combing reveals intrinsic temporal disorder in the replication of yeast chromosome VI. Journal of molecular biology *375*, 12-19.
Dammann, R., Lucchini, R., Koller, T., and Sogo, J.M. (1993). Chromatin structures and transcription of rDNA in yeast Saccharomyces cerevisiae. Nucleic acids research *21*, 2331-2338.
Dang, W., Kagalwala, M.N., and Bartholomew, B. (2006). Regulation of ISW2 by concerted action of histone H4 tail and extranucleosomal DNA. Molecular and cellular biology *26*, 7388-7396.
Dang, W., Sutphin, G.L., Dorsey, J.A., Otte, G.L., Cao, K., Perry, R.M., Wanat, J.J., Saviolaki, D., Murakami, C.J., Tsuchiyama, S.*, et al.* (2014). Inactivation of yeast Isw2 chromatin remodeling enzyme mimics longevity effect of calorie restriction via induction of genotoxic stress response. Cell metabolism *19*, 952-966.
Defossez, P.A., Prusty, R., Kaeberlein, M., Lin, S.J., Ferrigno, P., Silver, P.A., Keil, R.L., and Guarente, L. (1999). Elimination of replication block protein Fob1 extends the life span of yeast mother cells. Molecular cell *3*, 447-455.
Diffley, J.F., and Cocker, J.H. (1992). Protein-DNA interactions at a yeast replication origin. Nature *357*, 169-172.
Dror, V., and Winston, F. (2004). The Swi/Snf chromatin remodeling complex is required for ribosomal DNA and telomeric silencing in Saccharomyces cerevisiae. Molecular and cellular biology *24*, 8227-8235.
Dubey, D.D., Davis, L.R., Greenfeder, S.A., Ong, L.Y., Zhu, J.G., Broach, J.R., Newlon, C.S., and Huberman, J.A. (1991). Evidence suggesting that the ARS elements associated with silencers of the yeast mating-type locus HML do not function as chromosomal DNA replication origins. Molecular and cellular biology *11*, 5346-5355.
Eaton, M.L., Galani, K., Kang, S., Bell, S.P., and MacAlpine, D.M. (2010). Conserved nucleosome positioning defines replication origins. Genes & development *24*, 748-753.

Eng, J.K., McCormack, A.L., and Yates, J.R. (1994). An approach to correlate tandem mass spectral data of peptides with amino acid sequences in a protein database. Journal of the American Society for Mass Spectrometry *5*, 976-989.
Engels, K., Giannattasio, M., Muzi-Falconi, M., Lopes, M., and Ferrari, S. (2011). 14-3-3 Proteins regulate exonuclease 1-dependent processing of stalled replication forks. PLoS genetics *7*, e1001367.
Fazzio, T.G., Kooperberg, C., Goldmark, J.P., Neal, C., Basom, R., Delrow, J., and Tsukiyama, T. (2001). Widespread collaboration of Isw2 and Sin3-Rpd3 chromatin remodeling complexes in transcriptional repression. Molecular and cellular biology *21*, 6450-6460.
Fazzio, T.G., and Tsukiyama, T. (2003). Chromatin remodeling in vivo: evidence for a nucleosome sliding mechanism. Molecular cell *12*, 1333-1340.
Felsenfeld, G., and Groudine, M. (2003). Controlling the double helix. Nature *421*, 448-453.
Ferguson, B.M., and Fangman, W.L. (1992). A position effect on the time of replication origin activation in yeast. Cell *68*, 333-339.
Fischer, C.J., Yamada, K., and Fitzgerald, D.J. (2009). Kinetic mechanism for single-stranded DNA binding and translocation by Saccharomyces cerevisiae Isw2. Biochemistry *48*, 2960-2968.
Flanagan, J.F., and Peterson, C.L. (1999). A role for the yeast SWI/SNF complex in DNA replication. Nucleic acids research *27*, 2022-2028.
Foltman, M., Evrin, C., De Piccoli, G., Jones, R.C., Edmondson, R.D., Katou, Y., Nakato, R., Shirahige, K., and Labib, K. (2013). Eukaryotic replisome components cooperate to process histones during chromosome replication. Cell reports *3*, 892-904.
Fragkos, M., Ganier, O., Coulombe, P., and Mechali, M. (2015). DNA replication origin activation in space and time. Nature reviews Molecular cell biology *16*, 360-374.
Friedel, A.M., Pike, B.L., and Gasser, S.M. (2009). ATR/Mec1: coordinating fork stability and repair. Curr Opin Cell Biol *21*, 237-244.
Fyodorov, D.V., Blower, M.D., Karpen, G.H., and Kadonaga, J.T. (2004). Acf1 confers unique activities to ACF/CHRAC and promotes the formation rather than disruption of chromatin in vivo. Genes & development *18*, 170-183.
Ganley, A.R., Ide, S., Saka, K., and Kobayashi, T. (2009). The effect of replication initiation on gene amplification in the rDNA and its relationship to aging. Molecular cell *35*, 683-693.
Gelbart, M.E., Bachman, N., Delrow, J., Boeke, J.D., and Tsukiyama, T. (2005). Genome-wide identification of Isw2 chromatin-remodeling targets by localization of a catalytically inactive mutant. Genes & development *19*, 942-954.
Gilbert, C.S., Green, C.M., and Lowndes, N.F. (2001). Budding yeast Rad9 is an ATP-dependent Rad53 activating machine. Molecular cell *8*, 129-136.
Gilson, E., Roberge, M., Giraldo, R., Rhodes, D., and Gasser, S.M. (1993). Distortion of the DNA double helix by RAP1 at silencers and multiple telomeric binding sites. Journal of molecular biology *231*, 293-310.
Gkikopoulos, T., Schofield, P., Singh, V., Pinskaya, M., Mellor, J., Smolle, M., Workman, J.L., Barton, G.J., and Owen-Hughes, T. (2011). A role for Snf2-related nucleosome-spacing enzymes in genome-wide nucleosome organization. Science *333*, 1758-1760.
Goldmark, J.P., Fazzio, T.G., Estep, P.W., Church, G.M., and Tsukiyama, T. (2000). The Isw2 chromatin remodeling complex represses early meiotic genes upon recruitment by Ume6p. Cell *103*, 423-433.

Gonzalez-Prieto, R., Munoz-Cabello, A.M., Cabello-Lobato, M.J., and Prado, F. (2013). Rad51 replication fork recruitment is required for DNA damage tolerance. The EMBO journal *32*, 1307-1321.
Gravel, S., and Wellinger, R.J. (2002). Maintenance of double-stranded telomeric repeats as the critical determinant for cell viability in yeast cells lacking Ku. Molecular and cellular biology *22*, 2182-2193.
Greenwell, P.W., Kronmal, S.L., Porter, S.E., Gassenhuber, J., Obermaier, B., and Petes, T.D. (1995). TEL1, a gene involved in controlling telomere length in S. cerevisiae, is homologous to the human ataxia telangiectasia gene. Cell *82*, 823-829.
Greider, C.W., and Blackburn, E.H. (1985). Identification of a specific telomere terminal transferase activity in Tetrahymena extracts. Cell *43*, 405-413.
Hargreaves, D.C., and Crabtree, G.R. (2011). ATP-dependent chromatin remodeling: genetics, genomics and mechanisms. Cell research *21*, 396-420.
Hartley, P.D., and Madhani, H.D. (2009). Mechanisms that specify promoter nucleosome location and identity. Cell *137*, 445-458.
Hegnauer, A.M., Hustedt, N., Shimada, K., Pike, B.L., Vogel, M., Amsler, P., Rubin, S.M., van Leeuwen, F., Guenole, A., van Attikum, H*., et al.* (2012). An N-terminal acidic region of Sgs1 interacts with Rpa70 and recruits Rad53 kinase to stalled forks. The EMBO journal *31*, 3768-3783.
Heller, R.C., Kang, S., Lam, W.M., Chen, S., Chan, C.S., and Bell, S.P. (2011). Eukaryotic origin-dependent DNA replication in vitro reveals sequential action of DDK and S-CDK kinases. Cell *146*, 80-91.
Hendrich, B., and Bickmore, W. (2001). Human diseases with underlying defects in chromatin structure and modification. Human molecular genetics *10*, 2233-2242.
Hoggard, T., Shor, E., Muller, C.A., Nieduszynski, C.A., and Fox, C.A. (2013). A Link between ORC-origin binding mechanisms and origin activation time revealed in budding yeast. PLoS genetics *9*, e1003798.
Hustedt, N., Gasser, S.M., and Shimada, K. (2013). Replication checkpoint: tuning and coordination of replication forks in s phase. Genes *4*, 388-434.
Ide, S., Miyazaki, T., Maki, H., and Kobayashi, T. (2010). Abundance of ribosomal RNA gene copies maintains genome integrity. Science *327*, 693-696.
Iida, T., and Araki, H. (2004). Noncompetitive counteractions of DNA polymerase epsilon and ISW2/yCHRAC for epigenetic inheritance of telomere position effect in Saccharomyces cerevisiae. Molecular and cellular biology *24*, 217-227.
Iizuka, M., Matsui, T., Takisawa, H., and Smith, M.M. (2006). Regulation of replication licensing by acetyltransferase Hbo1. Molecular and cellular biology *26*, 1098-1108.
Imai, S., Armstrong, C.M., Kaeberlein, M., and Guarente, L. (2000). Transcriptional silencing and longevity protein Sir2 is an NAD-dependent histone deacetylase. Nature *403*, 795-800.
Joeng, K.S., Song, E.J., Lee, K.J., and Lee, J. (2004). Long lifespan in worms with long telomeric DNA. Nature genetics *36*, 607-611.
Jones, H.S., Kawauchi, J., Braglia, P., Alen, C.M., Kent, N.A., and Proudfoot, N.J. (2007). RNA polymerase I in yeast transcribes dynamic nucleosomal rDNA. Nature structural & molecular biology *14*, 123-130.
Kadauke, S., and Blobel, G.A. (2009). Chromatin loops in gene regulation. Biochimica et biophysica acta *1789*, 17-25.

Kall, L., Canterbury, J.D., Weston, J., Noble, W.S., and MacCoss, M.J. (2007). Semi-supervised learning for peptide identification from shotgun proteomics datasets. Nature methods *4*, 923-925.
Kanellis, P., Agyei, R., and Durocher, D. (2003). Elg1 forms an alternative PCNA-interacting RFC complex required to maintain genome stability. Current biology : CB *13*, 1583-1595.
Kapoor, P., Bao, Y., Xiao, J., Luo, J., Shen, J., Persinger, J., Peng, G., Ranish, J., Bartholomew, B., and Shen, X. (2015). Regulation of Mec1 kinase activity by the SWI/SNF chromatin remodeling complex. Genes & development *29*, 591-602.
Katou, Y., Kanoh, Y., Bando, M., Noguchi, H., Tanaka, H., Ashikari, T., Sugimoto, K., and Shirahige, K. (2003). S-phase checkpoint proteins Tof1 and Mrc1 form a stable replication-pausing complex. Nature *424*, 1078-1083.
Knott, S.R., Peace, J.M., Ostrow, A.Z., Gan, Y., Rex, A.E., Viggiani, C.J., Tavare, S., and Aparicio, O.M. (2012). Forkhead transcription factors establish origin timing and long-range clustering in S. cerevisiae. Cell *148*, 99-111.
Knott, S.R., Viggiani, C.J., Tavare, S., and Aparicio, O.M. (2009). Genome-wide replication profiles indicate an expansive role for Rpd3L in regulating replication initiation timing or efficiency, and reveal genomic loci of Rpd3 function in Saccharomyces cerevisiae. Genes & development *23*, 1077-1090.
Kobayashi, T. (2011). How does genome instability affect lifespan?: roles of rDNA and telomeres. Genes to cells : devoted to molecular & cellular mechanisms *16*, 617-624.
Kobayashi, T. (2014). Ribosomal RNA gene repeats, their stability and cellular senescence. Proceedings of the Japan Academy Series B, Physical and biological sciences *90*, 119-129.
Kobayashi, T., and Ganley, A.R. (2005). Recombination regulation by transcription-induced cohesin dissociation in rDNA repeats. Science *309*, 1581-1584.
Kobayashi, T., Heck, D.J., Nomura, M., and Horiuchi, T. (1998). Expansion and contraction of ribosomal DNA repeats in Saccharomyces cerevisiae: requirement of replication fork blocking (Fob1) protein and the role of RNA polymerase I. Genes & development *12*, 3821-3830.
Kobayashi, T., Horiuchi, T., Tongaonkar, P., Vu, L., and Nomura, M. (2004). SIR2 regulates recombination between different rDNA repeats, but not recombination within individual rRNA genes in yeast. Cell *117*, 441-453.
Kondo, T., Wakayama, T., Naiki, T., Matsumoto, K., and Sugimoto, K. (2001). Recruitment of Mec1 and Ddc1 checkpoint proteins to double-strand breaks through distinct mechanisms. Science *294*, 867-870.
Kubota, T., Hiraga, S., Yamada, K., Lamond, A.I., and Donaldson, A.D. (2011). Quantitative proteomic analysis of chromatin reveals that Ctf18 acts in the DNA replication checkpoint. Molecular & cellular proteomics : MCP *10*, M110 005561.
Kubota, T., Nishimura, K., Kanemaki, M.T., and Donaldson, A.D. (2013). The Elg1 replication factor C-like complex functions in PCNA unloading during DNA replication. Molecular cell *50*, 273-280.
Kubota, T., Stead, D.A., Hiraga, S., ten Have, S., and Donaldson, A.D. (2012). Quantitative proteomic analysis of yeast DNA replication proteins. Methods *57*, 196-202.
Kueng, S., Oppikofer, M., and Gasser, S.M. (2013). SIR proteins and the assembly of silent chromatin in budding yeast. Annual review of genetics *47*, 275-306.
Kuhn, H., Hierlmeier, T., Merl, J., Jakob, S., Aguissa-Toure, A.H., Milkereit, P., and Tschochner, H. (2009). The Noc-domain containing C-terminus of Noc4p mediates both formation of the Noc4p-Nop14p submodule and its incorporation into the SSU processome. PloS one *4*, e8370.

Kumar, S., and Burgers, P.M. (2013). Lagging strand maturation factor Dna2 is a component of the replication checkpoint initiation machinery. Genes & development *27*, 313-321.
Lee, C.K., Shibata, Y., Rao, B., Strahl, B.D., and Lieb, J.D. (2004). Evidence for nucleosome depletion at active regulatory regions genome-wide. Nature genetics *36*, 900-905.
Li, B., Carey, M., and Workman, J.L. (2007). The role of chromatin during transcription. Cell *128*, 707-719.
Li, J., Langst, G., and Grummt, I. (2006). NoRC-dependent nucleosome positioning silences rRNA genes. The EMBO journal *25*, 5735-5741.
Li, J.M., Tetzlaff, M.T., and Elledge, S.J. (2008). Identification of MSA1, a cell cycle-regulated, dosage suppressor of drc1/sld2 and dpb11 mutants. Cell Cycle *7*, 3388-3398.
Licklider, L.J., Thoreen, C.C., Peng, J., and Gygi, S.P. (2002). Automation of nanoscale microcapillary liquid chromatography-tandem mass spectrometry with a vented column. Analytical chemistry *74*, 3076-3083.
Linskens, M.H., and Huberman, J.A. (1988). Organization of replication of ribosomal DNA in Saccharomyces cerevisiae. Molecular and cellular biology *8*, 4927-4935.
Lipford, J.R., and Bell, S.P. (2001). Nucleosomes positioned by ORC facilitate the initiation of DNA replication. Molecular cell *7*, 21-30.
Lisby, M., Barlow, J.H., Burgess, R.C., and Rothstein, R. (2004). Choreography of the DNA damage response: spatiotemporal relationships among checkpoint and repair proteins. Cell *118*, 699-713.
Luger, K., Mader, A.W., Richmond, R.K., Sargent, D.F., and Richmond, T.J. (1997). Crystal structure of the nucleosome core particle at 2.8 A resolution. Nature *389*, 251-260.
Lundblad, V., and Szostak, J.W. (1989). A mutant with a defect in telomere elongation leads to senescence in yeast. Cell *57*, 633-643.
Maicher, A., Kastner, L., Dees, M., and Luke, B. (2012). Deregulated telomere transcription causes replication-dependent telomere shortening and promotes cellular senescence. Nucleic acids research *40*, 6649-6659.
Majka, J., Niedziela-Majka, A., and Burgers, P.M. (2006). The checkpoint clamp activates Mec1 kinase during initiation of the DNA damage checkpoint. Molecular cell *24*, 891-901.
Manning, B.J., and Peterson, C.L. (2014). Direct interactions promote eviction of the Sir3 heterochromatin protein by the SWI/SNF chromatin remodeling enzyme. Proceedings of the National Academy of Sciences of the United States of America *111*, 17827-17832.
Mantiero, D., Clerici, M., Lucchini, G., and Longhese, M.P. (2007). Dual role for Saccharomyces cerevisiae Tel1 in the checkpoint response to double-strand breaks. EMBO reports *8*, 380-387.
Mantiero, D., Mackenzie, A., Donaldson, A., and Zegerman, P. (2011). Limiting replication initiation factors execute the temporal programme of origin firing in budding yeast. The EMBO journal *30*, 4805-4814.
Marahrens, Y., and Stillman, B. (1992). A yeast chromosomal origin of DNA replication defined by multiple functional elements. Science *255*, 817-823.
Marshall, W.F. (2002). Order and disorder in the nucleus. Current biology : CB *12*, R185-192.
Masumoto, H., Sugino, A., and Araki, H. (2000). Dpb11 controls the association between DNA polymerases alpha and epsilon and the autonomously replicating sequence region of budding yeast. Mol Cell Biol *20*, 2809-2817.
McCarroll, R.M., and Fangman, W.L. (1988). Time of replication of yeast centromeres and telomeres. Cell *54*, 505-513.

McConnell, A.D., Gelbart, M.E., and Tsukiyama, T. (2004). Histone fold protein Dls1p is required for Isw2-dependent chromatin remodeling in vivo. Molecular and cellular biology *24*, 2605-2613.
McCune, H.J., Danielson, L.S., Alvino, G.M., Collingwood, D., Delrow, J.J., Fangman, W.L., Brewer, B.J., and Raghuraman, M.K. (2008). The temporal program of chromosome replication: genomewide replication in clb5{Delta} Saccharomyces cerevisiae. Genetics *180*, 1833-1847.
McDaniel, I.E., Lee, J.M., Berger, M.S., Hanagami, C.K., and Armstrong, J.A. (2008). Investigations of CHD1 function in transcription and development of Drosophila melanogaster. Genetics *178*, 583-587.
McGuffee, S.R., Smith, D.J., and Whitehouse, I. (2013). Quantitative, genome-wide analysis of eukaryotic replication initiation and termination. Molecular cell *50*, 123-135.
McKnight, J.N., and Tsukiyama, T. (2015). The conserved HDAC Rpd3 drives transcriptional quiescence in S. cerevisiae. Genomics data *6*, 245-248.
Miles, S., Li, L., Davison, J., and Breeden, L.L. (2013). Xbp1 directs global repression of budding yeast transcription during the transition to quiescence and is important for the longevity and reversibility of the quiescent state. PLoS genetics *9*, e1003854.
Mizuguchi, G., Shen, X., Landry, J., Wu, W.H., Sen, S., and Wu, C. (2004). ATP-driven exchange of histone H2AZ variant catalyzed by SWR1 chromatin remodeling complex. Science *303*, 343-348.
Mizuguchi, G., Tsukiyama, T., Wisniewski, J., and Wu, C. (1997). Role of nucleosome remodeling factor NURF in transcriptional activation of chromatin. Molecular cell *1*, 141-150.
Moreau, J.L., Lee, M., Mahachi, N., Vary, J., Mellor, J., Tsukiyama, T., and Goding, C.R. (2003). Regulated displacement of TBP from the PHO8 promoter in vivo requires Cbf1 and the Isw1 chromatin remodeling complex. Molecular cell *11*, 1609-1620.
Moretti, P., Freeman, K., Coodly, L., and Shore, D. (1994). Evidence that a complex of SIR proteins interacts with the silencer and telomere-binding protein RAP1. Genes & development *8*, 2257-2269.
Morrison, A.J., Highland, J., Krogan, N.J., Arbel-Eden, A., Greenblatt, J.F., Haber, J.E., and Shen, X. (2004). INO80 and gamma-H2AX interaction links ATP-dependent chromatin remodeling to DNA damage repair. Cell *119*, 767-775.
Morrison, A.J., Kim, J.A., Person, M.D., Highland, J., Xiao, J., Wehr, T.S., Hensley, S., Bao, Y., Shen, J., Collins, S.R*., et al.* (2007). Mec1/Tel1 phosphorylation of the INO80 chromatin remodeling complex influences DNA damage checkpoint responses. Cell *130*, 499-511.
Morrison, A.J., and Shen, X. (2009). Chromatin remodelling beyond transcription: the INO80 and SWR1 complexes. Nature reviews Molecular cell biology *10*, 373-384.
Muller, C.A., Hawkins, M., Retkute, R., Malla, S., Wilson, R., Blythe, M.J., Nakato, R., Komata, M., Shirahige, K., de Moura, A.P*., et al.* (2014). The dynamics of genome replication using deep sequencing. Nucleic acids research *42*, e3.
Murawska, M., Kunert, N., van Vugt, J., Langst, G., Kremmer, E., Logie, C., and Brehm, A. (2008). dCHD3, a novel ATP-dependent chromatin remodeler associated with sites of active transcription. Molecular and cellular biology *28*, 2745-2757.
Nagalakshmi, U., Wang, Z., Waern, K., Shou, C., Raha, D., Gerstein, M., and Snyder, M. (2008). The transcriptional landscape of the yeast genome defined by RNA sequencing. Science *320*, 1344-1349.
Navadgi-Patil, V.M., and Burgers, P.M. (2008). Yeast DNA replication protein Dpb11 activates the Mec1/ATR checkpoint kinase. J Biol Chem *283*, 35853-35859.

Nieduszynski, C.A., Hiraga, S., Ak, P., Benham, C.J., and Donaldson, A.D. (2007). OriDB: a DNA replication origin database. Nucleic Acids Res *35*, D40-46.
Nishimura, K., Fukagawa, T., Takisawa, H., Kakimoto, T., and Kanemaki, M. (2009). An auxin-based degron system for the rapid depletion of proteins in nonplant cells. Nature methods *6*, 917-922.
Nolis, I.K., McKay, D.J., Mantouvalou, E., Lomvardas, S., Merika, M., and Thanos, D. (2009). Transcription factors mediate long-range enhancer-promoter interactions. Proceedings of the National Academy of Sciences of the United States of America *106*, 20222-20227.
Papamichos-Chronakis, M., Krebs, J.E., and Peterson, C.L. (2006). Interplay between Ino80 and Swr1 chromatin remodeling enzymes regulates cell cycle checkpoint adaptation in response to DNA damage. Genes & development *20*, 2437-2449.
Papamichos-Chronakis, M., and Peterson, C.L. (2008). The Ino80 chromatin-remodeling enzyme regulates replisome function and stability. Nature structural & molecular biology *15*, 338-345.
Papamichos-Chronakis, M., Watanabe, S., Rando, O.J., and Peterson, C.L. (2011). Global regulation of H2A.Z localization by the INO80 chromatin-remodeling enzyme is essential for genome integrity. Cell *144*, 200-213.
Pasero, P., Bensimon, A., and Schwob, E. (2002). Single-molecule analysis reveals clustering and epigenetic regulation of replication origins at the yeast rDNA locus. Genes & development *16*, 2479-2484.
Patel, P.K., Arcangioli, B., Baker, S.P., Bensimon, A., and Rhind, N. (2006). DNA replication origins fire stochastically in fission yeast. Molecular biology of the cell *17*, 308-316.
Pellicioli, A., Lucca, C., Liberi, G., Marini, F., Lopes, M., Plevani, P., Romano, A., Di Fiore, P.P., and Foiani, M. (1999). Activation of Rad53 kinase in response to DNA damage and its effect in modulating phosphorylation of the lagging strand DNA polymerase. The EMBO journal *18*, 6561-6572.
Pfander, B., and Diffley, J.F. (2011). Dpb11 coordinates Mec1 kinase activation with cell cycle-regulated Rad9 recruitment. The EMBO journal *30*, 4897-4907.
Poot, R.A., Bozhenok, L., van den Berg, D.L., Steffensen, S., Ferreira, F., Grimaldi, M., Gilbert, N., Ferreira, J., and Varga-Weisz, P.D. (2004). The Williams syndrome transcription factor interacts with PCNA to target chromatin remodelling by ISWI to replication foci. Nature cell biology *6*, 1236-1244.
Postepska-Igielska, A., and Grummt, I. (2014). NoRC silences rRNA genes, telomeres, and centromeres. Cell Cycle *13*, 493-494.
Postepska-Igielska, A., Krunic, D., Schmitt, N., Greulich-Bode, K.M., Boukamp, P., and Grummt, I. (2013). The chromatin remodelling complex NoRC safeguards genome stability by heterochromatin formation at telomeres and centromeres. EMBO reports *14*, 704-710.
Raghuraman, M.K., Brewer, B.J., and Fangman, W.L. (1997). Cell cycle-dependent establishment of a late replication program. Science *276*, 806-809.
Raghuraman, M.K., Winzeler, E.A., Collingwood, D., Hunt, S., Wodicka, L., Conway, A., Lockhart, D.J., Davis, R.W., Brewer, B.J., and Fangman, W.L. (2001). Replication dynamics of the yeast genome. Science *294*, 115-121.
Remus, D., Beuron, F., Tolun, G., Griffith, J.D., Morris, E.P., and Diffley, J.F. (2009). Concerted loading of Mcm2-7 double hexamers around DNA during DNA replication origin licensing. Cell *139*, 719-730.

Rodriguez, J., McKnight, J.N., and Tsukiyama, T. (2014). Genome-Wide Analysis of Nucleosome Positions, Occupancy, and Accessibility in Yeast: Nucleosome Mapping, High-Resolution Histone ChIP, and NCAM. Curr Protoc Mol Biol *108*, 21 28 21-21 28 16.
Rodriguez, J., and Tsukiyama, T. (2013). ATR-like kinase Mec1 facilitates both chromatin accessibility at DNA replication forks and replication fork progression during replication stress. Genes Dev *27*, 74-86.
Rouse, J., and Jackson, S.P. (2002). Lcd1p recruits Mec1p to DNA lesions in vitro and in vivo. Molecular cell *9*, 857-869.
Roy, R., Meier, B., McAinsh, A.D., Feldmann, H.M., and Jackson, S.P. (2004). Separation-of-function mutants of yeast Ku80 reveal a Yku80p-Sir4p interaction involved in telomeric silencing. J Biol Chem *279*, 86-94.
Royce, T.E., Carriero, N.J., and Gerstein, M.B. (2007). An efficient pseudomedian filter for tiling microrrays. BMC bioinformatics *8*, 186.
Ruiz, C., Escribano, V., Morgado, E., Molina, M., and Mazon, M.J. (2003). Cell-type-dependent repression of yeast a-specific genes requires Itc1p, a subunit of the Isw2p-Itc1p chromatin remodelling complex. Microbiology *149*, 341-351.
Santoro, R., Li, J., and Grummt, I. (2002). The nucleolar remodeling complex NoRC mediates heterochromatin formation and silencing of ribosomal gene transcription. Nature genetics *32*, 393-396.
Shen, X., Mizuguchi, G., Hamiche, A., and Wu, C. (2000). A chromatin remodelling complex involved in transcription and DNA processing. Nature *406*, 541-544.
Sherriff, J.A., Kent, N.A., and Mellor, J. (2007). The Isw2 chromatin-remodeling ATPase cooperates with the Fkh2 transcription factor to repress transcription of the B-type cyclin gene CLB2. Molecular and cellular biology *27*, 2848-2860.
Shimada, K., Oma, Y., Schleker, T., Kugou, K., Ohta, K., Harata, M., and Gasser, S.M. (2008). Ino80 chromatin remodeling complex promotes recovery of stalled replication forks. Current biology : CB *18*, 566-575.
Simpson, R.T. (1990). Nucleosome positioning can affect the function of a cis-acting DNA element in vivo. Nature *343*, 387-389.
Sinclair, D.A., and Guarente, L. (1997). Extrachromosomal rDNA circles--a cause of aging in yeast. Cell *91*, 1033-1042.
Singer, M.S., Kahana, A., Wolf, A.J., Meisinger, L.L., Peterson, S.E., Goggin, C., Mahowald, M., and Gottschling, D.E. (1998). Identification of high-copy disruptors of telomeric silencing in Saccharomyces cerevisiae. Genetics *150*, 613-632.
Soutoglou, E., and Misteli, T. (2007). Mobility and immobility of chromatin in transcription and genome stability. Current opinion in genetics & development *17*, 435-442.
Strohner, R., Nemeth, A., Nightingale, K.P., Grummt, I., Becker, P.B., and Langst, G. (2004). Recruitment of the nucleolar remodeling complex NoRC establishes ribosomal DNA silencing in chromatin. Molecular and cellular biology *24*, 1791-1798.
Sugimoto, N., Yugawa, T., Iizuka, M., Kiyono, T., and Fujita, M. (2011). Chromatin Remodeler Sucrose Nonfermenting 2 Homolog (SNF2H) Is Recruited onto DNA Replication Origins through Interaction with Cdc10 Protein-dependent Transcript 1 (Cdt1) and Promotes Pre-replication Complex Formation. J Biol Chem *286*, 39200-39210.
Sugiyama, T., and Kowalczykowski, S.C. (2002). Rad52 protein associates with replication protein A (RPA)-single-stranded DNA to accelerate Rad51-mediated displacement of RPA and presynaptic complex formation. J Biol Chem *277*, 31663-31672.

Szyjka, S.J., Aparicio, J.G., Viggiani, C.J., Knott, S., Xu, W., Tavare, S., and Aparicio, O.M. (2008). Rad53 regulates replication fork restart after DNA damage in Saccharomyces cerevisiae. Genes & development *22*, 1906-1920.
Szyjka, S.J., Viggiani, C.J., and Aparicio, O.M. (2005). Mrc1 is required for normal progression of replication forks throughout chromatin in S. cerevisiae. Molecular cell *19*, 691-697.
Takahashi, Y.H., Schulze, J.M., Jackson, J., Hentrich, T., Seidel, C., Jaspersen, S.L., Kobor, M.S., and Shilatifard, A. (2011). Dot1 and histone H3K79 methylation in natural telomeric and HM silencing. Molecular cell *42*, 118-126.
Tanaka, H., Katou, Y., Yagura, M., Saitoh, K., Itoh, T., Araki, H., Bando, M., and Shirahige, K. (2009). Ctf4 coordinates the progression of helicase and DNA polymerase alpha. Genes to cells : devoted to molecular & cellular mechanisms *14*, 807-820.
Thomas, B.J., and Rothstein, R. (1989). The genetic control of direct-repeat recombination in Saccharomyces: the effect of rad52 and rad1 on mitotic recombination at GAL10, a transcriptionally regulated gene. Genetics *123*, 725-738.
Tkach, J.M., Yimit, A., Lee, A.Y., Riffle, M., Costanzo, M., Jaschob, D., Hendry, J.A., Ou, J., Moffat, J., Boone, C.*, et al.* (2012). Dissecting DNA damage response pathways by analysing protein localization and abundance changes during DNA replication stress. Nature cell biology *14*, 966-976.
Travesa, A., Duch, A., and Quintana, D.G. (2008). Distinct phosphatases mediate the deactivation of the DNA damage checkpoint kinase Rad53. J Biol Chem *283*, 17123-17130.
Udugama, M., Sabri, A., and Bartholomew, B. The INO80 ATP-dependent chromatin remodeling complex is a nucleosome spacing factor. Molecular and cellular biology *31*, 662-673.
Umezu, K., Sugawara, N., Chen, C., Haber, J.E., and Kolodner, R.D. (1998). Genetic analysis of yeast RPA1 reveals its multiple functions in DNA metabolism. Genetics *148*, 989-1005.
Unnikrishnan, A., Gafken, P.R., and Tsukiyama, T. (2010). Dynamic changes in histone acetylation regulate origins of DNA replication. Nature structural & molecular biology *17*, 430-437.
van Attikum, H., Fritsch, O., Hohn, B., and Gasser, S.M. (2004). Recruitment of the INO80 complex by H2A phosphorylation links ATP-dependent chromatin remodeling with DNA double-strand break repair. Cell *119*, 777-788.
Viggiani, C.J., and Aparicio, O.M. (2006). New vectors for simplified construction of BrdU-Incorporating strains of Saccharomyces cerevisiae. Yeast *23*, 1045-1051.
Viggiani, C.J., Knott, S.R., and Aparicio, O.M. (2010). Genome-wide analysis of DNA synthesis by BrdU immunoprecipitation on tiling microarrays (BrdU-IP-chip) in Saccharomyces cerevisiae. Cold Spring Harbor protocols *2010*, pdb prot5385.
Vignali, M., Hassan, A.H., Neely, K.E., and Workman, J.L. (2000). ATP-dependent chromatin-remodeling complexes. Molecular and cellular biology *20*, 1899-1910.
Vincent, J.A., Kwong, T.J., and Tsukiyama, T. (2008). ATP-dependent chromatin remodeling shapes the DNA replication landscape. Nature structural & molecular biology *15*, 477-484.
Vogelauer, M., Rubbi, L., Lucas, I., Brewer, B.J., and Grunstein, M. (2002). Histone acetylation regulates the time of replication origin firing. Molecular cell *10*, 1223-1233.
Warner, J.R. (1999). The economics of ribosome biosynthesis in yeast. Trends in biochemical sciences *24*, 437-440.
Weiner, A., Hughes, A., Yassour, M., Rando, O.J., and Friedman, N. (2010). High-resolution nucleosome mapping reveals transcription-dependent promoter packaging. Genome Res *20*, 90-100.

Wellinger, R.J., and Zakian, V.A. (2012). Everything you ever wanted to know about Saccharomyces cerevisiae telomeres: beginning to end. Genetics *191*, 1073-1105.
Whitehouse, I., Rando, O.J., Delrow, J., and Tsukiyama, T. (2007). Chromatin remodelling at promoters suppresses antisense transcription. Nature *450*, 1031-1035.
Winston, F., and Carlson, M. (1992). Yeast SNF/SWI transcriptional activators and the SPT/SIN chromatin connection. Trends in genetics : TIG *8*, 387-391.
Woodcock, C.L., and Ghosh, R.P. (2010). Chromatin higher-order structure and dynamics. Cold Spring Harbor perspectives in biology *2*, a000596.
Xue, Y., Van, C., Pradhan, S.K., Su, T., Gehrke, J., Kuryan, B.G., Kitada, T., Vashisht, A., Tran, N., Wohlschlegel, J.*, et al.* (2015). The Ino80 complex prevents invasion of euchromatin into silent chromatin. Genes & development *29*, 350-355.
Yabuki, N., Terashima, H., and Kitada, K. (2002). Mapping of early firing origins on a replication profile of budding yeast. Genes to cells : devoted to molecular & cellular mechanisms *7*, 781-789.
Yadon, A.N., Singh, B.N., Hampsey, M., and Tsukiyama, T. (2013). DNA looping facilitates targeting of a chromatin remodeling enzyme. Molecular cell *50*, 93-103.
Yadon, A.N., Van de Mark, D., Basom, R., Delrow, J., Whitehouse, I., and Tsukiyama, T. (2010). Chromatin remodeling around nucleosome-free regions leads to repression of noncoding RNA transcription. Molecular and cellular biology *30*, 5110-5122.
Yeeles, J.T., Deegan, T.D., Janska, A., Early, A., and Diffley, J.F. (2015). Regulated eukaryotic DNA replication origin firing with purified proteins. Nature *519*, 431-435.
Yen, K., Vinayachandran, V., and Pugh, B.F. (2013). SWR-C and INO80 chromatin remodelers recognize nucleosome-free regions near +1 nucleosomes. Cell *154*, 1246-1256.
Yoshida, K., Bacal, J., Desmarais, D., Padioleau, I., Tsaponina, O., Chabes, A., Pantesco, V., Dubois, E., Parrinello, H., Skrzypczak, M.*, et al.* (2014). The histone deacetylases sir2 and rpd3 act on ribosomal DNA to control the replication program in budding yeast. Molecular cell *54*, 691-697.
Yu, E.Y., Steinberg-Neifach, O., Dandjinou, A.T., Kang, F., Morrison, A.J., Shen, X., and Lue, N.F. (2007). Regulation of telomere structure and functions by subunits of the INO80 chromatin remodeling complex. Molecular and cellular biology *27*, 5639-5649.
Yusufzai, T., and Kadonaga, J.T. (2008). HARP is an ATP-driven annealing helicase. Science *322*, 748-750.
Zeman, M.K., and Cimprich, K.A. (2014). Causes and consequences of replication stress. Nature cell biology *16*, 2-9.
Zhao, X., Muller, E.G., and Rothstein, R. (1998). A suppressor of two essential checkpoint genes identifies a novel protein that negatively affects dNTP pools. Molecular cell *2*, 329-340.
Zou, L. (2013). Four pillars of the S-phase checkpoint. Genes & development *27*, 227-233.
Zou, L., and Elledge, S.J. (2003). Sensing DNA damage through ATRIP recognition of RPA-ssDNA complexes. Science *300*, 1542-1548.

VITA

Laura Jane Lee

Education: Ph.D. Molecular and Cellular Biology, March 2016
Fred Hutchinson Cancer Research Center/University of Washington
Seattle, Washington, U.S.A.

B.A. Honors in Molecular Biology, Cum Laude, June 2009
Scripps College
Claremont, California, U.S.A.
Advisor: Jennifer Armstrong, Ph.D.

Publications: **Lee, L.**, Tsukiyama, T. (2016). Working Title: The role of chromatin remodeling factors at repetitive elements. *In preparation*.

Lee, L.*, Rodriguez, J.*, Lynch, B. Tsukiyama, T. (2016). Nucleosome occupancy as a novel chromatin parameter for replication origin functions. *Submitted*.
*Authors contributed equally to this work.

Lee, L., Rodriguez, J., Tsukiyama, T. (2015). Chromatin remodeling factors Isw2 and Ino80 regulate checkpoint activity and chromatin structure in S phase. *Genetics.* 199(4):1077-1091.

Radman-Livaja, M., Quan T.K., Valenzuela, L., Armstrong J.A., van Welsem, T., Kim T., **Lee L.J.**, Buratowski, S., van Leeuwen F., Rando O.J., Hartzog, G.A. (2012). A key role for Chd1 in histone H3 dynamics at the 3' end of long genes in yeast. *PLoS Genet.* 8(7):e1002811.